TEXTILE RESEARCH JOURNAL

VOLUME XXV October 1955 *NUMBER 10*

PUBLICATION OF

TEXTILE RESEARCH INSTITUTE

Editorial Office: 10 East 40th Street, New York 16, N. Y.

TEXTILE RESEARCH JOURNAL

Change of Address

All functions of the Publications Department of Textile Research Institute now conducted in New York City will be transferred to the Institute's offices in Princeton, New Jersey at the end of this year. This includes the editorial and subscriptions departments of Textile Research Journal. All manuscripts and communications which are likely to arrive subsequent to December 26 should be mailed to the address below.

The Institute's policy of maintaining the Publications Department as a separate operation is to be continued and the present high standard of the Journal will be maintained. All papers including those submitted by T.R.I. staff members are submitted to independent review. Members of T.R.I. staff serve as reviewers only when requested to do so by the authors. Julian S. Jacobs will continue as Editor-in-Chief of the Journal and Director of the Publications Department.

Address after December 26, 1955 is:

TEXTILE RESEARCH INSTITUTE
Publications Department
Princeton, New Jersey

TEXTILE RESEARCH JOURNAL

VOL. XXV, No. 10 OCTOBER 1955

IN THIS ISSUE

THE TENSILE PROPERTIES OF MAN-MADE AND SYNTHETIC STAPLE YARNS. G. Susich and E. Th. Vadala 817

THE THERMAL INSULATION OF CARIBOU PELTS. Irene Moote . 832

MECHANICS OF ELASTIC PERFORMANCE OF TEXTILE MATERIALS. *PART XII:* RELATION OF CERTAIN GEOMETRIC FACTORS TO THE TEAR STRENGTH OF WOVEN FABRICS. N. A. Teixeira, M. M. Platt, and W. J. Hamburger 838

RATE OF DYEING. John H. Skinkle 861

MICROWAVE DIELECTRIC MEASUREMENTS ON SINGLE FIBERS. J. J. Windle and T. M. Shaw 865

MOLECULAR PROPERTIES OF MILKWEED CELLULOSE. T. E. Timell and J. L. Snyder 870

ON THE BULK COMPRESSION CHARACTERISTICS OF WOOL FIBERS. P. C. deMaCarty and J. H. Dusenbury 875

Correction, Volume XXV, No. 8 885

Letters to the Editor

THE EFFECT OF TEMPERATURE ON THE ADSORPTION OF IODINE BY CELLULOSE. A. G. Chitale 886

FABRIC EMBEDDING FOR MICROTOME SECTIONING. Ines V. deGruy 887

DENSITY GRADIENT RESOLUTION OF CORTICAL CELL FRACTIONS. Wilfred H. Ward and John J. Bartulovich 888

BOOK REVIEW 890

Editor: Julian S. Jacobs *Production Editor:* Elizabeth Jane Cassatt

Associate Editors

H. J. Ball, Earl E. Berkley, Henry Eyring, W. J. Hamburger, Milton Harris, K. L. Hertel, Harold P. Lundgren, H. Mark, E. R. Schwarz

TEXTILE RESEARCH JOURNAL, published monthly at Prince and Lemon Streets, Lancaster, Pa., is devoted to the interest of research in textile and allied industries. It is published by Textile Research Institute.

Entered as second-class matter, April 27, 1945, at the post office at Lancaster, Pa., under the Act of August 24, 1912. Accepted for mailing at special rate of postage provided for in paragraph (d-2), Section 34.40, P. L. & R. of 1948, authorized May 9, 1950.

Manuscripts and communications should be sent to the editorial office, 10 East 40th Street, New York 16, N. Y.

Subscription rates: $15.00 per year; additional for postage, 50 cents to Canada, $1.00 to all other countries. Single copies, $1.50 each.

Contents copyrighted © 1955 by Textile Research Institute. Advertising rates supplied on request.

CHEMISTS

1. PhD in organic chemistry or MS with 1 to 2 years research experience, preferably in polymers. For research related to the synthesis and application of chemical compounds connected with durable finishes for synthetic fabrics.
2. PhD or equivalent in physical chemistry, 5 to 8 years experience, some of which should have been in fiber research. To assist in planning and coordinating problems in basic fiber research covering relationship of molecular and micro structure to mechanical, thermal and other physical properties.
3. MS or PhD in physical, or in organic chemistry with strong physical background, 0 to 5 years experience. For fundamental studies on cellulose and its derivatives and in development of manufacturing processes for cellulose derivatives.

The diversity of the Celanese Corporation activities in chemicals, textiles and plastics . . . the continuing growth and expansion of the organization . . . provide opportunities for qualified men in the Research Laboratories in Summit, New Jersey, a pleasant residential community within 30 miles of metropolitan New York City.

Please submit resumes, including salary desired, to J. A. Berg.

Celanese

CORP. OF AMERICA

Morris Court **Summit, N. J.**

NEP TEST MACHINE

The Nep Test Machine was designed by the United States Department of Agriculture and is written up in the USDA Bulletin of November 1954 titled "Laboratory Equipment and Method for Making Nep Tests on Cotton Samples." To provide a rapid and satisfactory method of preparing specimens of raw cotton for nep evaluation, this laboratory-type machine has been devised to produce a relatively narrow web of fibers from a small sample of cotton. The design of this machine incorporates the principal mechanical assemblies of textile carding machines in order to simulate commercial production methods as closely as possible. The machine will process a 3-gram sample of blended cotton to produce a continuous web 4 inches wide and approximately equivalent in appearance and weight to card web produced for 40-gram sliver. Sufficient web is produced to provide 10 specimens which are placed on 4 x 9 inch boards for nep evaluation. (ASTM Designation D 1446-53T "Method of Test for Number of Neps in Cotton Fibers.")

CUSTOM SCIENTIFIC INSTRUMENTS, INC.

541 Devon Street **Kearny, N.J.**

Unusual Opportunity

INDEPENDENT COMMERCIAL LABORATORY has unusual opening for competent chemist experienced in wool technology.

Thorough knowledge of wool preparation and a familiarity with quality control techniques essential.

Plans for expansion of laboratory offer exceptional opportunity to person possessing resourcefulness and executive ability. Salary open. Our staff knows of this advertisement.

Address inquiries to

TEXTILE RESEARCH INSTITUTE

10 East 40th Street **New York 16, N. Y.**

Department "A"

TEXTILE RESEARCH JOURNAL

VOL. XXV, NO. 10 OCTOBER 1955

The Tensile Properties of Man-Made and Synthetic Staple Yarns[1]

G. Susich and E. Th. Vadala

Quartermaster Research and Development Center, Natick, Massachusetts

Abstract

The stress-strain properties, the tensile-recovery behavior, and the response to repeated tensioning (cycling) of sixteen staple yarns were investigated. Three man-made (Fiberglas, viscose, acetate) and seven synthetic (nylon, Orlon,[2] Dacron,[3] Dynel, Saran, polyvinyl chloride, Kuralon) textile materials were tested at standard conditions using the Instron Tensile Tester.

The tensile recovery was obtained by measuring the three elongation and work components. The total work of rupture was divided into the immediately recoverable work, creeping work, and unrecoverable work absorption. Dynamic tests were carried out by extending the yarns in 50 cycles to 80% of their elongation at break and measuring their response during and after this procedure.

A comparison was made between tensile properties of staple yarns and corresponding multifilaments of the same material. Cycling tests were found useful in evaluating those tensile characteristics which are significant for the performance of yarns in service. It was attempted to interpret the behavior of yarns in repeated tensioning and flex abrasion from their known tensile properties.

Introduction

Man-made and synthetic staple fibers are being increasingly applied in yarns and fabrics, either alone or in mixtures. They may be blended with one another, e.g., viscose with acetate, or with the natural fibers, cotton and wool, in order to impart to them desirable properties such as strength, durability, resistance to moisture, etc. The tensile behavior of multifilaments of man-made and synthetic fibers has probably been as widely investigated as that of yarns spun from the natural staple fibers. No comprehensive study exists, however, of the tensile behavior of corresponding staple yarns, although some of these (viscose, nylon) have been investigated thoroughly by various authors.

Synthetic staple fibers and, particularly, spun yarns duplicate the morphology of the natural fibers, cotton and wool, and the yarns spun from them more closely than continuous filaments. Yarn spun from staple fibers have a looser structure than multifilaments; they include more air space, and individual fibers stick out from the yarn surface. Figure 1 shows two-ply Fiberglas yarns; the left sample is spun from staple and the right sample from continuous filament. The staple yarn is thicker and has

[1] A part of this study was presented at the Spring Meeting of The Fiber Society at Charlottesville, Va., May 6, 1954.

[2] Du Pont acrylic fiber.

[3] Du Pont polyester fiber.

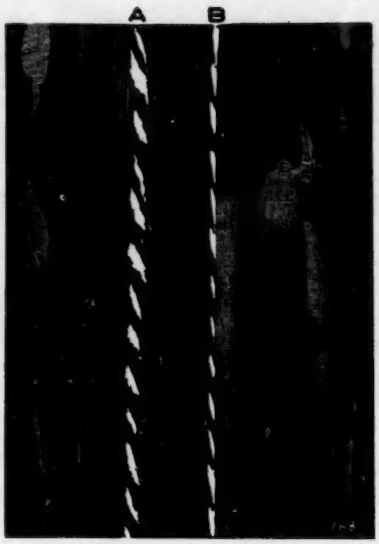

Fig. 1. Two-ply fiberglas yarns. *A*, staple yarn; *B*, multifilament.

a hairy surface. The single fibers protruding from the main yarn body are straight, demonstrating the inherent stiffness of glass fibers [8]. Fabrics woven from staple yarns generally show higher bulk, lighter weight, and better thermal insulation; they are more flexible and have a fuzzier surface and less luster than comparable fabrics made from multifilaments. Staple yarns are frequently superior to multifilaments in dye absorption and evenness of shades. This is partly due to the greater accessibility of the staple fibers. It must be mentioned, however, that staple fibers may be stretched less than continuous filaments and that their chemical composition may even be different from that of multifilaments, with resultant enhanced dyeability.

The tensile behavior of staple yarns can be markedly different from that of multifilaments. Therefore, a systematic study of the tensile properties of staple yarns was carried out using testing techniques which permit some conclusions to be drawn regarding their behavior in practical use.

The present investigation deals with the tensile properties of ten different textile materials under standardized conditions, 21.2°C (70°F) and 65% R.H.

Tensile properties are obtained by evaluating the stress-strain curve from the beginning of stress and strain up to the point where rupture occurs. The conventional stress-strain diagram represents the relationship between stress and strain, including the initial modulus, yield point and breaking point, and the work necessary for rupture. It will be worthwhile to discuss the significance of the yield point and work of rupture.

In testing textiles little attention is generally paid to the yield point, probably because it is far less definite than the breaking point. Nevertheless, it is an important characteristic since marked changes in tensile behavior occur at the yield point. These changes cause numerous problems in the practical use of textiles, especially if accompanied by greater amounts of plastic flow. Moreover, fibers are subjected in service almost exclusively to stresses and strains which are closer to the yield point than to the breaking point. With the exception of a very few cases (e.g., wet wool) the yield point coincides with the "elastic limit" and also denotes the limit of linear relationship between stress and strain (Hookean behavior). Data of initial modulus or compliance [4] are of little value without knowing up to what point on the stress-strain curve they are valid.

The total energy absorption of fibers is expressed by the area under the stress-strain curve which characterizes the resistance of fibers to mechanical destruction. Although work absorption is frequently more indicative of fiber behavior [5] than breaking tenacity or extensibility, relatively little information on this property is available in the current textile literature [see data of Meredith, Smith, Kaswell, and Coplan, pp. 21–26, 318 of reference 6]. If the "work factor" [6] reflecting the shape of the stress-strain curve is known, total work of rupture can be easily calculated from ultimate values of stress and strain by multiplication of their product by the "work factor" and a conversion factor for the required energy unit. Work absorption can be expressed in any work units: ergs, gram-centimeters, foot-pounds, or even calories. In this report it will be discussed on

[4] Compliance denotes the ratio of strain to stress, and it is reciprocal to the elastic modulus.

[5] For example, of abrasion resistance according to Hamburger [4] and of felting of wool tops according to Bogaty, Sookne, and Harris [3].

[6] "Work factor" is the ratio between the area below the stress-strain curve and the area of a rectangle having as sides the ultimate values of stress and strain.

the basis of gram-centimeters per grex [1a] for one meter fiber length.

Tensile recovery and response of yarns to repeated tensioning have been included in this investigation, although these characteristics are not obtainable from the conventional stress-strain curves. In order to make any judgment of the tensile behavior of yarns, it is imperative to know to what extent and at what rate their length recovers after the tension imposed has been released. This was investigated by analyzing the stress-strain relationship and measuring three elongation components: immediate and delayed elastic recovery and permanent set. The testing procedure and the different methods of demonstrating elongation components by three curves and by three areas of rectangular and quadratic graphs have been previously described [9].

The demonstration of the elongation components by three curves permits the separation of the total work absorption into three components: the immediately recoverable, the creeping recoverable, and the nonrecoverable work. It is known that in extending fibers a portion of the total energy absorption is regained spontaneously after the tension is released. This part of the total work absorption is the elastic work and may be divided into that component which recovers immediately and that which recovers after a while. The remaining portion of the total work does not recover. It seems to be lost in the first deformation; more accurately, it is stored as potential energy or is transformed into heat and dissipated to the environment.

Knowledge of the response of yarns to repeated tensioning is essential for the understanding of their behavior in service. Yarns are subjected in practice not to one but to repeated stretchings under widely varying conditions. Any stress exceeding the yield point, and even stresses below the yield point if frequently repeated, will affect the properties of a viscoelastic material. It was shown in a previous study [10] that the alterations of fibers after they have been extended are partly reversible and partly permanent and may be desirable (stress hardening) or undesirable (fatigue). The changes depend upon inherent fiber properties and environmental conditions, temperature, humidity, and swelling, upon the degree, rate, and duration of stress or strain to which the fibers are subjected, and upon the relaxation time after the deformation. In this study, selected staple yarns were repeatedly extended under rather severe conditions. The behavior during repeated tensioning (cycling) and the changed stress-strain relationship, including the total energy absorption, were evaluated.

Materials Tested

Almost all types of man-made and synthetic fibers available at present in the form of staple yarns were investigated. Spun yarns of glass, viscose, cellulose acetate, 6–6 nylon, polyacrylonitrile (Orlon), polyester of terephthalic acid and ethylene glycol (Dacron), copolymer of 60% polyvinyl chloride and 40% polyacrylonitrile (Dynel), polyvinylidene chloride (Saran), polyvinyl chloride (Fibravyl, Thermovyl), and polyvinyl alcohol (Kuralon) fibers were tested. Most of them are textile materials well known in this country. The polyvinyl chloride fibers were French products [7]. Fibravyl is the staple fiber corresponding to the continuous-filament Rhovyl and starts to shrink at approximately 78°C (172°F). Thermovyl has a slightly higher heat stability [100°C (212°F)] and is less stretched than Fibravyl. The Kuralon samples were of Japanese origin and consisted of acetalized polyvinyl alcohol [2, 12]. Formaldehyde crosslinks make polyvinyl alcohol insoluble in water and thus suitable for textile purposes.

In addition to inherent material properties due to the chemical composition, the morphology of individual staple fibers—fineness, cross-section, staple length, crimp, etc., the form factors of the yarns—size, construction, and twist, and stretching and finishing in processing affect tensile properties. These factors were by no means identical for all available yarns and in order to indicate within what limits the properties tested may vary some fiber materials (Kuralon, 6-6 nylon, Orlon, and Dacron) were tested in different forms.

The characteristics of the fibers tested are listed in Table I. Although yarn size of staple yarns is generally expressed in cotton or worsted counts, the universal yarn numbering system using grex [1*a*] was adopted for the designation of yarn fineness in order to facilitate the comparison of all the yarns tested. The conventional "twist multiplier" [7] was included in the table, and it appears in parenthesis for those yarns for which size is not expressed in cotton count.

[7] Twist multiplier $= \frac{\text{Turns per inch}}{\sqrt{\text{Cotton count}}}$.

TABLE I. Materials Tested

No.	Designation	Count	Actual Fineness of Yarn (grex)	Fineness of Staple (grex)	Average Staple Length in Cm	Average Staple Length in Inches	Twist Single/Ply per Cm	Twist Single/Ply per Inch	Twist Multiplier Single/Ply	Source
1	Fiberglas ESE 31/1	Special	1576	1.0*	25.4	10.0	3.34	8.5 Z	(6.6)	Owens Corning Fiberglas Corp., Ashton, R. I.
2	Kuralon 80/2†	Cotton	144	1.7						Omni Products Corp., New York, N. Y.
3	Orlon 16/1	Cotton	369	2.8	16.5	6.5	2.36	6 Z	1.50	Champlain Spinners, Inc., White Hall, N. Y.
4	Saran 16/1	Worsted	533	11.1	10.2	4.0	4.9	12.5	(3.1)	Livingston Worsted Mills, Inc., Holyoke, Mass.
5	Viscose 20/1	Cotton	296	3.3	5.1	2.0	6.3	16	3.58	American Viscose Corp., Marcus Hook, Pa.
6	Fibravyl 75/1	Metric	138	2.0	9.0	3.6	5.9	15	(2.30)	Rhodia, Inc., New York, N. Y.
7	Kuralon 40/1‡	Cotton	146	2.2						Omni Products Corp., New York, N. Y.
8	Acetate 20/1	Cotton	296	3.3	3.8	1.5	5.7	14.6	3.26	
9	Nylon 60/1	Cotton	98	1.7	3.8	1.5	9.8	25	3.24	Aberfoyle, Mfg. Co. Philadelphia, Pa.
10	Orlon 15/1	Cotton	391	3.3	6.4	2.5	5.5	14	3.62	Newnan Cotton Mills, Newnan, Ga.
11	Dacron 29/2	Worsted	595	3.3	6.4–12.7	2.5–5.0				Nathan Schwartz & Sons, Inc., Philadelphia, Pa.
12	Dynel 20/1 (Experimental)	Cotton	296	3.6	5.1	2.0				Carbide & Carbon Chemical Co., Charlottesville, Va.
13	Nylon 30/2	Cotton	405	3.3	3.8	1.5	7.1/3.9	18/10	3.29/2.58	Durham Hosiery Mills, Durham, N. C.
14	Dacron 20/1	Cotton	295	3.3	6.4	2.5	5.5	14 Z	3.14	Dixie Mercerizing Co., Chattanooga, Tenn.
15	Dacron 60/2§	Worsted	309	3.3	7.6	3.0	8.7/9.5	22/24	(2.85/4.39)	Phaar Worsted Mills Inc., McAdenville, N. C.
16	Thermovyl 30/1	Metric	324	5.5	9.0	3.6	3.74	9.5	(1.73)	Rhodia, Inc., New York, N. Y.

* 0.28 mils (7.1 μ) in diameter.
† Spun on draft break system, degree of acetalization 30.8%.
‡ Spun on cotton system, degree of acetalization 37.4%.
§ Type 5400.

Stress-Strain Relationship

The yarns were tested on the Instron Tensile Tester Model TTB [5] using a 12.7-cm (5.0-in.) gauge length at a pretension of 0.5–1.0% of the breaking load and a jaw separation corresponding to 100% elongation of the specimen per minute. Ten specimens of each yarn were tested. From the load-elongation curves obtained, one having ultimate values closest to the mean values of extensibility and work of rupture was selected to represent the average behavior.

Stress-strain curves are shown in Figures 2, 3, and 4*B* where normalized stress values (uncorrected tenacities) are correlated to the initial yarn grex. Data obtained from these curves are listed in Table II.

Yield Point

As yield point, that point on the curve was taken which was closest to the intersection of the two straight lines representing the two linear portions below and above the region where the first marked change in the stress-strain relationship occurs. The yield point appears as elongation and tenacity values in Table II and is always at the beginning of the stress-strain curve.

Initial Modulus

The tangent to the initial linear portion of the stress-strain curve represents the initial modulus. The yield tenacity (g/gx) values listed in Table II designate the tension in grams which would be neces-

TABLE II. Stress-Strain Properties

No.	Designation	Yarn Fineness (grex)	Yield Point*			Breaking Point*				Total Work of Rupture (g-cm/gx for 1 m fiber length†)
						Elongation at Break		Uncorrected Tenacity at Break		
			Initial Modulus (g/gx)	Yield Elongation (%)	Yield Tenacity (g/gx)	in Per Cent	Coefficient of Variation (%)	in G/gx	Coefficient of Variation (%)	
1	Fiberglas ESE 31/1	1576	81.1	0.56	0.18	1.8	8.9	1.47	10.9	0.94
2	Kuralon 80/2	144	29.4	2.4	0.57	11.2	4.5	2.44	17.8	12.8
3	Orlon 16/1	369	36.3	2.5	0.77	13.7	7.3	1.86	15.6	15.0
4	Saran 16/1	553	4.2	4.4	0.19	14.3	9.8	0.73	21.0	5.0
5	Viscose 20/1	296	25.7	2.1	0.44	16.2	8.6	1.26	7.9	12.3
6	Fibravyl 75/1	138	20.3	2.8	0.44	18.9	5.8	1.41	17.0	15.5
7	Kuralon 40/1	146	18.8	2.3	0.33	20.0	8.6	1.44	19.4	15.5
8	Acetate 20/1	296	17.3	3.5	0.51	21.9	22.9	0.88	13.6	13.8
9	Nylon 60/1	98	8.0	6.0	0.48	22.0	13.2	2.21	24.5	20.2
10	Orlon 15/1	391	18.7	5.0	0.70	24.0	15.0	1.38	12.3	22.9
11	Dacron 29/2	595	16.6	4.2	0.65	24.1	4.6	2.21	5.1	29.0
12	Dynel 20/1	296	13.1	3.8	0.43	27.5	5.8	1.10	8.1	19.1
13	Nylon 30/2	405	5.9	4.5	0.25	31.7	9.5	2.40	10.8	35.6
14	Dacron 20/1	295	15.6	3.1	0.41	38.5	3.5	1.92	7.9	39.0
15	Dacron 60/2	309	19.9	4.3	0.55	39.7	4.3	2.78	5.4	56.8
16	Thermovyl 30/1	324	6.9	5.9	0.31	100.0	13.2	0.29	24.8	32.1

* Demonstrated in Figures 2, 3, and 4*B*.
† Based on uncorrected tenacities and demonstrated in Figure 9*A*.

sary, for each grex of the yarn, to extend its length by 100%, assuming that it could be extended to such an amount and that the initial linear relationship between stress and strain would remain constant during this procedure. It was found that the initial moduli of Saran, nylon, and Thermovyl are rather low, while that of Fiberglas is exceptionally high, and that the moduli of all the other yarns are between 13 and 36 g/gx. The moduli of staple yarns are generally lower than those of corresponding multifilaments, due mainly to the yarn structure. The relative ranking of the initial moduli for different staple yarns is, however, similar to that of corresponding continuous yarns.

Breaking Point

Disregarding the low extensibility of Fiberglas (1.8%) and the unusually high elongation of Ther-

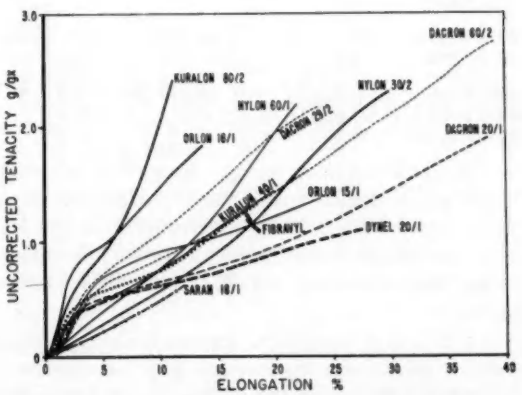

Fig. 2. Stress-strain curves of synthetic staple yarns.

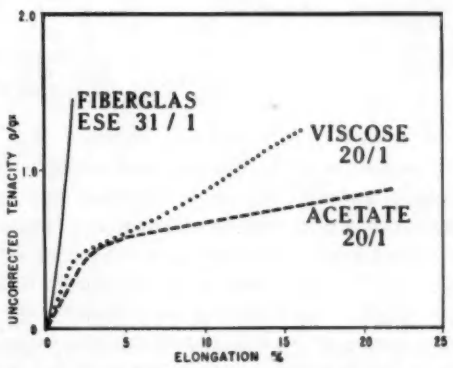

Fig. 3. Stress-strain curves of man-made staple yarns.

TABLE III. Different Evaluations of the Stress-Strain Relationship

		Initial Modulus		Yield Point				Breaking Point					
				Stress				Stress				Work of Rupture	
No.	Designation	Load (g)*	Uncorr. (g/gx)†	Load (g)*	Uncorr. Tenacity (g/gx)†	Corr. Tenacity (g/gx)‡	Strain (%)	Load (g)*	Uncorr. Tenacity (g/gx)†	Corr. Tenacity (g/gx)‡	Strain (%)*,†,‡	in G-cm/m	Uncorr. (g-cm/gx/m)	Corr. (g-cm/gx/m)
4	Saran 16/1	2300	4.2	107	0.19	0.20	4.4	405	0.73	0.84	14.3	2760	5.0	5.5
6	Fibravyl 75/1	2800	20.3	61	0.44	0.45	2.8	194	1.41	1.67	18.9	2140	15.5	16.9
16	Thermovyl 30/1	2220	6.8	100	0.31	0.33	5.9	93	0.29	0.58	100.0	1040	32.1	47.5
	(Maximum)	—	—	—	—	—	—	121	0.37		35.0	—	—	—

* Shown in Figure 4*A*.
† Shown in Figure 4*B* and Table II.
‡ Shown in Figure 4*C*.

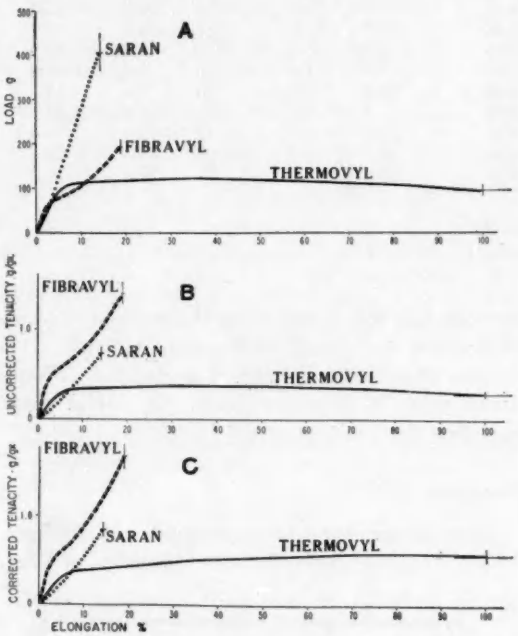

Fig. 4. Different demonstrations of the stress-strain relationship.

movyl (100%), extensibilities between 11.2 and 39.7% were observed. These values are higher than the elongation of cotton yarns, and they represent a wider range than that observed for wool yarns. The extensibilities of staple yarns are in general similar to those of the corresponding multifilaments [9, 10]. Where higher extensibilities were found (e.g., for 30/2 nylon, and 20/1 and 60/2 Dacron), they are most likely due to a smaller amount of orientation (stretching) in producing the staple yarns.

The breaking tenacity of the yarns varies between 0.29 and 2.78 g/gx and is lower than that of corresponding multifilaments. This is apparent from comparison of the relatively low breaking tenacities of Fiberglas (1.47 g/gx) and of the two nylon spun yarns (2.21 and 2.40 g/gx) with those of the multifilaments (Fiberglas, 5.81; nylon, 5.52 g/gx [9]). The lower tenacity of staple yarns is sometimes due to insufficient fiber-to-fiber friction, perhaps also to damage suffered in mechanical spinning (Fiberglas), and sometimes to lower drawing rates (nylon).

The total work of rupture varies between 0.94 (Fiberglas) and 56.8 g-cm/gx for 1 m fiber length (60/2 Dacron). It is not surprising that the energy absorption of staple yarns is lower than that of multifilaments. The following energy absorptions in g-cm/gx/m were observed for Orlon, 6–6 nylon, and Dacron.

Staple Yarn		*Multifilament*[8]	
16/1 Orlon	15.0	100/40 Orlon	37.3
15/1 Orlon	22.9		
60/1 Nylon	20.2	100/40/2.5 Nylon	85.8
30/2 Nylon	35.6		
29/2 Dacron	29.0	100/40 Dacron	60.7
20/1 Dacron	39.0		
60/2 Dacron	56.8		

The relatively low energy absorption of nylon staple yarns compared with that of the Dacron staple yarns tested can easily be understood from the low tenacities of nylon and the high extensibilities (indicating less stretching) of 20/1 and 60/2 Dacron yarns.

[8] Obtained from stress-strain data shown in Figure 6 and Table II of reference 9. These energy values are low in comparison with those of the corresponding undrawn fibers since 109.3, 212, and 696 g-cm/gx/m work were observed for undrawn Orlon, Dacron, and 6–6 nylon, respectively.

TABLE IV. Elongation Components at the Breaking Point

		Actual Values (in per cent of original length)				Relative Values* (in per cent of total elongation at break)		
		Immediate Elastic Recovery	Delayed Recovery	Permanent Set	Total Elongation	Immediate Elastic Recovery	Delayed Recovery	Permanent Set
1	Fiberglas ESE 31/1	0.83	0.78	0.19	1.8	46	43	11
2	Kuralon 80/2	2.0	6.0	3.2	11.2	18	54	28
3	Orlon 16/1	2.6	7.5	3.6	13.7	19	55	26
4	Saran 16/1	5.3	8.1	0.9	14.3	37	57	6
5	Viscose 20/1	2.7	3.6	9.9	16.2	17	22	61
6	Fibravyl 75/1	3.5	8.2	7.2	18.9	19	43	38
7	Kuralon 40/1	2.2	7.8	10.0	20.0	11	39	50
8	Acetate 20/1	2.6	3.8	15.5	21.9	12	17	71
9	Nylon 60/1	4.4	13.0	4.6	22.0	20	59	21
10	Orlon 15/1	4.0	8.0	12.0	24.0	16	34	50
11	Dacron 29/2	3.1	8.0	13.0	24.1	13	33	54
12	Dynel 20/1	3.2	7.8	16.5	27.5	12	28	60
13	Nylon 30/2	4.1	17.0	10.6	31.7	13	53	34
14	Dacron 20/1	3.5	9.0	26.0	38.5	9	24	67
15	Dacron 60/2	4.4	8.4	26.9	39.7	11	21	68
16	Thermovyl 30/4	5.0	11.8	83.2	100.0	5	12	83

* Demonstrated on the top of quadratic graphs in Figure 5.

Fig 5

RECOVERY BEHAVIOR DEMONSTRATING RELATIVE VALUES OF ELONGATION COMPONENTS

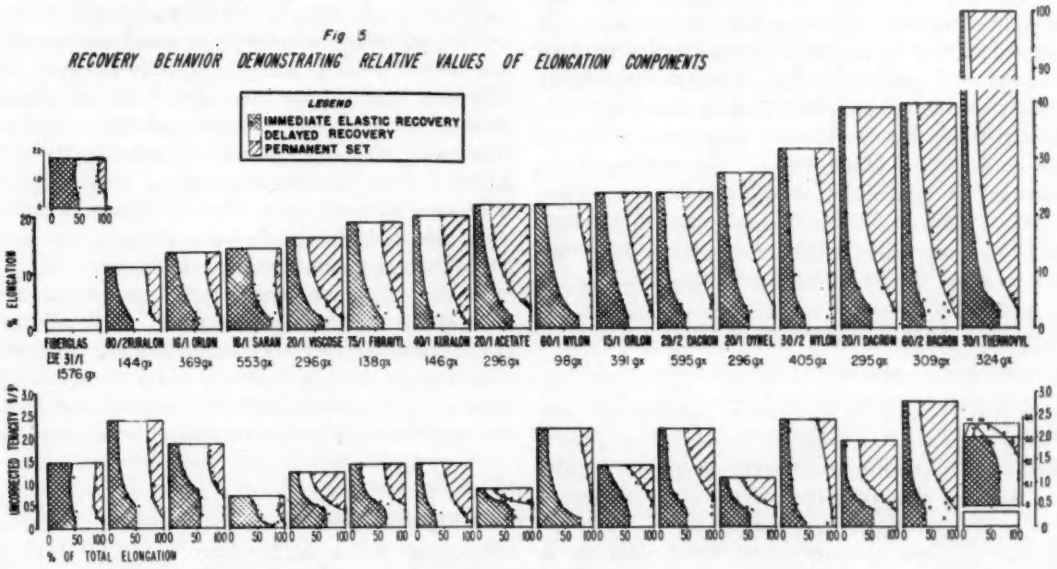

It must be mentioned that there are different ways of evaluating the stress-strain relationship of yarns. Some of them are demonstrated in Figure 4*A-C*. The load-elongation curves of Saran, Fibravyl, and Thermovyl as obtained directly in the Instron Tensile Tester are shown in Figure 4*A*. Figure 4*B* demonstrates the stress-strain relationship of these fibers by tenacity values based on the initial yarn grex. When tenacities are based on the actual yarn grex, which decreases [9] during the stretching procedure, the curves of Figure 4*C* are obtained. Using "corrected tenacities," of course, affects values of initial modulus, yield tenacity, breaking tenacity, and also work of rupture. Table III shows that the difference between uncorrected and corrected data is

[9] The diminishing yarn fineness can be calculated for any strain value from the initial grex and the elongation, assuming that uniform extension takes place along the entire length of the yarn.

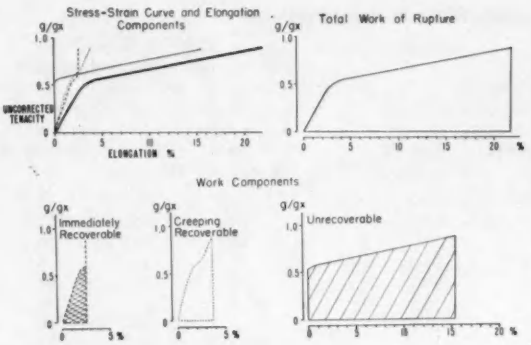

Fig. 6. Energy components of a 20/1 acetate staple yarn (296 gx).

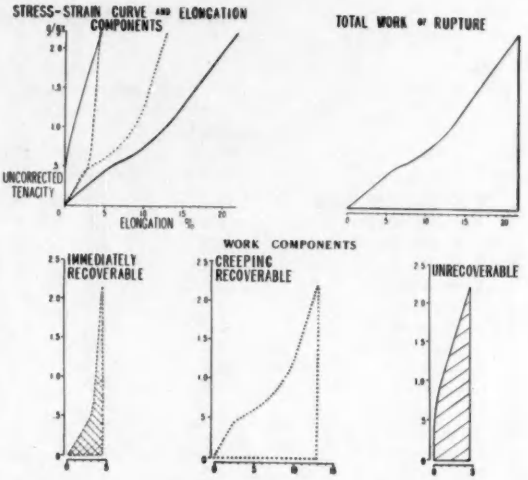

Fig. 7. Energy components of a 60/1 nylon staple yarn (98 gx).

slight at low strain and is considerable at high strain values, e.g., for the ultimate stress and work of rupture of Thermovyl.

The stress-strain relationship of Thermovyl is unusual in that the maximal tension does not appear at rupture but at a much earlier point, corresponding to approximately 35% elongation if stress is expressed by load in grams or by uncorrected tenacity (Figure 4*A* and *B*). The maximal tension is reached at a markedly higher elongation (approximately 85%), however, when uncorrected tenacities are demonstrated (Figure 4*C*). The analysis of the stress-strain relationship shows that the unconventional behavior of Thermovyl is due to the predominance of plastic flow which causes a marked stress decay during the stretching procedure.

Tensile Recovery Behavior

Elongation Components

Relative values of elongation components are shown from the beginning of the stretching procedure up to rupture by rectangular graphs in Figure 5. They are plotted against actual values of elongation in the upper row and against actual values of uncorrected tenacity in the lower row.[10] Numerical data of actual and relative elongation components at the breaking point are listed in Table IV.

The Fiberglas and Saran yarns are the most elastic samples. The elongation of Fiberglas recovers to a great extent immediately, 46% of the total elongation at the breaking point. The two nylon samples are also highly elastic; their recovery is, however, mainly delayed (creep). Of the two polyvinyl alcohol and polyvinyl chloride yarns tested, the stronger and less extensible samples (80/2 Kuralon and Fibravyl) have higher recovery. Viscose, acetate, Dynel, 20/1 and 60/1 Dacron, and Thermovyl are characterized by high values of unrecoverable elongation. Their permanent set at the breaking point is between 50 and 83% of the total elongation. The elongation components of most staple yarns are similar to those of corresponding multifilaments [9, 10], indicating that recovery remains essentially unaffected by the yarn structure. It must be mentioned, however, that the recovery of the 20/1 and 60/1 Dacron yarn is markedly lower than that observed for a multifilament,[11] owing to the lower drawing ratio used in manufacturing the staple yarns.

Work Components

In Figures 6 and 7 the actual values of elongation components for a 20/1 acetate and a 60/1 nylon staple yarn are shown by three curves in order to illustrate the separation of work components. The areas under the curves representing the immediate elastic recovery (dashed line), delayed recovery (dotted line), and permanent set (light solid line) demonstrate the immediately recoverable, creeping

[10] The distinction between maximal and ultimate load for Thermovyl made it necessary to extend the rectangular graph above the breaking tenacity in the lower row of Figure 5.

[11] At the breaking point 33 and 32% of the elongation were recoverable for the Dacron staple yarns, while the corresponding value is 55% for Dacron multifilaments (Table II, Column 6 of reference 10).

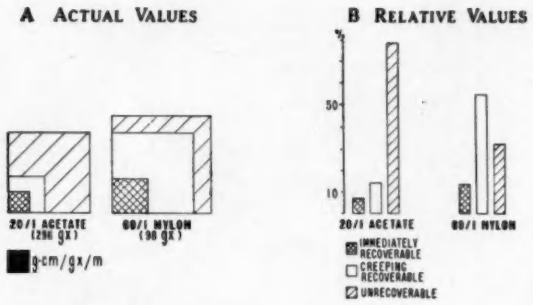

Fig. 8. Demonstration of energy components.

recoverable, and unrecoverable work absorption. The sum of these three areas is the total work of rupture as obtained from the conventional stress-strain curve.

Since the visual comparison of areas having markedly different shapes is inconvenient, the actual values of work components of the two yarns are demonstrated in Figure 8*A* by three parts of quadrates representing the total work absorption.

The acetate and nylon yarns have practically identical extensibilities (21.9 and 22.0%). Due to the higher breaking tenacity of nylon, its total work absorption is somewhat higher than that of acetate (20.2 compared with 13.8 g-cm/gx/m). Comparison of the two quadratic graphs in Figure 8 shows the striking difference between the two materials. While the predominant portion of the total energy is unrecoverable for acetate (11.0 g-cm/gx/m or 79% of the total energy), it is creeping recoverable for nylon (11.1 g-cm/gx/m or 55% of the total energy). The immediately recoverable energy is also higher for nylon. Accordingly, the nylon staple yarn has a much higher elastic energy than the acetate yarn. These differences between the two yarns are also apparent from the relative values of their energy components, demonstrated by three bars in Figure 8*B*. Only 21% of the total energy is recoverable for acetate, while the corresponding value for nylon is 68%. The high elastic energy absorption of nylon explains its exceptionally high resistance when subjected to repeated stresses.

The tensile-recovery behavior of different fibers can thus be compared on the basis of energy as well as of elongation. The relative values of energy components for acetate and nylon, shown in Figure 8*B*, are similar to those of elongation components at the breaking point listed in Table IV. This explains why elongation components can frequently be used in evaluating fiber behavior when in fact energies are involved.

Total work absorption is not significant in determining the resistance of fibers to destruction when subjected to repeated stresses. Immediately recoverable work has to be taken into account when yarns are frequently deformed at high speed (e.g., in sewing). Both recoverable work components, immediately and creeping recoverable energy absorption, have to be considered either when fibers are frequently stressed at a rather low speed or for any repeated tensile deformations separated from each other by relaxation periods. The unrecoverable work component is for the most part undesirable and is useless, except in a few cases. In cycling tests the unrecoverable work absorption is eliminated in the first extension. If such cycling tests are performed at moderate strain rates, both elastic work components are regained in the unloading phase of the cycle, indicating a reversible structural rearrangement in the fibers during the loading phase.

Actual and relative values of work components of the yarns tested are shown graphically in Figure 9, and corresponding numerical data are listed in Table

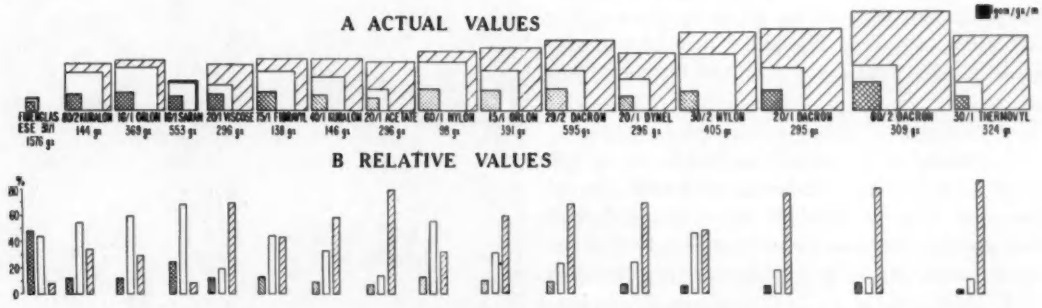

Fig. 9. Energy components.

V. Yarns are arranged in order of increasing extensibility. The highest total work absorption (56.8 g-cm/gx/m) was not found for the most extensible yarn (Thermovyl) but for 60/2 Dacron. The predominant portion (80%) of the energy absorbed, however, for this yarn is unrecoverable. The highest elastic energy absorptions (sum of immediately and creeping recoverable work) were found for the two nylon yarns (13.7 and 18.5 g-cm/gx/m), although their work recovery is to a great extent creeping. A relatively high percentage of the total work (48%) was instantaneously recoverable for Fiberglas, but due to low tenacity and extensibility the total work absorption of this material was the lowest (0.45 g-cm/gx/m) of all the yarns tested.

Response to Repeated Tensioning

Behavior of eleven yarns during and after repeated tensioning was investigated by extending them repeatedly in the Instron Tensile Tester under rather severe conditions. Details of testing conditions and results of these cycling tests are listed in Table VI and are shown in Figure 10. Yarns of 20.3-cm (8.0-in.) length were cycled 50 times between zero tension and 80% of their extensibility at a constant strain rate corresponding to 62.5% elongation of the specimen per minute. After a relaxation period of 1 hr without tension, the changed stress-strain relationship was tested in the same way as described on page 820.

Conditioning Level [12]

The cycling procedure to 80% of the extensibility was necessarily carried out to different actual elongation levels, which were between 9.0 and 31.7%. Neither the actual nor the relative tensions to which the yarns were subjected were, of course, the same for the eleven yarns. The conditioning tension varied between 72 and 90% of the ultimate values. Even this tension prevailed only in the first loading cycle because notable load decay occurred during cycling.

Load Decay

Stress decay in viscoelastic materials is not surprising since marked irreversible structural changes occur when they are extended above the yield point. These changes are evidenced then by altered mechanical properties. The load decay was pronounced

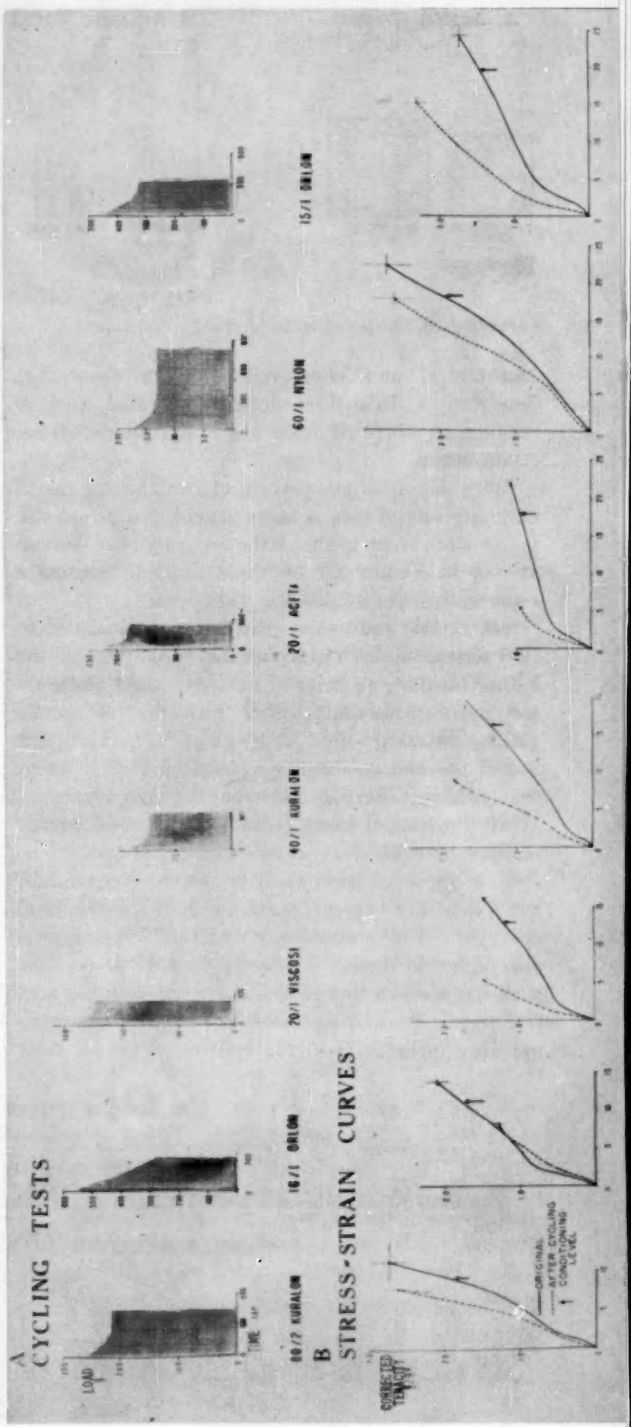

[12] The term conditioning level is derived from "mechanical conditioning" [10] and designates the stress, strain, or energy level to which the yarn was subjected during cycling.

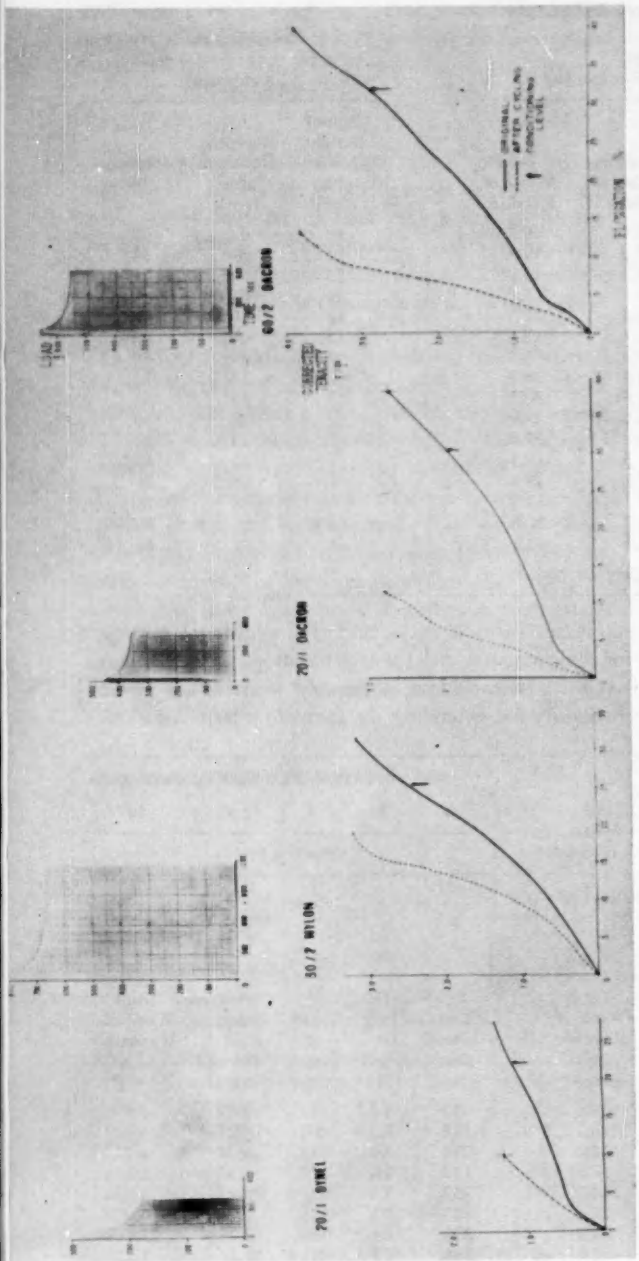

Fig. 10. Cycling tests and alteration of the stress-strain relationship.

in the first cycles and decreased later. No noticeable stress decay occurred in the last cycles of 80/2 Kuralon and 60/1 nylon, indicating that for these yarns a fairly elastic and stable structural rearrangement was attained by cycling. It can be expected that the remaining nine yarns will continue to change their properties following the 50th cycle, some of them (e.g., 16/1 Orlon) rapidly; others (e.g., 40/1 Kuralon, acetate) at a rather slow rate.

Cycling Time

Markedly different times (between 234 and 1095 sec) were necessary to complete 50 cycles on the eleven yarns. Not extensibility but the recovery at the conditioning level was critical for the cycling time. When two yarns having the same extensibility but different recoveries are repeatedly extended to the same level at a constant strain rate, the more elastic yarn needs a longer time for recovery in the unloading cycle. Also, it has to be extended for a longer time in the following loading cycle. The conditioning elongation was practically identical for the 20/1 acetate and 60/1 nylon yarn. Figure 10 shows, however, that 50 cycles (between 0 load and 17.5/17.6% elongation) required a much longer time for nylon (785 sec) than for acetate (234 sec). This is due to the essentially higher elastic recovery of nylon shown in Figure 8*A* and *B*.

The time necessary to perform 50 cycles in the Instron Tensile Tester cannot be obtained from the recovery behavior of the yarns shown in Figure 5. The immediate elastic recovery demonstrated took place more rapidly than the recovery in the Instron Tester during the unloading cycle, and the delayed elastic recovery was obtained for a relaxation time of 300 sec. This was much longer than the time in the unloading cycles (between 2.1 and 9.5 sec). The time necessary to perform 50 cycles could be estimated, however, from the recovery observed in the first unloading cycle at the conditioning level. This recovery value is somewhere between immediate and delayed elastic recovery and can be termed "cycling recovery." It is readily available from the recovery tests performed to obtain the data demonstrated in Figure 5. A comparison of estimated and observed cycling times (columns 17 and 18 in Table VI) shows, however, that the times actually observed are, without exception, shorter than the estimated times (56–90% of the estimated times). This can be explained by the fact that the cycling time was obtained from the recovery after one extension, while

TABLE V. Work Components *

No.	Designation	Actual Values (in g-cm/gx for 1 m fiber length) Immediately Recoverable Work	Creeping Recoverable Work	Unrecoverable Work	Total Work of Rupture	Relative Values (in per cent of total work of rupture) Immediately Recoverable Work	Creeping Recoverable Work	Unrecoverable Work
1	Fiberglas ESE 31/1	0.45	0.41	0.08	0.94	48	44	8
2	Kuralon 80/2	1.6	6.9	4.3	12.8	12	54	34
3	Orlon 16/1	1.9	8.8	4.3	15.0	12	59	29
4	Saran 16/1	1.2	3.4	0.4	5.0	24	68	8
5	Viscose 20/1	1.5	2.3	8.5	12.3	12	19	69
6	Fibravyl 75/1	2.1	6.8	6.6	15.5	13	44	43
7	Kuralon 40/1	1.4	5.1	9.0	15.5	9	33	58
8	Acetate 20/1	0.9	1.9	11.0	13.8	7	14	79
9	Nylon 60/1	2.6	11.1	6.5	20.2	13	55	32
10	Orlon 15/1	2.3	7.0	13.6	22.9	10	31	59
11	Dacron 29/2	2.7	6.5	19.8	29.0	9	23	67
12	Dynel 20/1	1.2	4.6	13.3	19.1	7	24	69
13	Nylon 30/2	2.1	16.4	17.1	35.6	6	46	48
14	Dacron 20/1	2.5	7.1	29.4	39.0	6	18	76
15	Dacron 60/2	4.6	7.0	45.2	56.8	8	12	80
16	Thermovyl 30/1	1.1	2.1	5.3	32.1	3	11	86

* Based on uncorrected tenacities and demonstrated in Figure 9*A* and *B*.

it was observed during 50 extensions. The recovery of yarns improves in cycling in that an increasing portion of the elongation recovers at a more rapid rate. Besides this, the permanent deformation also increases in each cycle, and this additional portion of the elongation need not be extended in subsequent cycles. Both factors noticeably shorten the times necessary for extending the yarns to a required elon-

TABLE VI. Cycling Tests and

		1	2	3	4	5	6	7	8	9	10
		Before Cycling					After Cycling				
No.	Designation	Yarn Fineness (grex)	Elong. at Break (%)	Load at Break (g)	Corrected Tenacity at Break (g/gx)	Total Work of Rupture (g-cm/gx/m)*	Yarn Fineness (grex)	Elong. at Break (%)	Load at Break (g)	Corrected Tenacity at Break (g/gx)	Total Work of Rupture (g-cm/gx/m)*
2	Kuralon 80/2	144	11.2	351	2.72	13.5	139	7.7	337	2.62	8.9
3	Orlon 16/1	369	13.7	684	2.11	16.7	347	8.2	408	1.27	6.2
5	Viscose 20/1	296	16.2	373	1.47	13.6	270	5.4	378	1.47	4.7
7	Kuralon 40/1	146	20.0	210	1.73	17.7	132	9.0	222	1.83	8.6
8	Acetate 20/1	296	21.9	260	1.07	16.1	259	5.5	232	0.95	3.5
9	Nylon 60/1	98	22.0	217	2.70	24.4	93	17.5	205	2.59	20.0
10	Orlon 15/1	391	24.0	536	1.71	25.2	350	15.4	689	2.26	21.7
12	Dynel 20/1	296	27.5	325	1.40	22.4	254	10.1	302	1.31	7.7
13	Nylon 30/2	405	31.7	970	3.16	69.0	367	19.4	990	3.22	42.8
14	Dacron 20/1	295	38.5	567	2.67	49.0	239	11.7	579	2.70	18.6
15	Dacron 60/2	309	39.7	860	3.88	73.0	254	13.3	853	3.82	27.2

* Based on corrected tenacities and demonstrated in Figure 9.

gation level in cycling, and they explain the discrepancy between estimated and observed cycling times.

Length Increase

The most obvious change which occurs when viscoelastic fibers are extended above their yield point is the increase of fiber length due to permanent set. The recovery behavior shown in Figure 5 demonstrates permanent set values after a single extension up to the conditioning level. They permit at least the estimation of length increase in 50 cycles.[13] A comparison of estimated and observed length increases listed in columns 21 and 22 of Table VI shows that a somewhat higher fiber length (111–237% of the estimated value) was actually observed, indicating higher permanent set values in 50 cycles than those observed in a single loading cycle. This increase in permanent set is due partly to internal fine structural rearrangements (orientation) occurring in subsequent cycles and partly to slippage of individual staple fibers in the yarn structure. In the 16/1 Orlon yarn fiber slippage apparently occurred because an essential load decay took place during the cycling operation, and this did not diminish during the last cycles, despite the essentially lower tensions (597 g in the first, 316 g in the 50th cycle) to which the yarn was subjected. Fiber slippage in this yarn was also revealed by the markedly higher yarn length after cycling than that estimated from a single loading. In contrast to this behavior, a rearrangement in the fine structure (orientation) must have taken place during the cycling for the 15/1 Orlon yarn. This is evidenced by increased tenacity at break (stress hardening), apparent from the stress-strain curves of Figure 10. Any increase of yarn length is necessarily connected with reduced cross-section and grex. Altered yarn grex and length after cycling affect, of course, normalized values of stress and strain. The difficulties in comparing normalized stress and strain values correctly after the fibers have been extended were discussed in a previous paper [10]. In the present study, yarns after cycling were considered as new samples having new tensile properties and changed fiber length and fineness (grex), to which strain and stress values were respectively correlated.

[13] Immediately after cycling, the yarns are unstable [10] and a slight shrinkage (0.9–2.1%) takes place spontaneously. Therefore, increase of fiber length was referred here to a relaxation time of 1 hr.

Alteration of the Stress-Strain Properties

11	12	13	14	15	16	17	18	19	20	21	22	23	24	25
Details of Repeated Tensioning														
	Conditioning Load		Load Decay			Cycling Time (sec)				Length Increase (%)				
Cond. Elong. (%)	(a) Grams	(b) Per Cent of Ultimate	(a) Grams	(b) Per Cent of 12a	"Cycling Recovery" (%)†	(a) Estimated	(b) Observed	(c) Observed Per Cent of Estimated	Permanent Set at the Conditioning Level‡	(a) Estimated§	(b) Observed after 50 Cycles§,‖	(c) Observed Per Cent of Estimated	"Overall Extensibility" (%)§	Shrinkage (%)¶
9.0	253	72	39	15	4.5	432	390	90	24	2.2	3.5	159	11.5	1.0
11.0	597	87	316	53	4.7	452	285	63	25	2.7	6.4	237	15.1	1.3
12.9	315	85	67	21	3.5	335	234	70	58	7.5	9.5	127	15.4	1.0
16.0	183	87	45	25	5.1	490	362	74	47	7.5	10.1	134	20.0	1.3
17.5	234	90	54	23	3.7	356	234	66	68	11.9	14.4	121	20.7	0.9
17.6	156	72	30	19	11.9	1141	785	70	17	3.0	5.2	173	23.6	1.4
19.2	436	81	131	30	6.0	576	324	56	44	8.4	11.9	142	29.1	2.1
22.0	267	82	94	35	6.5	624	363	58	54	11.8	16.6	141	28.4	1.5
25.4	803	83	160	20	15.8	1518	1095	72	26	6.6	10.5	159	31.9	1.5
30.8	436	77	86	20	7.1	681	444	65	65	20.0	23.1	116	37.5	1.4
31.7	661	77	104	16	8.0	767	600	78	64	20.3	22.6	111	38.9	1.4

† Actual values from the first recovery cycle at the conditioning level.
‡ Relative values shown in Figure 5.
§ Correlated to the original fiber length before cycling.
‖ Length increase measured after 1 hr relaxation.
¶ Shrinkage in 1 hr correlated to the original length before conditioning.

Stress-Strain Relationship

The extensibilities listed in column 7 of Table VI were obtained from the stress-strain curve after cycling and are expressed as percentage of the new length. Besides the new extensibility, the overall extensibility is also listed (column 24) in Table VI. The overall extensibility is the sum of the length increase during cycling and the elongation occurring after the cycling procedure. It is expressed as percentage of the original fiber length. Calculation of the overall extensibility was thought to be necessary to learn whether the cycling affected the total extensibility of the yarns tested.

Tenacity values of Figure 10*B* and Table VI were normalized to the diminishing grex during the stretching procedure. These corrected tenacities have the advantage of permitting a meaningful evaluation of any real strengthening or weakening of fibers due to stretching. They are more realistic than uncorrected values because the grex does not remain unchanged during stretching.

Figure 10*B* shows that the shape of the stress-strain curve is in most cases markedly altered after cycling. With the exception of 16/1 Orlon, the yarns have a slightly higher modulus after cycling and the yield point is generally less pronounced. The two nylon yarns are the only exception because their first yield point became more pronounced. In some cases (e.g., 30/2 nylon and 20/1 and 60/2 Dacron) a new yield point appears close to the breaking point. This "second yield point" depends upon the conditioning level and indicates the unaffected end portion of the original curve.

The extensibility after cycling is always markedly lower than originally (30–80% of the original). This is the result of eliminating the permanent set. The decrease was relatively slight for 60/1 nylon and 80/2 Kuralon (80 and 69% of the original). Decrease in extensibility was most pronounced for the 20/1 acetate (25% of the original) and the 20/1 and 60/2 Dacron yarns (30 and 34%). Even these essential diminutions occurred, however, without marked alteration of the total extensibility. The values of overall extensibility (column 24, Table VI) remained practically identical with the original elongation (column 2) for all the yarns tested except for the 16/1 and 15/1 Orlon yarns. The breaking tenacities of most yarns after cycling are also almost identical to the corresponding original values when corrected tenacities are compared. The resistance to tension is thus not much affected by even such a severe treatment as 50 extensions to a point fairly close to rupture. There are only two notable exceptions to this rule: 16/1 and 15/1 Orlon. The marked weakening (fatigue) of 16/1 Orlon is the result of insufficient fiber-to-fiber friction. The low twist (6 turns per inch) of this yarn allows fiber slippage evidenced by marked stress decay, considerably increased fiber length, and overall extensibility. In contrast to this behavior, an increased tenacity at break (stress hardening) was observed for 15/1 Orlon (having a twist of 14 turns per inch) due to orientation during the cycling procedure.

The energy absorption of the yarns tested decreased after cycling, the total work of rupture remaining between 8.9 and 42.8 g-cm/gx/m (column 10, Table VI) as compared to original values between 13.5 and 73.0) g-cm/gx/m.[14] This diminished resistance to destruction indicates some fatigue of all the yarns tested. The fatigue was slight for the 16/1 Orlon yarn, due to a compensation by stress hardening, and for the highly elastic fibers—60/1 nylon, 80/2 Kuralon, and 30/2 nylon. The largest decrease in energy absorption was found for the acetate yarn (to 22% of its original value) as a result of markedly reduced extensibility and slightly diminished breaking tenacity.

Figure 10*B* also shows that the variation of the breaking point after cycling generally remains similar to the original. In some cases, however, an enhanced or diminished variation was found either in respect to tenacity or extensibility, or both.

The behavior of staple yarns during and after cycling is not essentially different from that of multifilaments [10], where unchanged tenacity and decreased new extensibility and work of rupture were frequently observed with little influence on the overall extensibility. Marked alterations in the shape of the stress-strain relationship, increase or decrease of the initial modulus, and appearance of new yield points are also familiar phenomena for multifilaments after they have been extended.

The behavior of the 16/1 Orlon yarn demonstrates strikingly the usefulness of cycling tests. The stress-strain relationship, breaking tenacity, and total en-

[14] These energy values are somewhat higher than the corresponding values listed in Table II (12.8–56.8 g-cm/gx/m) because they are derived from corrected tenacities and these are always higher than uncorrected tenacity values.

ergy of rupture, and even the recovery behavior including elastic work components of this sample do not indicate a low fatigue resistance. The marked deterioration of fiber quality due to excessive fiber slippage was clearly evidenced, however, after the yarn was subjected to repeated tensioning.

Dynamic tests were also informative for the two Kuralon yarns. It is known that resistance to tensional stress generally prevents damage by abrasion. As stated by Hamburger [4], some correlation exists between abrasion resistance and high elastic energy absorption in tension. Testing different samples of cotton, nylon, Dacron, Orlon, and Kuralon spun yarns, it was shown [11] that the flex-abrasion resistance to cotton, nylon, Dacron, and Orlon was lower for the less recoverable, and more extensible, yarn. Higher flex-abrasion resistance was observed, however, for the more recoverable and less extensible 80/2 Kuralon than for the 40/1 yarn, using the Stoll-Quartermaster Tester but not the Walker Abrader.[15] Apparently a too low extensibility and a poor transverse resistance is critical for the rather severe abrasive tests using the Stoll-Quartermaster Tester.

Tensional fatigue tests performed in this study show a slightly decreased corrected tenacity for the 80/2 sample after cycling while that of the 40/1 yarn increased, apparently as a result of stress hardening. The relatively low resistance of the 80/2 yarn to flexing and to frequently repeated tensile deformations under severe conditions is due to an "overstretching" in producing or processing the fiber. This is also evidenced by poor resistance to forces acting perpendicular to the fiber length, which is not apparent in conventional tensile tests but becomes evident in knot tests.[16]

Summary

The investigation of spun yarns demonstrates the similarities and differences in the tensile behavior of man-made and synthetic staple yarns compared to multifilaments containing the same fiber material. Energy absorption values have been determined, differentiating between three energy components. Only repeated deformation can reveal those tensile characteristics of fibers which are important for their performance in service where they are subjected to frequent stresses and strains under widely varied conditions. Evaluation of yarn properties must not, therefore, be limited to those observed in the first deformation process, but should include their alterations after the yarns have been extended. If the tensile recovery behavior of viscoelastic fibers is known, some alterations which occur in repeated tensioning may be estimated.

Acknowledgment

Sincere gratitude is expressed to Drs. S. J. Kennedy and S. D. Bailey, Research Directors, Quartermaster Research and Development Command, for their interest in this study.

The authors are greatly indebted to the firms listed in Table I for their cooperation in furnishing the samples tested, including their characteristics. The permission of the Owens-Corning Fiberglas Corporation, New York City, to reproduce Figure 1 is also gratefully acknowledged.

Thanks are also due to Mrs. G. Buri and Mrs. V. Rivlin for reviewing this paper and to Mr. J. Salmon and his assistants of the Quartermaster Research and Development Laboratories, Philadelphia, Pa., for the preparation of the figures.

Literature Cited

1. Abrams, E., and Whitten, H. P., "Abrasion Resistance of Multifilaments and Staple Yarns on Modified Walker Abrader," TEXTILE RESEARCH JOURNAL **24**, 980–989 (1954).

1a. American Society for Testing Materials, "Recommended Practice for Designation of Linear Density of Fibers, Yarns and Other Textile Materials in Universal Units (D861–52)," in *A.S.T.M., Standards 1952*, Philadelphia, Pa., Part 7, p. 133 (January, 1953).

2. Anon., "Vinylon from Japan, a New Synthetic Fiber," *Textile World* **101**, 123, 232, 233 (April, 1951).

3. Bogarty, H., Sookne, A. M., and Harris, M., "The Felting of Wool as Related to the Elastic and Swelling Behavior of the Fiber," TEXTILE RESEARCH JOURNAL **21**, 822–826 (1951).

[15] The flex abrasion damage of 80/2 Kuralon was 13.7 times higher, while for the 40/1 Kuralon it was only 11.5 times higher than that of a nylon multifilament using the Stoll-Quartermaster Abrasion Tester. Using the Walker Abrader, the abrasion resistance (based on cycle numbers at break) of the 80/2 and 40/1 Kuralon yarn was in the ratio of 21 to 108 under comparable conditions. (See Table VII, Abrams and Whitten [1].)

[16] The relative knot tenacity and extensibility of the 80/2 Kuralon yarn are definitely lower (63 and 82%) than those of the 40/1 yarn (89 and 90%).

4. Hamburger, W. J., "Mechanics of Abrasion of Textile Materials," TEXTILE RESEARCH JOURNAL **15**, 169–177 (1945).
5. Hindman, H., and Burr, G. S., "The Instron Tensile Tester," *Trans. Am. Soc. Mech. Engrs.* **71**, 789–796 (1949).
6. Kaswell, E. R., *Textile Fibers, Yarns, and Fabrics,* Reinhold Publishing Corporation, New York, N. Y. (1953).
7. Mouchiroud, G., "The Blending of Polyvinyl Chloride Fibers with Other Fibers," *J. Textile Inst.* **43**, 466–472 (1952).
8. Sen, K. R., "Analytical Study of Hairiness of Yarns," *Indian Textile J.* **62**, 300–304 (1952).
9. Susich, G., and Backer, S., "Tensile Recovery Behavior of Textile Fibers," TEXTILE RESEARCH JOURNAL **21**, 482–509 (1951).
10. Susich, G., "Mechanical Conditioning of Textile Fibers," TEXTILE RESEARCH JOURNAL **23**, 545–572 (1953).
11. Susich, G., "Abrasion Damage of Textile Fibers," TEXTILE RESEARCH JOURNAL **24**, 210–228 (1954).
12. Tomonari, T., "Synthetic Fibers of Japan," Chapter 9, pp. 234–250 in McFarlane, S. B., *Technology of Synthetic Fibers,* Fairchild Publications, Inc., New York, N. Y. (1953).

Manuscript received March 22, 1955.

The Thermal Insulation of Caribou Pelts[1]

Irene Moote[2]

Abstract

The thermal insulation of samples of three caribou pelts, six other pelts, and one pile fabric was measured in still air and in winds up to about 26 mph. In still air the values, including ambient air layer, ranged from 2.0 clos for the pile fabric to 5.4 clos for the winter caribou. In a 25-mph wind the insulation afforded by most of the samples dropped to about 50% of the still-air value; notable exceptions were winter caribou, which dropped to only 58%, and winter deer, which dropped as low as 38%.

Introduction

The study of arctic clothing has of recent years become a subject of some importance, and it is natural that those who were first interested in this field of investigation should have attached considerable significance to the means by which the Eskimo clothed himself to face the elements, namely, the caribou skin. A certain school of thought arose which believed that caribou clothing had exceptional qualities extremely difficult if not impossible to duplicate by other means.

The work described in this communication was undertaken to decide whether caribou really did differ particularly from any other skin which was thickly covered with hair or if availability was the reason for its use by the Eskimo. The investigation therefore was not planned with a view to comparing the thermal insulation required by different animals in different climates, which is of course a subject of great interest to biologists [9]; the aim of the work was rather to find out if caribou skin used as a material for garments was superior to any other kind of fur.

The investigation comprised essentially the measurement of the thermal conductance of the various samples in still air and in winds up to about 26 mph, with the hair side of the pelt in the wind. The thickness and weight of each sample were measured later in order to aid in the general assessment of caribou as an insulator.

Methods

The hot-plate apparatus used for measuring the thermal conductances was similar to that described by Cleveland [2]. It was constructed by the Textile Section, Division of Chemistry (N.R.C., Canada), and has been described by Larose [7]. It

[1] Contribution from the Division of Physics, National Research Laboratories, Ottawa, Canada. Issued as N.R.C. Report No. 3740.

[2] Physicist, at present at S. Mildred's College, Toronto.

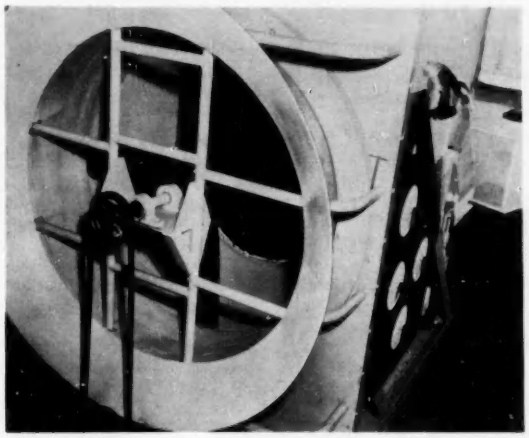

Fig. 1. Full-length view of wind tunnel, showing fan, controls for regulating speed of fan, outlet of tunnel above the apparatus, and the wind screen for still air tests.

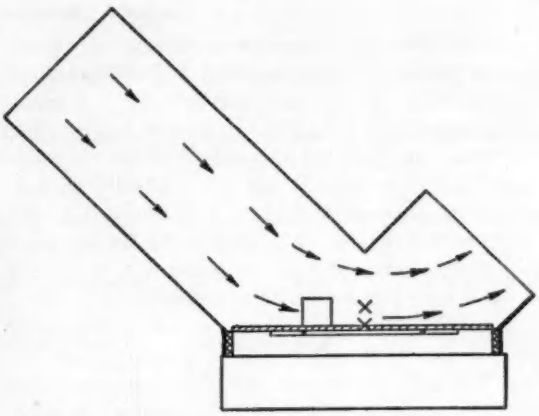

Fig. 2. Longitudinal section of that part of the wind tunnel over the apparatus, showing the air flow over the sample, the anemometer at one station, and the thermocouples at the surface of the sample and in the air above it.

consisted, briefly, of an electrically heated brass plate 10 in. square surrounded by a 2-in. guard ring with a lower plate to prevent heat flow downward. Thermocouples on the central plate, guard ring, and lower plate enabled the operator to keep the guard ring and lower plate to within 0.02°C of the central plate, while the latter was held at a temperature of around 37°C.

The apparatus stood in a wind tunnel, a photograph of which is shown in Figure 1. The wind was generated by a powerful 36-in. fan running in the cylindrical part of the tunnel, and air was forced into a rectangular cross-section 22½ in. wide by 12 in. deep, which was arranged at an angle of 45° to the surface of the plate, as illustrated in Figure 2. The fan was driven by a dc motor and speeds could thus be varied from 5 to 26 mph. To measure the wind velocity a Negretti and Zambra vane anemometer was used. It was placed on the surface of the sample at five positions, shown by circles in Figure 3. The average of the readings was taken as the wind-velocity value. The crosses in Figure 3 indicate the positions of the thermocouples.

Since very slight air movement in a "still air" measurement of conductance makes an appreciable change in value, special provision had to be made to shield the sample from draughts. The last portion of the wind tunnel was therefore constructed to lift off and permit a wooden frame covered with two layers of cheesecloth to be placed over the plate.

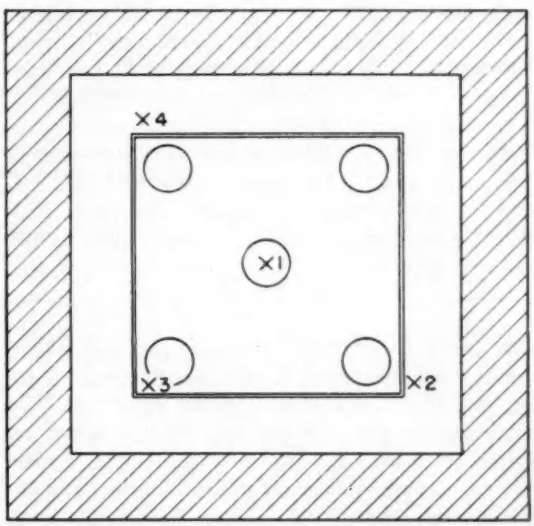

Fig. 3. Top view of the apparatus showing by crosses the positions of the thermocouples in the hot plate and guard ring and by circles the five stations for measuring wind velocity.

This screen can be seen in Figure 1, standing near the hot plate but not in use. The room in which the wind tunnel was situated was controlled at approximately 75°F.

Since there are wide differences in the thermal insulation values of caribou skins, three samples

TABLE I. Description of the Fur Samples

Type of Fur	Part of Pelt Used	Skin	Hair Structure	Hair Density
Caribou (Winter)	Neck and back	Chrome tanned, thick	Cellular and brittle, fairly coarse,	Very great
Caribou (Summer)	Back and flank	Untanned, a bit stiff, thinner than winter caribou	Cellular, not brittle and finer	Somewhat less than that of winter caribou
Caribou (Thin summer)	Back and flanks	Untanned, quite stiff, not flat, very thin	Cellular, not brittle and finer	Less than summer caribou
Deer (Winter)	Back	Chrome tanned, thick	Cellular, brittle and coarse	About half that of winter caribou
Arctic Wolf	Back and flanks	Tanned, quite thin and soft	Solid, not brittle, guard hairs coarse, underfur soft and fine	Guard hairs not very dense, underfur very dense
Raccoon	Back and flanks	Commercially tanned and stitched	Solid, guard hairs coarse, underfur soft and fine	Guard hairs not very dense, underfur very dense
Beaver	Back and flanks	Commercially tanned, very soft and thick	Solid, both guard hairs (very few) and underfur sheared	Underfur very dense on flanks, much less dense on back
Muskrat	Back and flanks of four pelts	Commercially tanned and stitched together	Solid, guard hairs less coarse, and underfur very soft and fine	Less dense than the other furs
Rabbit	Many small pieces	Commercially tanned and stitched together	Solid, no guard hairs, underfur sheared and dyed black	Same as muskrat
Pile fabric		Cotton ground fabric	Single mohair pile woven on ground fabric	50 tufts per square inch

were taken, a winter pelt, a summer pelt, and a light summer pelt presumably from a young animal. Taking several samples of each of the other furs was not important provided that pelts from a variety of species were used and provided the sample of each was of normal commercial grade. These pelts included deer, arctic wolf, raccoon, beaver, muskrat, and rabbit. The beaver was sheared and lacked the guard hairs; the rabbit was sheared and dyed black and actually came off an old worn coat. A sample of mohair pile fabric was included in the tests. Some details of the actual samples used are given in Tables I and II.

A sample for test was placed, with the fur side upward, flat on the hot plate and tacked in position, usually with the hair pointing downwind. One thermocouple was placed near the center of the surface of the sample and another one in the air $1\frac{1}{2}$ in. directly above it. This height seemed reasonable since Larose [7] found that the temperature of the ambient air layer did not vary significantly from heights of 0.6 in. to 8.0 in. above the surface. Thermal equilibrium was considered to have been reached if, with constant current in the central plate circuit, no appreciable change was observed in No. 1 thermocouple for a period of 1 hr. The conductance could then be calculated from the equation

$$C = \frac{I^2R}{JA(t_1 - t_2)}$$

where I and R are respectively current and resistance of central plate; J, the mechanical equivalent of heat; A, area of central plate; t_1, the temperature of the central plate; and t_2, the temperature either at the surface of the sample or $1\frac{1}{2}$ in. above, depending on whether the resistance of the ambient air film

TABLE II. Some Physical Properties of the Fur Samples

Type of Fur	Thickness in Inches under Pressure of 0.10 lb/in.²	Thickness in Inches under Pressure of 0.0 lb/in.²	Weight (oz)	Length of Hair (in.) Guard	Length of Hair (in.) Underfur
Caribou (Winter)	1.13	1.29	15.2	—	2.0
Caribou (Summer)	0.30	0.47	7.8	1.8	0.7
Caribou (Thin summer)	0.22	0.29	5.3	1.6	0.5
Deer (Winter)	0.82	0.94	12.5	—	2.2
Arctic Wolf	0.47	1.08	9.3	3.6	1.3
Raccoon	0.24	0.52	9.3	2.3	1.2
Beaver	0.31	0.66	10.0	0.6*	0.6*
Muskrat	0.13	0.27	7.1	1.5	0.7
Rabbit	0.17	0.37	8.6	0.6*	0.6*
Mohair Pile Fabric	0.42	0.50	11.2	0.5	0.5

* Hair sheared to an even length.

was to be excluded or included. When the heat is measured in calories, the temperature in degrees centigrade, the area in square meters, and the time in seconds, the thermal resistance (R) in clo units [6] can be calculated directly from the equation $CR = 1.543$.

Results and Discussion

In plotting the results resistance rather than conductance values have been used. Figures 4 and 5 show resistance plotted against wind velocity when the ambient air film is included. Winter caribou is clearly shown to be the best of all the samples tested. However, Figure 5, in which the three caribou samples are compared, shows that summer caribou is only about half as good as winter caribou. Comparing the two diagrams it is easy to see that summer caribou only rated about as high as sheared beaver while the light summer caribou was about as good as muskrat. The comparison of caribou with deer in Figure 4 is of interest, because the resistance values in still air differed only slightly, but in wind the pelt of the forest animal was much inferior to the pelt of the animal of wind-swept arctic wastes. By examining the pelts one can see quite easily why this is so: the caribou hair stands up like soft close-packed bristles, while the hair on the deerskin can be pressed down with the hand much more readily. Raccoon and arctic wolf both turned out to be better than summer caribou.

In Figure 6 the effect of wind on the ambient air layer is illustrated. Broken lines refer to resistance calculations excluding the air layer and solid lines, those including the air layer. As one might expect, the air layer exerts a negligible effect at high wind velocities. It is at low wind velocities that the air layer is important, and some rather puzzling results were obtained, indicating a rise of resistance with wind velocity if the velocity was low and the resistance excluded the air layer. This effect was quite pronounced for a sample of raccoon measured with the fur lying "upwind." All the other samples referred to in Figure 6 were measured with the fur

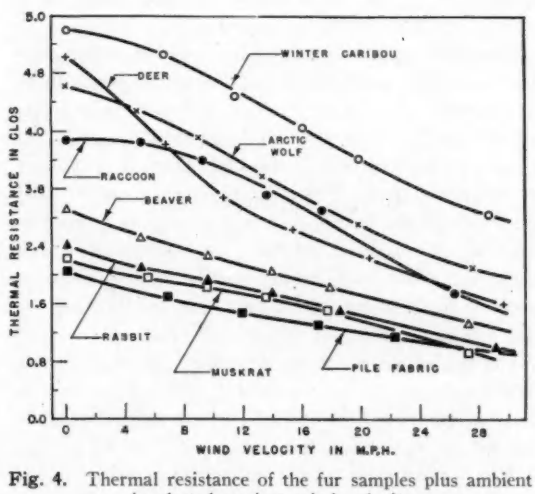

Fig. 4. Thermal resistance of the fur samples plus ambient air plotted against wind velocity.

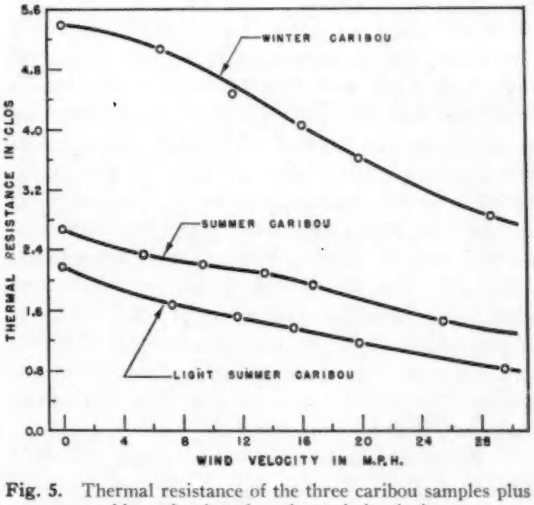

Fig. 5. Thermal resistance of the three caribou samples plus ambient air plotted against wind velocity.

lying downwind. The author suggests that the explanation of this finding is that the wind blows the hair out so that the depth of the fur is actually increased and the thermocouple is then below the surface. Too definite conclusions must not, however, be drawn about this rather academic point, since the exact position of the surface of an unsheared fur is somewhat indefinite.

While the graphs in Figures 4 and 5 give a fairly good estimate of caribou, there are some special aspects which possibly warrant consideration in making a comparison with other furs: namely, (a) the effect which wind has in decreasing thermal resistance, (b) the thermal resistance when thickness is taken into account, and (c) the thermal resistance when weight is taken into account.

a. The effect of wind in decreasing the insulation of a fur can be judged superficially from the slopes of the graphs. Table III gives this comparison in actual figures and shows that winter caribou stands out as superior to any of the others; winter deer is very poor.

b. When thickness is taken into account, Table IV indicates that caribou should be rated as poor. Of course, it must be conceded that the measurement of thickness is difficult and an error in this factor can give a misleading impression, but the evidence that caribou is superior to other furs on this basis of comparison is certainly lacking.

It is of interest to note in passing that the average of the nine natural fur samples which were tested gives a figure of 4.4 for the clo value per inch of pelt thickness using an uncompressed thickness value. The average of clo values per inch found by several investigators [3, 4, 8] for the resistance of fabrics when the thickness was measured under a pressure of 0.1 lb/in.^{2} is about 4. Using thickness values measured under 0.1 lb/in.^{2} pressure in the calculations for the furs led to impossible values for muskrat and raccoon, which were much higher than the value for still air at 25°C given by Fourt and Harris [5] at 6.8 clo/in. The ruling of the Canadian Government Purchasing Standards Committee [1] that thickness of pile fabrics should be measured under 0.10 lb/in.^{2} pressure cannot then be applied to furs unless the thermal conductivity tests are also to be carried out under a 0.10 lb/in.^{2} pressure.

c. When weight is taken into account the third column of Table V again fails to show any superiority for caribou. The figures in this column were

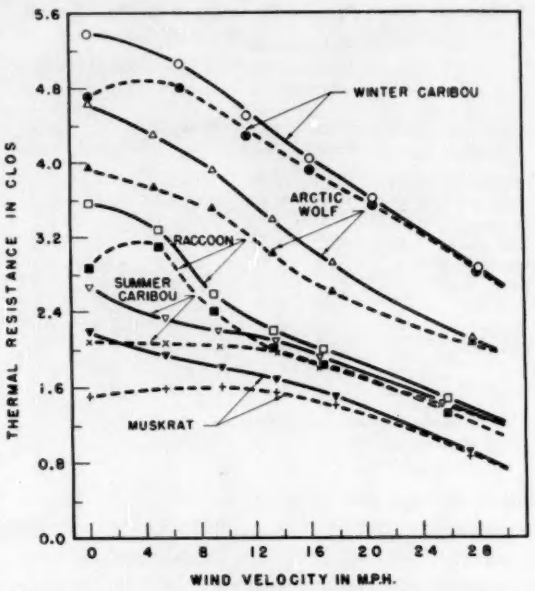

Fig. 6. Comparison of the thermal resistance of the sample only and of the sample plus the ambient air for five of the furs.
○——○ Thermal resistance of sample plus ambient air vs. wind velocity.
●- - - -● Thermal resistance of sample only vs. wind velocity.

obtained by dividing the clo value by the weight per square yard, and they give a measure of the insulation which a wearer gets for the weight of clothing he carries. In the fourth column of the table percentage of fur to total weight of hide plus hair is given: caribou shows up poorly.

Altogether these more specific ways of rating caribou with the exception of (a) fail to demonstrate its superiority over other pelts. Where caribou has special quality is in the wind-resistant nature of its close-packed hair and in the high thermal resistance of the winter pelt. Since, however, Stefansson [10] distinctly states that Eskimos prefer pelts from animals killed in July, August, or September rather than in the last three months of the year one cannot account for the use of caribou skin for clothing by the insulation value of the winter pelt.

On the whole the work described above leads one to the conclusion that availability rather than superiority accounts for the use of caribou skins for clothing by the natives of the Arctic.

The exceptional wind resistance of caribou fur which this investigation has brought to light is a

TABLE III. Ratio of Thermal Resistance in Following Wind Velocities to the Thermal Resistance in Still Air in Per Cent

Type of Fur	10 Mph	25 Mph	30 Mph
Caribou (Winter)	89	58	50
Caribou (Summer)	81	55	47
Caribou (Thin summer)	72	44	37
Deer (Winter)	64	38	32
Arctic Wolf	83	50	42
Raccoon	90	49	40
Beaver	78	50	41
Muskrat	82	50	33
Rabbit	79	50	42
Pile Fabric	78	51	42

TABLE IV. Thermal Resistance per Unit Thickness

		Under Pressure of 0.0 lb/in.²	
Type of Fur	Resistance* in Clos	Thickness (in.)	Clo/in.
Caribou (Winter)	4.72	1.29	3.7
Caribou (Summer)	2.09	0.47	4.5
Caribou (Thin summer)	1.33	0.29	4.6
Deer (Winter)	4.33	0.94	4.6
Arctic Wolf	3.94	1.08	3.7
Raccoon	3.09	0.52	5.9
Beaver	2.23	0.66	3.4
Muskrat	1.51	0.27	5.6
Rabbit	1.37	0.37	3.7
Pile Fabric	1.50	0.50	3.0

* Thermal resistance in still air of sample only.

point of interest in the design of pile fabrics because apparently for good wind resistance the hair must be close packed and moderately stiff. From a purely utilitarian viewpoint where it is not necessary to simulate fur in appearance, wind resistance can be far more easily accomplished by means of a thin flexible windproof fabric on the outside of the insulation.

Acknowledgment

The author wishes to make grateful acknowledgment to Dr. C. D. Niven under whose direction this work has been carried out and who has given helpful criticism in the writing of this paper.

TABLE V. Thermal Resistance per Unit Weight

Type of Fur	Resistance* in Clos	Weight (oz/yd²)	Clo/oz/yd²	Weight of Fur (% of total weight)
Caribou (Winter)	4.72	52	0.091	48
Caribou (Summer)	2.09	26	0.080	44
Caribou (Thin summer)	1.33	17	0.078	39
Deer (Winter)	4.33	42	0.103	56
Arctic Wolf	3.94	31	0.127	66
Raccoon	3.09	32	0.097	61
Beaver	2.23	34	0.066	41
Muskrat	1.51	24	0.063	51
Rabbit	1.37	29	0.047	52
Pile Fabric	1.50	38	0.039	49

* Thermal resistance in still air of sample only.

Literature Cited

1. *Canadian Government Purchasing Standards Schedule of Methods of Testing Textiles,* No. 4-GP-2-1947.
2. Cleveland, R. S., *J. Research Natl. Bur. Standards* **19**, 675–684 (1937).
3. Clothing Test Methods, *Committee on Aviation Medicine Report 390,* National Research Council, Washington, p. 91 (1945).
4. Cochrane, M. I., and Siple, P. A., *Principles of Environmental Stress on Soldiers,* Research and Development Branch, Office of the Quartermaster General, Washington, pp. 15–16 (1944).
5. Fourt, L., and Harris, M., in *Physiology of Heat Regulation and the Science of Clothing,"* edited by L. Newburgh, W. B. Saunders Company, Philadelphia, pp. 300–301 (1949).
6. Gagge, A. P., Burton, A. C., and Bazett, H. C., *Science* **94**, 428–430 (1941).
7. Larose, P., *Can. J. Research* **A25**, 169–190 (1947).
8. Schiefer, H. F., Stevens, H. T., Mack, P. B., and Boyland, P. M., *J. Research Natl. Bur. Standards* **32**, 261–284 (1944).
9. Scholander, P. F., Walters, V., Hock, R., and Irving, L., *Biol. Bull.* **99**, 225–236 (1950).
10. Stefansson, V., *Arctic Manual,* The MacMillan Company, New York, p. 248 (1944).

Manuscript received April 27, 1955.

Mechanics of Elastic Performance of Textile Materials

Part XII: Relation of Certain Geometric Factors to the Tear Strength of Woven Fabrics[1]

N. A. Teixeira, M. M. Platt, and W. J. Hamburger[2]

Fabric Research Laboratories, Inc., Boston, Massachusetts

Abstract

Tongue-tear tests were made on samples of acetate fabrics, varying certain controlled factors: weave, texture, yarn twist, and yarn structure. An analysis of the resulting experimental data showed certain relationships between these fabric factors and tear strength. A qualitative discussion was made of tearing action—the influence on tear strength of various types of fabric distortion at or near the tear such as yarn pull-out force, crimp, cover factors, and dimensional stability in the plane of the fabric. Then the relationships between these types of distortion and the variable fabric factors were examined. The actual "mechanism of tear" in the tongue-tear test was theoretically investigated from the nature of the frequency distribution of load drops through the geometry of the tear structure to the synthesis of the tear diagram. Then the effects of the tails and the untorn fabric were studied; finally, all components were studied together.

I. Introduction

As our knowledge of the structure and behavior of fibers increases, the translation of their properties into those of yarn and fabric constructions becomes ever more important. Various laboratory tests have been developed and used to determine the ability of fabric structures to utilize the strength of the component yarns. In order to study the effect of geometry of woven fabrics on the utilization of yarn properties, the tests applied should yield results dependent on the very factors which differentiate a fabric from its component yarns.

The loading of the fabric should cause both a deformation and a resistance to this deformation more characteristic of the material as a fabric than of the sum of the properties of the yarns of which the fabric was constructed. Thus a strip-tensile test will not yield results which differ greatly from a test of the stressed yarns as a bundle since, if the crossyarns are removed after the specimen is in the jaws, the test may still be run and the results will not differ too much from those of the strip-tensile test. The grab test, on the other hand, is more dependent upon the crossyarns. A better test of the fabric would be one in which the weave and the entire structure are so important that removal of any one set of yarns will completely nullify the test. In the tongue-tear test, the fabric structure is essential, and neither warp nor filling yarn system could be removed without completely eliminating the test itself. This is not true of the trapezoid-tear test, for instance, since only the yarns held in the jaws and which have been loaded with predetermined elongation unbalance are important. If a very sleazy fabric is being torn, in the tongue tear, it is possible to have the fabric destroyed as a fabric without breaking any of the yarns.

Furthermore, since many service failures involve some sort of a propagated failure through the fabric structure, the results of tear tests can often be correlated with service tests. The following discussion on tear, therefore, will be based entirely on studies

[1] The preceding parts in this series appeared in the following issues of TEXTILE RESEARCH JOURNAL: I, February, 1948; II, December, 1948; III, January, 1950; IV and V, August, 1950; VI, October, 1950; VII, May, 1951; VIII, March, 1952; IX, October, 1952; X, November, 1952; XI, October, 1954.

[2] The authors gratefully acknowledge the sponsorship of this research by the Department of the Army, Office of the Quartermaster General, Research and Development Division; Textile, Clothing, and Footwear Branch. This work has also appeared as *Textile Series Report Number 86*, issued by the OQMG.

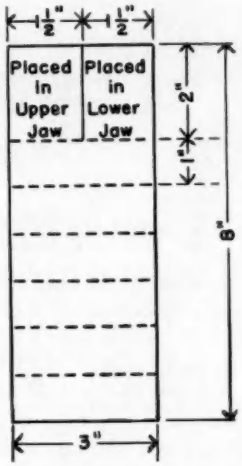

Fig. 1. Specimen of fabric.

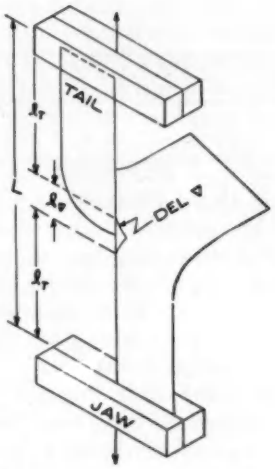

Fig. 2. Fabric in jaws of tensile tester.

of the tongue-tear testing of fabrics. The object of the work reported herein is twofold:

First, the mechanics of fabrics undergoing tongue tear will be investigated from a theoretical view to isolate those factors of fabric construction which seem to determine the tear strength and also to make test results in the tear testing of fabrics a little more intelligible.

Second, empirical results, obtained from tests on a series of fabrics with controlled form factors, will be presented and evaluated according to the conclusions drawn from the theoretical study.

II. Mechanics of Fabric in Tongue Tear

A. The Tongue-Tear Test

1. *Description of test.* In the tongue-tear test as performed in this investigation, a specimen 8 in. long and 3 in. wide was cut as shown in Figure 1. The dotted horizontal lines represent lines drawn 1 in. apart on the fabric. This specimen was then placed in the jaws of a tensile tester so that ½ the slit section was placed in the top jaw and ½ in the lower jaw, as shown in Figure 2.

Whenever possible, the length of tongue clamped in each of two 3-in. jaws was such that zero jaw separation resulted. (In a few cases the fabrics tore across parallel to the jaw when the tear was started so that 1 or 2 in. of initial jaw separation were required for the tear to progress normally down the middle of the specimen.)

The lower jaw was then moved downward at a constant speed. A strip chart recorder, with an indicating system capable of traversing the 10 in. of chart in 1 sec, recorded the load transmitted to the upper jaw.

As the tear reached each of the horizontal 1-in. marks, the pen which records the load was pipped to mark on the chart the end of 1 in. of tear.

The actual load-measuring system consisted of a bonded strain gage-type load cell with its amplifying equipment. This type of instrument, such as the Instron Tensile Tester, which was used here, is essential for proper study of tear, since the variations in load are much too fast to be measured with any of the high-inertia low-speed recording devices. Furthermore, the servo-controlled jaw speed establishes the elongation coordinate of the load-elongation diagram.

2. *Definitions.* The following definitions apply to Figure 2.

The del is the triangular shaped distortion at the active region of tearing, named (by Krook and Fox [3]) after the del operator used in vector analysis, "∇."

L = Total jaw separation
l_T = Length of each tail (unextended)
l_∇ = Length of the del

The following definitions apply to the load-elongation diagram obtained in tear, shown in Figure 3. P_u (called the "tear force") is the upper load limit

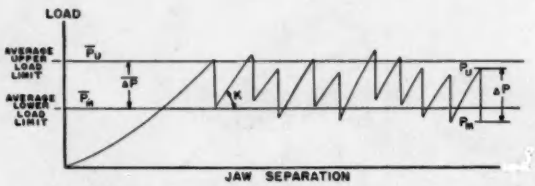

Fig. 3. Load-elongation diagram of tongue-tear test.

of each peak or the highest load supported before a yarn rupture. P_m is the lower load limit of each peak or the load on the jaws just after a yarn has ruptured. ΔP is the load drop resulting from the rupture of a yarn or yarns in a given peak. P_u/B.S. is the upper load limit of each peak divided by the breaking strength of the yarns being broken. This is called the "normalized tear force." E is the tear energy per inch of tear, usually calculated for the third inch of tear.

$$E \approx \frac{P_u + P_m}{2} \Delta L$$

where ΔL is the amount of jaw movement during the particular inch of tear for which the energy is being calculated. N is the number of peaks per inch of fabric torn. K is the effective spring constant of the specimen being loaded. This K can be resolved into components, as indicated by Figure 4.

The following definitions apply to Figure 4. $2K_T$ is the spring constant of one of the tails. K_T is the spring constant of both tails in series. K_f is the spring constant of the fabric being loaded in parallel with the del. K_∇ is the effective spring constant of the del. $K_o = K_f + K_\nabla$ is the spring constant of the specimen if the tails are of zero length. According to the rule for series springs:

$$1/K = (1/K_o) + (1/2K_T) + (1/2K_T)$$
$$= (1/K_o) + (1/K_T)$$

Let C_T be the spring coefficient of the tails; i.e., the force required to stretch a 1-in. length of tail 1 in. Then

$$K_T = C_T/2l_T$$

and

$$1/K = (1/K_o) + (2l_T/C_T)$$

or

$$K = (K_oC_T)/(C_T + 2K_ol_T)$$

Thus the plot of $1/K$ vs. $2l_T$ is a straight line with $1/K_o$ for the intercept at the axis of ordinates and a slope equal to $1/C_T$, assuming that $K_o = K_f + K_\nabla$ remains constant.

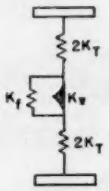

Fig. 4. Mechanical representation of tongue-tear specimen.

3. *Brief explanation of tearing action.* A schematic diagram of a specimen being torn is shown in Figure 5. When the lower jaw descends, the tails are loaded as springs in series until the crossyarns are pulled out and into the vertical plane as shown. Then, as these del yarns fail progressively *in tension*, the tails get longer and the fabric around the del becomes strained. When the tails get longer, they become more extensible and begin to extend and contract according to the discontinuous loading of the del. Each time one of the del yarns breaks, the drop in tension causes the tails to contract as the del jumps to the next configuration, and the associated energy of contraction may also cause the rupture of more yarns.

Krook and Fox proved that the crossyarns failed in tension and that the tearing was a result of a progressive tensile failure of the crossyarns rather than any shearing action perpendicular to the surface of the fabric.

B. *Outline of Theoretical Development*

In order to understand the tearing action and the sawtooth shape of the diagram, it is necessary to separate the action at the del from the action in the tails. At the jaws there is applied a constant rate of extension which strains the fabric and eventually causes tensile failure of the del yarns. The del, however, being composed of yarns with finite spacing, is loaded as a discontinuous function of its elongation. Because the rate of extension of the entire specimen is fixed, when the first del yarn (the longest yarn) breaks, the del does not extend as a simple parallel structure weakened by the loss of one component. Actually, there is a sudden discontinuous shift from one del structure to another, and the second del structure is at a lower load and the first yarn extended less than the corresponding amounts in the previous del at the time of the yarn rupture. When the new del structure is formed, a new point of equilibrium must be

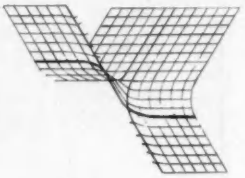

Fig. 5. Distortion of fabric structure in region of tear.

established between the tails, the del, and the fabric structure in parallel with the del. This mechanical readjustment will be analyzed in greater detail later in this paper. The contraction of the tails which takes place at this time is so fast and may exert so large a force on the del that another yarn is broken. This action is called snapback. The mechanism of snapback will also be described in greater detail in the body of this presentation.

Since the rupture of a yarn is a point of discontinuity in the loading of the del, there should be a peak, or discontinuous drop, in load in the tear diagram for each yarn broken.

If the peaks in the load-elongation diagram are counted in the length of chart corresponding to 1 in. of tear, the result is often less than the number of yarns per inch in the fabric. This apparent anomaly disappears if the individual load drops, or ΔP's, corresponding to the peaks, are measured. Some of the drops will be two or three times the size of others. Distribution studies, to be described later, show that some peaks represent the simultaneous rupture of two or more yarns. In this manner, however, all the yarns may be accounted for.

With each yarn accounted for in the tear diagram, the next step in the analysis is to investigate the del-shaped region where the tearing action occurs in order to determine the manner in which the yarns being ruptured are brought under load. Visual examination of specimens being subjected to tongue tear reveals the del to be an area bounded by two sides of seemingly hyperbolic curvature and a third straight side which coincides with the most elongated yarn. The yarns within the del are not evenly spaced and are actually the yarns perpendicular to the direction of tear. These yarns are under pure tension, and their length and spacing depend upon the del geometry, which is influenced by several parameters of the fabric, as will be discussed in the section on del structure.

Knowing the load-elongation characteristics of the yarns and the arrangement of the yarns in the del, it is possible to synthesize the load-elongation diagram of the del itself for a hypothetical fabric. This synthesis has been performed graphically and mathematically. To proceed from the load-elongation diagram of the del to the load-elongation diagram of the tear specimen itself necessitates the investigation of two other components of the fabric undergoing tear.

First, and most important, is the fabric structure being loaded in parallel with the del. The configuration and load-supporting properties of this fabric depend upon the same parameters that influence the shape of the del and very strongly affect the tear strength of the fabric.

The second component is formed by the two tongues or tails, which are mechanically in series with the del and the fabric around the del. The force required to tear a fabric is usually much lower than the tensile strength of a strip $1\frac{1}{2}$ in. wide, and at these loads the tails act practically as a linear spring whose spring constant is inversely proportional to the length of the tails. As mentioned above, these tails may control the number of yarns which break at one time.

It is possible to analyze the mechanics of this system of three components and determine the relationships between the loading at the del and the loading at the jaws. It is also possible to deduce some aspects of the distribution of load between the del and the fabric in parallel with the del, although it is not possible to determine directly the loading diagram of the paralleled fabric structure itself.

In this manner, the attempt will be made in the following section to develop, from the yarn properties and the fabric geometry, the load diagram of the fabric undergoing tongue tear.

C. The Frequency Distribution of Load Drops

Assuming one yarn break per peak in the load-elongation diagram of a tongue-tear test, the drop in load at the jaw should correspond to the loss in load-supporting ability of the del, after compensating for the elements in series and in parallel with the ruptured yarn. When the number of peaks in the length of chart corresponding to 1 in. of tear proved to be less than the number of yarns per inch in certain fabrics, each individual load drop was measured. These load drops, when plotted against the frequency of their occurrence, produced a double- or triple-humped frequency polygon. Furthermore, the second hump had a modal value of about twice that of the first hump and the third hump had a modal value of three times that of the first hump.

TABLE I. Corrected Values* for $\overline{\Delta P}$ and N

Plain-Weave Fabric No.	Twist (t.p.i.)	Actual Texture	Yarn B.S. (lb)	From Tear Diag. N†	From Tear Diag. $\overline{\Delta P}$‡ (lb)	From Dist. Curve N†	From Dist. Curve $\overline{\Delta P}$‡ (lb)
300AW		74	0.84	48	1.10	74	0.65
300AF		53	0.83	51	0.67	51	0.68
301AW	6	58	0.88	56	0.85	55	0.90
301AF		53	0.80	49	1.00	51	0.94
302AW		56	0.89	51	1.22	55	1.15
302AF		34	0.77	38	1.47	38	1.45
400AW		74	0.79	55	0.90	73	0.64
400AF		54	0.78	51	0.63	53	0.66
401AW	12	58	0.89	53	0.88	55	0.86
401AF		48	0.86	47	0.93	47	0.99
402AW		56	0.89	52	1.03	55	1.00
402AF		32	0.89	31	1.53	31	1.55
500AW		73	0.67	38	0.98	70	0.57
500AF		39	0.87	39	0.95	38	0.94
501AW	24	57	0.71	36	1.13	63	0.59
501AF		41	0.88	40	0.82	40	0.84
502AW		55	0.73	35	1.30	55	0.66
502AF		35	0.84	34	1.75	55	1.16

* Values are for third inch of tear.

† N = Number of peaks per inch of fabric torn.

‡ ΔP = Load drop resulting from the rupture of a yarn or yarns in a given peak; $\overline{\Delta P}$ = Mean of ΔP's in the third inch of tear.

Assuming that, in the case of a double-humped diagram, the second hump indicated the simultaneous rupture of two yarns, each load drop in the second hump was considered as two load drops of half the measured value and a new frequency polygon was plotted. The resulting modified distribution contained the same number of load drops as there were crossyarns in the fabric, thus accounting for all the yarns broken.

Table I shows the results of determining the frequency distribution of ΔP's for the plain-weave fabrics. This table lists the following: (1) The actual thread count of the yarns being torn; (2) the breaking strength of the crossyarns as determined from strip-tensile tests; (3) the uncorrected $\overline{\Delta P}$ as averaged on the chart; (4) the number of peaks per inch of tear counted on the chart; (5) the mean ΔP from the corrected frequency polygon; and (6) the number of equivalent peaks from the corrected frequency polygon.

A sample double-humped curve is shown in Figure 6, which also demonstrates how the original curve is corrected for double breaks.

Inspection of the data in Table I will show that the $\overline{\Delta P}$ is sometimes larger than the yarn breaking

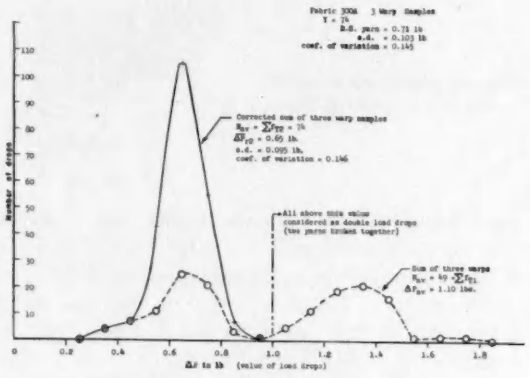
Fabric 300A 3 Warp Samples
Corrected sum of three warp samples
All above this value considered as double load drops (two yarns broken together)
Sum of three warps
Number of drops
ΔP in lb (value of load drops)

Fig. 6. Distribution of load drops.

strength and sometimes lower. The explanation of this fact will attend the analysis of the complete system including the untorn fabric and the tails, but, briefly, the answer lies in the fact that these two components act differently on the ratio between the ΔP and the yarn breaking strength.

The distribution of ΔP for 1 in. of tear is broadened by the gradual decrease in ΔP as the tear progresses. This decrease is related to the decrease in K_T as the tails lengthen.

The results of this work on the frequency distribution of ΔP in the tear-load diagram have been very useful in accounting for each yarn broken and in determining the effect on the jaw of each individual yarn.

D. The Geometry of the Del Structure

From observations on fabrics under tongue tear shown by Krook and Fox [3], a hyperbolic curvature was observed in the sides of the del. Visual inspection of the fabrics torn in these laboratories also revealed this curvature.

Based upon these observations, the following calculations were made, with expectations that the geometric form of the del might later serve in the analysis of the tearing action itself.

1. *General geometry of the del.* Assuming that the del is shaped as shown in Figure 7, then

h = Depth of del

l_∇ = Length of del

If the side from y_o to x_o is hyperbolic, then, since the displaced asymptotes are perpendicular, this must be a rectangular hyperbola. The equation of

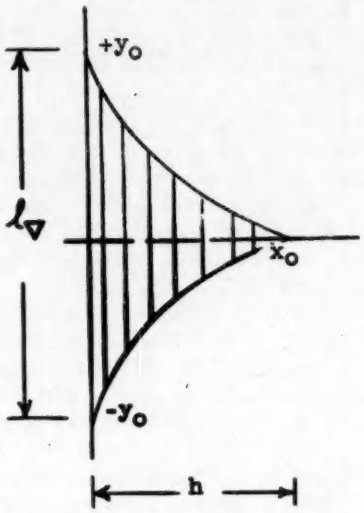

Fig. 7. Assumed shape of del.

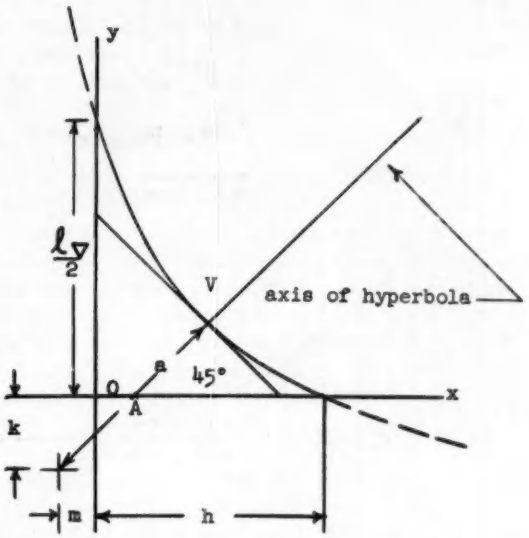

Fig. 8. Boundary geometry of the del.

a rectangular hyperbola with the asymptotes parallel to the coordinate axes and with its origin displaced by "k" from the x-axis and by "m" from the y-axis is

$$(y + k)(x + m) = \pm(a^2/2)$$

where a is the shortest distance from the point $(-m, -k)$ measured along the axis of the hyperbola, as shown in Figure 8.

For the positive quadrant only, the equation is

$$y + k = \frac{a^2}{2(x + m)}$$

For the entire del

$$\left[y = \pm\left(\frac{a^2}{2(x + m)} - k\right)\right]$$

where $0 < x < h$

$$\text{when } x = 0,\ y_0 = \left(\frac{a^2}{2m} - k\right) = \frac{l_\nabla}{2}$$

$$\text{when } y = 0,\ x_0 = \left(\frac{a^2}{2k} - m\right) = h$$

As an experimental check, this equation will be applied to data obtained from a fabric used by Krook and Fox.

In this fabric, $l_\nabla = 33$ and $h = 16.5$ (both measurements in arbitrary units). Since

$$\frac{l_\nabla}{2h} = \frac{\dfrac{a^2 - 2km}{m}}{\dfrac{a^2 - 2km}{k}} = \frac{k}{m}$$

and

$$l_\nabla/h = 2$$

then

$$k/m = 1$$

$$h = (a^2/2k) - m = 16.5$$

$$33k = a^2 - 2k^2$$

$$a^2 = 33k + 2k^2$$

Since $k = m$, point A in Figure 8 coincides with the origin, point O, and VO was measured as 7.5 units. Therefore

$$a = 7.5 + k\sqrt{2}$$

Substituting

$$(7.5 + k\sqrt{2})^2 = 33k + 2k^2$$

and

$$k = m = 4.77$$

$$a^2 = 33\ (4.77) + 2\ (4.77)^2 = 202.9$$

The equation then becomes

$$y = \pm\left(\frac{101}{x + 4.8} - 4.8\right) \qquad 0 < x < h$$

and is shown plotted in Figure 9 together with measured points along the curve.

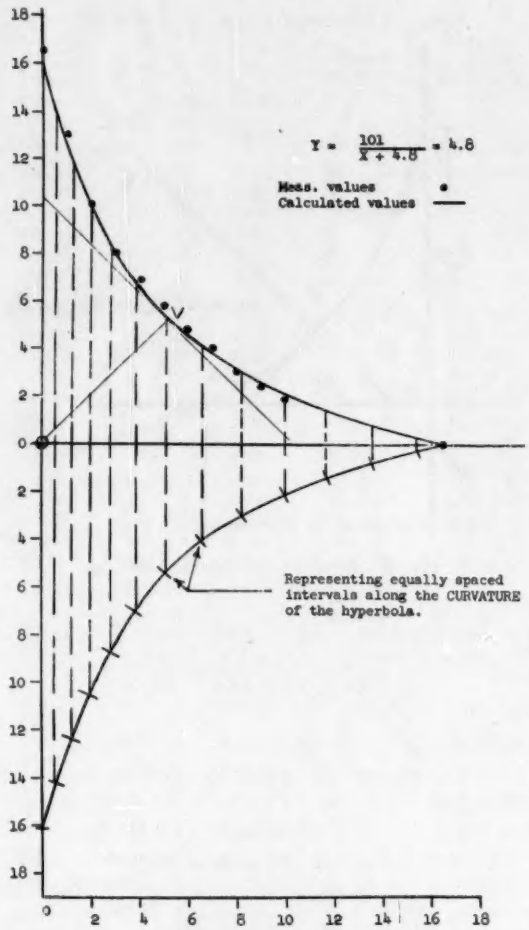
Y = 101/(X + 4.8) + 4.8
Meas. values •
Calculated values —
Representing equally spaced intervals along the CURVATURE of the hyperbola.

Fig. 9. Calculated del shape with measured values for comparison of fit.

2. *Yarn spacing within the del.* More important than the overall geometry of the del, however, is the spacial distribution of the yarns within the del. In a specimen under load, the longer yarns seem to be closer together than are the shorter del yarns.

If the yarns were considered to be pinpointed at the boundary curves of the del, then the spacing would be that which resulted from deforming the fabric near the del to produce approximately hyperbolically curved sides. In Figure 9, equal intervals were laid out along the curved sides. Then, vertical lines were drawn from these points to represent the yarns. The result is an uneven spacing in which the yarn-to-yarn distance increases linearly toward the narrow or cusp end of the del. Beyond this point the spacing would be that of the yarns in the jammed fabric ahead of the del.

This representation is indicative of the mechanism of yarn loading in the simplest types of tear. According to this schematic picture, the longer del yarns, those bearing more of the load, will be closer together when the ratio of l_v to h is greater. The closer these yarns are to each other, the better the elongation balance among them and the greater their combined load-carrying capacity.

3. *Influence of fabric geometry on load characteristics of the del.* a. Formation of the del structure. The shape and size of the del and the nature of the fabric structure loaded in parallel with the del depend upon the distortability of the fabric which occurs at comparatively low loads (not above the force required at the jaw to break the individual yarns involved). At the beginning of a tongue-tear test, when the load on the tails is first applied, several forms of this distortion are exhibited: (1) The crossyarns pull out of the fabric and become del yarns; (2) the crimp is taken out of both sets of yarns near the del, and crimp interchange occurs within the untorn fabric; (3) the untorn fabric ahead of the del becomes jammed in the direction of tear; and (4) at the junction of the tails and the untorn fabric ahead of the del, trellis-type distortion also takes place (i.e., the rectangular interstices become parallelograms with their long diagonals parallel to the del yarns).

b. Effects of fabric factors on the del.

(1) The more easily the crossyarns pull out of the fabric, the longer are the del yarns and the longer is the del. Smooth strong yarns which pull out of the fabric rather than break make for a long del. Also, the less grip the fabric matrix has on the individual yarns, the better the chances for forming a long del structure. A basket weave with strong low-twist yarns will deform to give such a del.

(2) Any crimp which is removed from the crossyarns near the tearing area acts to lengthen the del. There is also some crimp interchange which occurs in the untorn fabric ahead of the del and which subsequently results in jamming this portion of the fabric.

(3) If the fabric were already jammed in the direction of tear, no further elongation of the del could result from the jamming action of the tear.

The elongation of the del resulting from jamming of the fabric, therefore, depends upon how far the original undistorted fabric was from the jammed state in the direction of tear. Thus the lower the cover factor in the direction of tear, the more del elongation should be derived from the crimp interchange in the fabric ahead of the del.

(4) The trellis-type distortion in which both sets of yarns tend to parallel the del yarns seems greater when the cover factor and crimp in both directions are lower. For a given cover factor in the direction of tear, however, the effect of the trellis action is greater when the cover factor in the perpendicular direction is lower. The trellis action is very much dependent upon weave differences and especially upon the presence of long floats.

4. *Effect of these forms of distortion on tear strength.* (a) First, when the del is made longer and less deep, that is with a high l_T to h ratio, the del yarns are brought closer together for better load distribution and higher load capacity. This means that in order to exert a rupture load on a del yarn, the force at the jaw must be greater. (b) Second, when the fabric ahead of the del is distorted so that both sets of yarns tend to be parallel with the del yarns and bunch together to support a larger portion of the total force, the jaw again must exert a greater force to apply the rupture load to a del yarn.

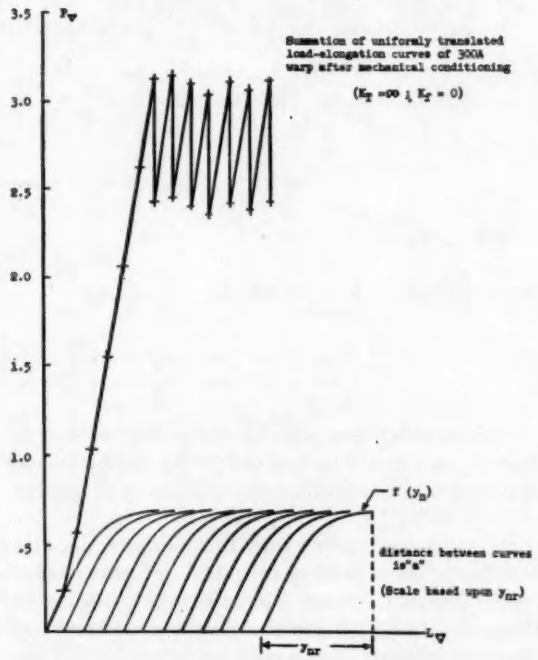

Fig. 10. Synthesis of load-elongation diagram of del.

E. Synthesis of the Tear Diagram of the Del

The section on the distribution of load drops showed that each yarn break in the del was reflected in the load at the jaws, and the analysis of the del structure showed how these yarns were arranged in the del. Earlier, a qualitative explanation was given of the tearing action and the movement of the crossyarns into the del was described.

Based upon this background, this section describes the synthesis of the load-elongation diagram of the del structure itself during a tongue tear.

1. *Graphical synthesis.* In an ideally uniform plain-weave fabric, with one load drop for each yarn ruptured, the peaks in the tear diagram would be equally spaced and there would be as many peaks per inch of tear as there were yarns per inch being torn.

Because of the repeated stressing which occurs ahead of the tearing action, the load-elongation diagram of a mechanically conditioned (acetate warp) yarn (from fabric 300A) was used. The curve was drawn upon stiff paper to be used as a stencil in duplicating the curves.

The curves were spaced $1/Y$ in. apart (where Y is the number of yarns per inch of fabric perpendicular to the direction of tear) and added to produce a plot of P_T, the load on the del, vs. elongation. This curve, shown in Figure 10, exhibits the sawtooth shape commonly associated with tongue-tear diagrams. Actually, this type of diagram with equally spaced yarns is more indicative of trapezoid tear in which the del cannot form and in which the tails are quite short. Unfortunately, however, the elongation to rupture of a yarn depends upon its gage length and it is difficult to determine the actual gage length of the yarns broken in the del. It may be possible at a later date to photograph or otherwise measure the actual length of the del in these fabrics and from this value calculate an effective gage length. Then the yarns could be tested at this length and a better load-elongation diagram derived.

In this case, the load on the del was assumed equal to the load at the jaws in the actual test and the scale adjusted so that a spacing of $1/Y$ would

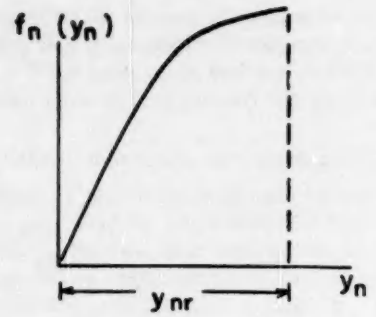

Fig. 11. Diagram of mathematical synthesis of del.

produce a peak P_∇ corresponding to P_u in the actual tear diagram.

This method is time-consuming and rather inflexible for changes in yarn spacing and curve shape. A more general method can be derived mathematically.

2. *Mathematical synthesis.* Let the load-elongation curve of the nth yarn be represented by the function $f_n(y_n)$ where y_n is the elongation of the nth yarn, whose length is l_{yn}, and y_{nr} is the ultimate elongation of the nth yarn. (See Figure 11.) Let a_n be the spacing between yarns (n) and $(n+1)$.

If these individual curves are properly summed, the result should be a diagram of P_∇, the load on the del, vs. L_∇, the elongation of the del. In this analysis the spring constant of the tails must be considered infinite and the fabric in parallel with the del neglected. The functions representing the individual curves must be multiplied by a unit step-function [2] such as

$$u[L_\nabla] \begin{cases} \text{equal to zero when } L_\nabla \text{ is less than zero.} \\ \text{equal to one when } L_\nabla \text{ is greater than zero.} \end{cases}$$

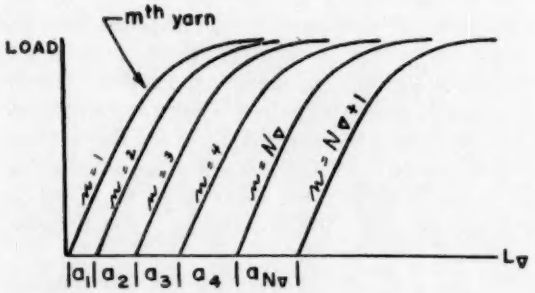

Fig. 12. Schematic representation of loading curves of yarns in del.

Thus

$u[L_\nabla - L_1]$ is zero until $L_\nabla = L_1$ and equal to 1 for L_∇ greater than L_1

and

$u[L_\nabla - L_1] - u[L_\nabla - L_2]$ is equal to zero except from L_1 to L_2, when it is equal to 1.

Multiplying the yarn load-elongation curve by such a function allows the use of the curve as a discontinuous function.

The expression for the first yarn curve, therefore, is

$$f_1(L_\nabla)\{u[L_\nabla] - u[L_\nabla - y_{1r}]\}$$

and for the nth yarn curve is

$$f_n(L_\nabla - \sum_{n=1}^{n} a_{(n-1)})\{u[L_\nabla - \sum_{n=1}^{n} a_{(n-1)}] - u[L_\nabla - \sum_{n=1}^{n} a_{(n-1)} - y_{nr}]\}.$$

The sum of these expressions is

$$\begin{aligned} P_\nabla = {} & f_1(L_\nabla)\{u[L_\nabla] - u[L_\nabla - y_{1r}]\} \\ & + f_2(L_\nabla - a_1)\{u[L_\nabla - a_1] - u[L_\nabla - a_1 - y_{2r}]\} \\ & + f_3(L_\nabla - a_1 - a_2)\{u[L_\nabla - a_1 - a_2] - u[L_\nabla - a_1 - a_2 - y_{2r}]\} + \cdots \\ & + f_n(L_\nabla - \sum_{n=1}^{n} a_{(n-1)})\{u[L_\nabla - \sum_{n=1}^{n} a_{(n-1)}] - u[L_\nabla - \sum_{n=1}^{n} a_{(n-1)} - y_{nr}]\} + \cdots \end{aligned}$$

where $a_o = 0$, or

$$P_\nabla = \sum_{n=1}^{\infty} f_n[L_\nabla - \sum_{n=1}^{n} a_{(n-1)}]\{u[L_\nabla - \sum_{n=1}^{n} a_{(n-1)}] - u[L_\nabla - \sum_{n=1}^{n} a_{(n-1)} - y_{nr}]\}.$$

This expression represents the entire concatenation of yarn curves as laid out in the graphical case but does not limit itself to any uniformity of spacing or yarn shape.

Before going further with this analysis, another look at the del structure is required. In the section on del geometry it was shown that the spacing of the yarns in the del was certainly not uniform and that the longer yarns were closer together. Furthermore, if the del is considered as supporting the

whole load, the untorn fabric neglected, then only the yarns in the del need be added to obtain the load. This considerably simplifies the last equation. This expression, by means of the unit step functions, automatically eliminates all the yarns not under load at any value of L_∇ but includes the fault of the graphical method in that the yarn curves are not added in the same way that the individual yarns contribute to the load in the del.

Let the limits of the summation, therefore, include only the number of yarns in the del, N_∇.

Then, during the mth peak, that is, between the ruptures of yarns $m-1$ and m, the yarns being loaded are yarns numbered 1 through N_∇ where the mth yarn is number 1.

These yarn curves will be added with the spacing between curves increasing linearly from a_1 to aN_∇. All the curves will be considered identical, that is,

$$f_1(y_1) = f_2(y_2) = f_n(y_n) = f(y)$$

and

$$y_{1r} = y_{2r} = y_{nr} = y_r$$

Using the stencil for the 300A acetate warp yarn, after mechanical conditioning, the graphical representation is as shown in Figure 12.

Using the mathematical expressions for the curves, the load on the del may be written as

$$\begin{aligned} P_\nabla = {} & f(L_\nabla)\{u[L_\nabla]-u[L_\nabla-y_r]\} \\ & +f(L_\nabla-a_1)\{u[L_\nabla-a_1]-u[L_\nabla-a_1-y_r]\} \\ & +f[L_\nabla-(a_1+a_2)]\{u[L_\nabla-(a_1+a_2)] \\ & \qquad -u[L_\nabla-(a_1+a_2)-y_r]\}+\cdots \\ & +f\Big[L_\nabla-\sum_{n=1}^{n} a_{n-1}\Big]\Big\{u\Big[L_\nabla-\sum_{n=1}^{n} a_{n-1}\Big] \\ & \qquad -u\Big[L_\nabla-\Big(\sum_{n=1}^{n} a_{n-1}\Big)-y_r\Big]\Big\}+\cdots \end{aligned}$$

Summing all the yarns in the del

$$\begin{aligned} P_\nabla = \sum_{n=1}^{N\nabla} & f\Big[L_\nabla-\sum_{n=1}^{n} a_{n-1}\Big]\Big\{u\Big[L_\nabla-\sum_{n=1}^{n} a_{n-1}\Big] \\ & -u\Big[L_\nabla-\Big(\sum_{n=1}^{n} a_{n-1}\Big)-y_r\Big]\Big\} \end{aligned}$$

In this expression the yarn spacing may be exactly the spacing determined from the del structure. The maximum del load, just before yarn rupture, will depend upon the number of yarns in the del, their spacing, and the shape of their load-elongation curves. It is more important that the yarns be closely spaced than that there be many in the del.

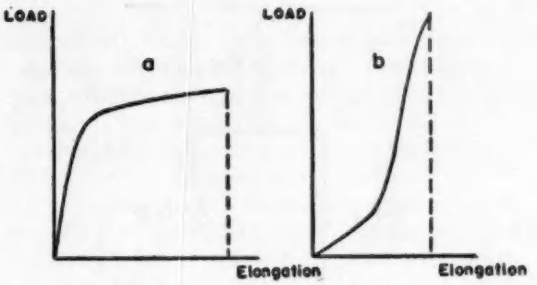

Fig. 13. Comparison of load-elongation curves.

Analysis of the equation or examination of the diagram of Figure 12 will show that a curve shaped like that in Figure 13*a* will be better than one like that shown schematically in Figure 13*b*, even though the latter yarns have a higher breaking strength.

It may also be shown by Figure 12 how a variation in the ultimate elongation of these yarns could cause multiple yarn breaks. If the second yarn in the del had an ultimate elongation which was less than that of the first yarn by an amount equal to the spacing between them, then both yarns would fail simultaneously.

Although the yarns in the del are not equally spaced, even in an ideally uniform fabric, the peaks representing the yarn breaks would be equally spaced. Each time a yarn breaks, the entire del structure is renewed and for a uniform fabric the jaw would have to move an equal amount to break each yarn.

F. The Analysis of the Effect of the Tails and the Untorn Fabric on the Tear Force

Even if the loading function of the del structure were completely defined, the mechanism of tear would only be partially explained. Two other parts of the system must be investigated; namely, the untorn fabric in parallel with the del and the tongues, or tails, acting in series with the del and its parallel fabric structure.

1. *The spring analogue.* In the first part of this paper the tongue-tear specimen was schematically represented by three springs, as shown in Figure 14, where K_T represents the tails and K_f stands for the fabric in parallel with the del, which is considered to act as K_∇.

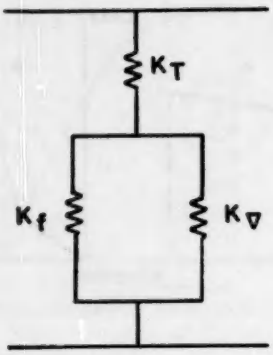

Fig. 14. Components of spring constant K.

As indicated previously, if K is the total spring constant of the system and K_o is equivalent to the parallel combination of K_f and K_∇, then

$$K = (K_o K_T)/(K_o + K_T)$$

If this combination be extended by a force equal to P, then the elongation of the tails will be equal to P/K_T and the elongation of the del will be equal to P/K_o. For every load that is placed on the series combination of K_T and K_o, there is an equilibrium position which may be determined very readily by graphical means [5].

In Figure 15, the line marked K_T, which is the load-elongation diagram of the tails, has been plotted using the origin at the left, while from the right-hand origin the load-elongation diagram for the del and the fabric in parallel with the del, K_o, has been drawn. The K_o used in this construction consists of K_f plus K_1, where K_1 may be considered as one yarn in the del, and K_2, which is another del yarn. Since K_f, K_1, and K_2 are in parallel, their loading diagrams may be added directly. The two main lines in this figure are K_T and K_o. Since these two springs are in series, the same load is on each of them, and their equilibrium point must be their intersection on this diagram. Point O_1 is the point of equilibrium just as K_o is loaded to its breaking point. When K_1 breaks, a new equilibrium point must be achieved between K_T and K_o', where $K_o' = K_o - K_1 = K_f + K_2$. This new equilibrium point is O_2 and the shift from O_1 to O_2 has taken place without any change in the total elongation, that is, without any jaw movement.

From this diagram the amount of tail contraction may be determined. It is also possible to determine the ratio of the load drop on the whole system, ΔP, to the drop in load-carrying capacity of K_o, or ΔP_o. In Figure 16 the region near the operating points has been expanded to facilitate calculation. The diagram of Figure 16 is more general than the example in Figure 15, and $K_o = K_f + K_\nabla$.

In an actual case of fabric tear the yarns are so close together that the failure of a yarn does not reduce K_o appreciably, since another yarn is already being brought into the del. The load on K_o may drop at a yarn break, but the slope of the line does

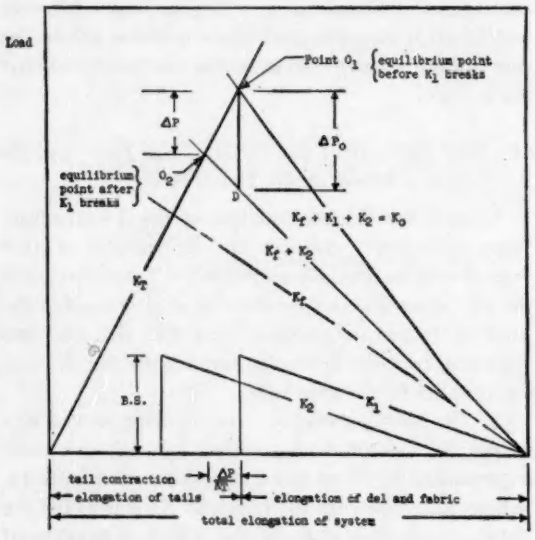

Fig. 15. Graphical presentation of spring system.

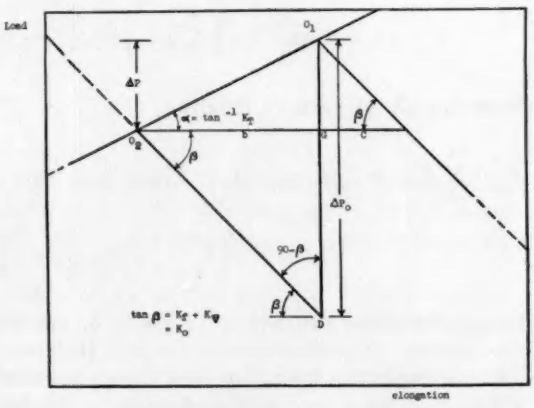

Fig. 16. Trigonometric analysis of section from figure 15.

not change much from one peak to another. Therefore, $K_o = K_o'$

$$\tan \alpha = O_1G/O_2G = \Delta P/b = K_T$$
$$\tan \beta = DG/O_2G = (\Delta P_o - \Delta P)/(b) = K_o$$
$$\Delta P_o/b = K_o + \Delta P/b = K_o + K_T$$
$$\frac{\Delta P}{\Delta P_o} = \frac{\Delta P/b}{\Delta P_o/b} = \frac{K_T}{K_o + K_T} = \frac{1}{(K_o/K_T) + 1}$$

Since $K_T = C_T/2l_T$

$$\frac{\Delta P}{\Delta P_o} = \frac{1}{(2K_o/C_T)l_T + 1}$$

(The actual dependence of ΔP on l_T will be discussed later in this section.)

To show the effect of K_T on the appearance of multiple breaks, Figure 17 was drawn for a simple three-spring system. K_1 and K_2, equal springs, are in parallel, and the parallel combination is in series with K_T. There is slack in K_2 so that K_2 does not begin to take on load until K_1 has already been partially stretched. This figure shows that when the tail contraction is equal to or greater than the slack for two identical springs with the same rupture load value both springs will be broken at the same time. This is true for springs having no mass and no damping. With the introduction of mass, the rapid movement of the tails could cause an inertia force to be applied to the del yarns. This force would not be detectable at the jaw.

2. *The effect of the fabric loaded in parallel with the del.* Were it not for this paralleled fabric, represented by K_f, the tear load diagram could be completely synthesized from the yarn characteristics, the yarn spacing, and the spring constant of the tails. The series combination of K_T and K_Y (synthesized graphically according to the method of the last section) is shown in Figure 18.

It is quite difficult, however, to determine the behavior of the fabric in parallel with the del. One clue to its behavior comes from calculations of the ratio $\Delta P/\Delta P_o$ where ΔP is the load drop at the jaws and ΔP_o is the load drop which would occur if the tails were of infinite stiffness.

Neglecting K_f, ΔP_o would be equal to the breaking strength of the yarn ruptured, as shown in Figure 18. Table II lists the values of ΔP_o as calculated for the continuous-filament plain-weave fabrics and lists also the difference between ΔP_o and the breaking strength of the yarn.

The relationships between the various K's and the load drops are shown diagrammatically in Figure 19 for Fabric 300A warp, since, for fabrics having single yarn breaks, the graphical procedure becomes less involved. This diagram shows the difference between ΔP_o and the breaking strength of the yarn in a simple case.

During the loading of a del yarn up to the time of its rupture, K_f acts as a supporting member in parallel with the del yarns, continuously bearing part of the gradually increasing load. When the del yarn is ruptured, there is a sudden discontinuity in the load and the tails are discontinuously in-

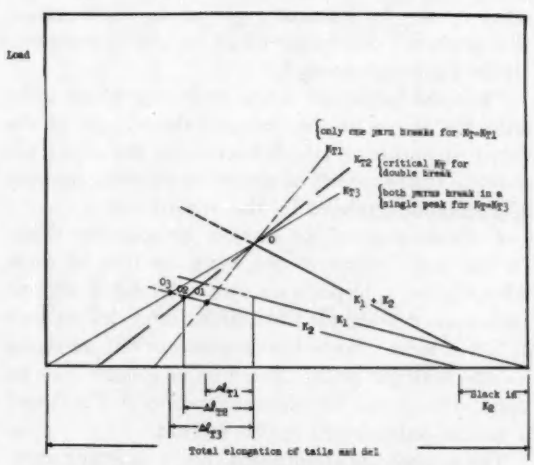

Fig. 17. The effect of K_T on multiple breaks.

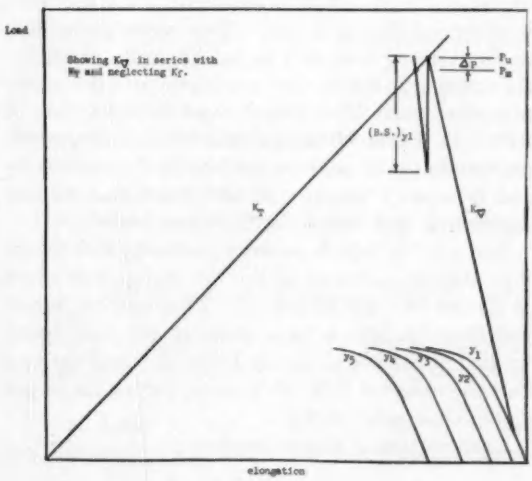

Fig. 18. Synthesis of tear diagram neglecting K_f.

TABLE II. Calculations Showing the Effect on ΔP of K_f

Fabric	K_o (lb/in.)	K_T (lb/in.)	K_o+K_T (lb/in.)	K_T/K_o+K_T	ΔP^* (lb)	ΔP_o (lb)	Yarn B.S. (lb)	ΔP_o—B.S.† (lb)
300AW	41	97	138	0.72	0.65	0.91	0.71	0.20
300AF	43	56	99	0.57	0.68	1.20	0.77	0.53
301AW	56	53	109	0.49	0.90	1.85	0.74	1.11
301AF	43	103	146	0.70	0.94	1.34	0.71	0.63
302AW	76	76	152	0.50	1.15	2.30	0.76	1.54
302AF	70	75	145	0.48	1.45	3.00	0.58	2.42
400AW	31	65	96	0.68	0.64	0.94	0.66	0.28
400AF	39	45	84	0.54	0.66	1.23	0.74	0.49
401AW	41	71	112	0.63	0.86	1.36	0.76	0.60
401AF	38	83	121	0.69	0.99	1.44	0.77	0.67
402AW	52	76	138	0.55	1.00	1.81	0.78	1.03
402AF	50	68	118	0.58	1.55	2.69	0.74	1.85
500AW	34	69	103	0.67	0.57	0.85	0.67	0.18
500AF	50	35	85	0.41	0.94	2.28	0.78	1.50
501AW	42	43	85	0.50	0.59	1.17	0.67	0.50
501AF	39	36	75	0.48	0.84	1.75	0.74	1.01
502AW	90	33	123	0.27	0.66	2.46	0.73	1.73
502AF	56	38	94	0.41	1.16	2.84	0.69	2.15

* From corrected distribution curves

$$\Delta P_o = \frac{\Delta P}{\left(\frac{K_T}{K_o + K_T}\right)}.$$

† ΔP_o—(B.S.) yarn = Drop in load caused by discontinuity in K_f.

creased in length by approximately twice the distance between crossyarns. The fabric in parallel with the del is usually already in a jammed state and cannot contract to take up load, very much like a coiled spring with the coils touching each other. As a result there is also a discontinuity in the loading of K_f, causing a cyclic loading of the fabric ahead of the del which is apparent if the specimen is observed during a test. This repeated loading and unloading also acts to mechanically condition the crossyarns before they are drawn into the region of active tear. The drop in load on K_f is part of ΔP_o. In Table II the column headed ΔP_o—B.S. represents the discontinuous drop in the load on K_f and becomes a measure of how much load K_f was supporting just before the del yarns broke.

For a fabric which permits jamming and trellis-type distortion ahead of the del region, the effect of K_f can be quite beneficial. This jammed fabric will then support a large share of the load being applied at the jaws. From Table II it may be seen that the values of ΔP_o—B.S. are larger for the looser more distortable fabrics.

Examination of the expression

$$\Delta P_o = \Delta P\left(\frac{K_o}{K_T} + 1\right)$$

which may be rewritten as

$$\Delta P_o = \Delta P\left(\frac{K_\nabla}{K_T} + \frac{K_f}{K_T} + 1\right)$$

shows that the amount of fabric assistance depends upon the relative extensibilities of the tails and the fabric loaded in parallel with the del. For short tails K_∇/K_T is quite small and K_f/K_T is the dominant term. In a gauze type fabric, for instance, it is probably this factor which results in comparatively high tear strength.

Thus the factors in fabric geometry which influence the shape of the del and the nature of the fabric structure in parallel with the del affect not only the load capacity of the del but also the amount of assistance rendered by the untorn fabric.

3. Calculation of the number of multiple peaks. In the early stages of the work on tear at these laboratories, a hypothesis was formulated and an expression derived for the number of peaks per inch of fabric torn. Since that expression still accounts for the multiple peaks caused by snapback (not by variability in the ultimate elongation of the yarns) it will be redeveloped in this section.

The hypothesis maintained that a constant number of yarns were broken per peak by actual jaw

separation and a gradually increasing number of yarns per peak broken by snapback or tail contraction. As the number of yarns broken by snapback increased, the number of peaks per inch of fabric torn must decrease, since each inch of fabric has a constant number of yarns.

The tail contraction is $2\Delta l_T$, which is equal to $\Delta P/K_T$ and was considered as an additional jaw movement since the effect of tail contraction was the same to the del structure as a jaw displacement.

Let

M = Equivalent number of peaks caused by tail contraction at each rupture

and if

N_o = Number of peaks per inch of fabric torn at zero tail length (extrapolated value)

and

Y/N_o = Yarns per peak due to jaw separation

Then

$$M = (\Delta l_T)(N_o) = (\Delta P/2K_T)N_o$$

and

$$\left\{\begin{matrix}\text{Yarns broken per}\\ \text{major peak due to}\\ \text{tail contraction}\end{matrix}\right\} = (\Delta P N_o/2K_T) \times (Y/N_o) = (\Delta P Y/2K_T)$$

Let

T = Total number of yarns broken per peak

$$= \left\{\begin{matrix}\text{Yarns per peak}\\ \text{due to actual}\\ \text{jaw separation}\end{matrix}\right\} + \left\{\begin{matrix}\text{Yarns per peak}\\ \text{due to tail con-}\\ \text{traction}\end{matrix}\right\}$$

$$T = \frac{Y}{N_o} + \frac{\Delta P Y}{2K_T} = Y\left(\frac{1}{N_o} + \frac{\Delta P}{2K_T}\right)$$

$$N = \left\{\begin{matrix}\text{Peaks per inch}\\ \text{of fabric torn}\end{matrix}\right\} = \frac{Y}{T}$$

$$= \frac{1}{(1/N_o) + (\Delta P/2K_T)}$$

$$= \frac{2N_oK_T}{2K_T + \Delta P N_o}$$

$K_T = C_T/2l_T$ and $2K_T = C_T/l_T$

then

$$N = (N_oC_T)/(C_T + \Delta P N_o l_T)$$

or

$$1/N = 1/N_o + (\Delta P l_T/C_T)$$

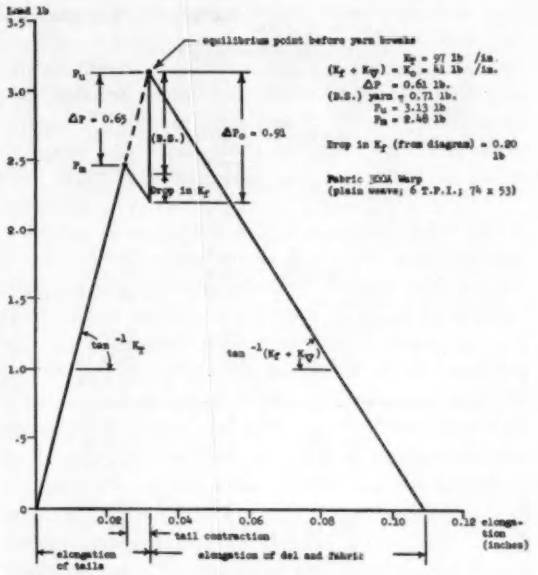

Fig. 19. Schematic presentation of tear data showing effect of drop in K_T.

This equation says in a different way what was presented in Figure 17 with its associated discussion. The N referred to in the equation includes a double peak as one peak.

4. *Effect of tail length on* ΔP. Since ΔP is included in the expression for the peaks per inch of fabric torn as a function of l_T, the relationship between ΔP and l_T will be analyzed here. From Figure 23,

$$\Delta P/\Delta P_o = (K_T)/(K_o + K_T) = (C_T)/(2K_o l_T + C_T)$$

$$\Delta P = \Delta P_o C_T/(2K_o l_T + C_T)$$

The empirical dependence of ΔP on l_T is known for one fabric, Number 301A, for which a plot of successive ΔP's was made. This fabric, therefore, will be used as an example.

The above equation for ΔP vs. l_T is hyperbolic and may be rectified to be read:

$$1/\Delta P = (2K_o/\Delta P_o C_T)l_T + (1/\Delta P_o)$$

Thus $1/\Delta P$ plotted vs. l_T would be a straight line with a slope of $2K_o/\Delta P_o C_T$ and an intercept of $1/\Delta P_o$.

From Table II, $\Delta P_o = 1.85$ and $K_o = 56$, and for this fabric $C_T = 265$. The equation becomes

$$1/\Delta P = 0.23\, l_T + 0.54$$

TABLE III. Construction of Desized Form Factor Fabrics

Continuous-Filament Fabrics				Staple-Fiber Fabrics			
Nominal Twist (t p.i.)*	Nominal Texture (w×f)	Weave	Actual Texture (w×f)	Nominal Twist (t.p.i.)*	Nominal Texture (w×f)	Weave	Actual Texture (w×f)
	68×52	1/1	74×53		68×52	1/1	76×50
		3/1	77×53			3/1	77×51
		2/2	77×53			2/2	78×52
	50×52	1/1	58×53		50×52	1/1	60×51
6		3/1	56×54	11		3/1	58×51
		2/2	55×54			2/2	57×51
	50×32	1/1	56×34		50×32	1/1	56×32
		3/1	58×35			3/1	55×32
		2/2	58×34			2/2	55×32
	68×52	1/1	74×54		68×52	1/1	74×53
		3/1	76×56			3/1	76×52
		2/2	77×57			2/2	77×52
	50×52	1/1	58×48		50×52	1/1	60×50
12		3/1	59×54	19		3/1	59×51
		2/2	58×54			2/2	58×52
	50×32	1/1	56×32		50×32	1/1	57×32
		3/1	56×32			3/1	59×33
		2/2	57×35			2/2	57×34
	68×52	1/1	73×39		68×52	1/1	74×49
		3/1	77×56			3/1	78×51
		2/2	77×55			2/2	77×53
	50×52	1/1	57×41		50×52	1/1	58×50
24		3/1	59×55	27		3/1	60×51
		2/2	59×57			2/2	59×52
	50×32	1/1	55×35		50×32	1/1	56×32
		3/1	57×35			3/1	59×32
		2/2	56×35			2/2	57×33

* In turns per inch.

Substituting values of l_T, the following results are derived, shown together with the experimental points for comparison.

	Calculated		*Experimental*	
l_T	$1/\Delta P$	ΔP	$1/\Delta P$	ΔP
2	1.00	1.00	0.98	1.02
2.5	1.11	0.90	1.09	0.91
3	1.23	0.83	1.22	0.82
4	1.46	0.69	1.52	0.66
5	1.69	0.59	1.92	0.52

When the experimental curve was rectified, the resulting straight line had a slope of about 0.26 and an intercept of about 0.5. This would make the experimental equation

$$1/\Delta P = 0.26\, l_T + 0.5$$

G. Summary of Theoretical Section

The results of this theoretical analysis point to certain prime factors affecting the tear resistance of fabrics. The tear strength of a fabric will depend upon: (1) The amount and type of distortion at or near the del; (2) the relative extensibility of the fabric loaded in parallel with the del; (3) the shape of the load-elongation curve of the del yarns after mechanical conditioning, since the yarns are worked and reworked at gradually increasing loads as they

advance to the breaking position; (4) the breaking strength of the mechanically conditioned del yarns; (5) the ultimate elongation and the variability in the ultimate elongation of the conditioned del yarns; and (6) the extensibility of the fabric which transmits the load to the del, represented in these tests by the tails.

These factors in turn depend upon the following form factors of the fabric: (1) The reciprocal of the force required to pull a yarn out of the fabric; (2) the crimp level and crimp balance; (3) the interyarn spacing in the fabric or the reciprocal of the cover factor; (4) the deformability of the fabric in its own plane, which leads to trellis action; and (5) the load-elongation curve of the conditioned yarn.

III. Experimental Study

The fabrics studied were those described in Table III. These fabrics were torn on the Instron Tensile Tester using a jaw speed of 2 in. per min and a chart speed of 20 in. per min.

Some of the fabrics pulled apart or tore across the tails, and no data are available for them at this speed. The presence of dashes in the data tables IV, V, and VI results indicates that such data are not available for the reason mentioned above.

The data were studied to learn the effects on tear strength of such form factors as weave, texture, yarn twist, and yarn structure (staple or continuous filament).

A. Effect of Weave on Tear Strength

In a weave with many crossovers per inch, the gripping action between warp and filling threads will tend to be high and thus increase the yarn pullout force over what it would have been for a fabric with long floats. This increase in pullout force resulting from weave will decrease the realizable tear strength of the fabric. Thus, the plain weave should be weaker in tear (for a given yarn strength and texture) than the basket weave, as substantiated by the data.

A looser weave with longer floats should also be more deformable in its own plane and allow greater trellis-type distortion.

There should be an optimum condition of crimp where the amount of crimp, the crimp balance, and the degree of crimp interchange under load allow for the type of distortion which results in a long shallow del structure. To the extent that the weave affects the crimp for a given texture and yarn size, the weave also influences the tear strength. The data have not been analyzed for the effects of crimp on tear strength or of weave on crimp since the crimp was not too well-controlled in these samples.

The most important factor in tear strength which is influenced by the weave is the dimensional stability of the fabric in its own plane. Even if the cover factor be high, a weave with many long floats will allow greater distortion due to jamming and trellis action. For the purposes of comparison, visual examination of a plain-weave and a basket-weave tongue-tear specimen, each of the same texture and yarn content, shows how much more deformable the basket weave is and how the deformed structure in the basket weave distributes the load between the fabric and the del more than in the plain weave. The del structure in the basket weave also allows more yarns to share the tear load.

Compared strictly on the basis of weave, the 2/2 (basket) weave is more than twice as strong as the 1/1 (plain) weave, and the 3/1 (twill) weave is about 1½ times stronger than the 1/1 (plain) weave. The data on tear energy, tear force, and normalized tear force are presented in Table IV, where the effects of weave are discernible. In Table V the data for the 3 twists in Table IV have been averaged, with allowance for blank spaces. Data on

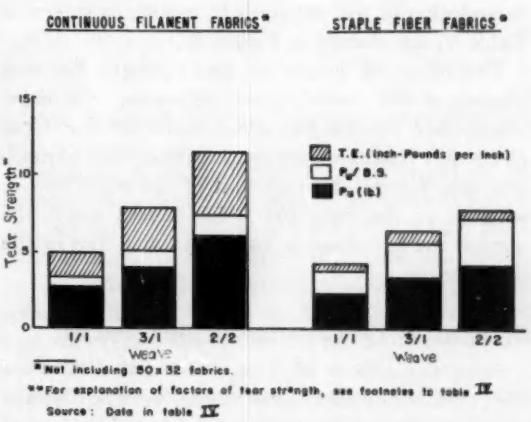

Fig. 20. Relation of tear strength to weave.

TABLE IV. Tear Strength vs. Fabric Factors

Nominal Texture	Twist* (t.p.i.)	Weave	Tear Energy† (w)	Tear Energy† (f)	P_u in lb‡ (w)	P_u in lb‡ (f)	P_u/B.S.§ (w)	P_u/B.S.§ (f)
			Continuous-Filament Fabrics					
		1/1	5.79	4.88	3.13	2.68	3.73	3.23
	6	3/1	10.65	7.36	5.20	3.87	5.71	4.90
		2/2	14.94	9.36	7.37	5.50	8.57	7.33
		1/1	5.28	5.31	2.77	2.72	3.51	3.49
68×52	12	3/1	9.02	9.05	4.73	4.82	5.26	5.13
		2/2	14.13	8.97	6.83	5.10	7.34	5.80
		1/1	4.66	5.07	2.62	2.75	3.91	3.16
	24	3/1	6.46	6.06	3.08	3.10	4.16	3.97
		2/2	9.87	8.23	5.10	4.30	6.14	5.06
		1/1	6.14	4.95	3.10	2.80	3.52	3.50
	6	3/1	8.80	7.95	4.60	4.30	5.97	5.18
		2/2	18.83	10.89	8.97	6.87	11.65	8.38
		1/1	5.59	5.50	2.83	2.98	3.18	3.47
50×52	12	3/1	10.05	7.52	5.17	4.30	6.46	4.78
		2/2	14.33	11.64	6.93	6.57	8.45	7.55
		1/1	4.56	4.73	2.57	2.55	3.62	2.90
	24	3/1	6.88	7.22	3.20	3.60	4.44	5.14
		2/2	12.06	11.12	5.97	6.47	7.37	7.89
		1/1	8.54	5.03	4.33	3.20	4.87	4.16
	6	3/1	—	8.96	—	4.47	—	5.75
		2/2	—	—	—	—	—	—
		1/1	7.64	5.53	3.87	3.33	4.35	3.74
50×32	12	3/1	18.28	12.49	8.40	6.80	10.63	7.91
		2/2	—	11.43	—	6.67	—	8.13
		1/1	5.56	5.64	3.12	3.10	4.27	3.69
	24	3/1	11.08	8.19	5.90	4.88	7.47	5.61
		2/2	—	—	—	—	—	—

the relation of tear strength to weave, as shown in Table V, are plotted in Figure 20.

The effect of weave on tear strength becomes greater as the thread count decreases. On those staple-fiber fabrics for which data on the loose (50 × 32) basket weave are available, the normalized tear force is 3 times that of the plain weave, whereas on the tight (68 × 52) basket weave the normalized tear force is less than twice that of the plain weave.

B. Effects of Yarn Structure on Tear Strength

Since the effects of yarn twist and fiber type (i.e., continuous filament or staple) were not always separable, they will be discussed together in this section.

In every case, the fabrics constructed of continuous-filament yarns were stronger in tear than those made of staple-fiber yarns. For ease in comparing the effects of yarn structure, the tear-force data from Table IV have been plotted in Figure 21*a* and *b*. A comparison based on these curves, however, is not quite fair since the continuous-filament yarns have higher tensile strengths than their staple-fiber counterparts. For this reason the tear force values have been normalized by dividing them by the individual yarn breaking strength. These normalized tear-force data as shown in Table IV are plotted against twist in Figure 22*a* and *b*.

The results of this normalization have interesting ramifications. First, the continuous-filament fabrics are not always stronger than the staple fiber fabrics. Secondly, and perhaps more important,

TABLE IV.—Continued

Nominal Texture	Twist* (t.p.i.)	Weave	Tear Energy† (w)	Tear Energy† (f)	P_u in lb‡ (w)	P_u in lb‡ (f)	P_u/B.S.§ (w)	P_u/B.S.§ (f)
			Staple-Fiber Fabrics					
		1/1	4.43	3.49	2.23	1.97	3.19	2.77
	11	3/1	6.99	5.38	3.22	2.87	4.41	4.42
		2/2	8.49	5.59	4.17	3.08	5.96	4.97
		1/1	3.83	3.63	1.93	1.92	3.78	3.25
68×52	19	3/1	7.08	5.56	3.30	2.95	4.93	4.92
		2/2	9.36	6.05	4.55	3.33	8.92	5.64
		1/1	4.00	2.99	2.00	1.55	4.55	3.10
	27	3/1	5.67	4.48	2.60	2.33	4.41	4.57
		2/2	7.08	5.26	3.50	2.83	5.83	5.15
		1/1	4.36	4.01	2.12	2.23	3.07	3.54
	11	3/1	6.71	6.89	3.45	3.43	5.75	5.28
		2/2	7.92	7.02	4.10	4.00	7.07	6.35
		1/1	4.00	4.27	1.90	2.00	3.11	3.51
50×52	19	3/1	6.17	7.76	3.33	3.57	5.46	5.76
		2/2	10.50	8.03	4.87	4.47	8.12	7.21
		1/1	3.89	2.98	1.97	1.62	4.02	3.52
	27	3/1	5.66	5.06	2.72	2.70	4.69	5.19
		2/2	8.53	6.70	3.95	3.68	7.45	7.08
		1/1	5.71	3.22	2.77	1.97	4.01	3.23
	11	3/1	9.22	6.73	4.83	3.92	7.92	7.26
		2/2	14.55	7.69	6.93	4.13	11.55	7.25
		1/1	5.33	3.69	2.60	2.08	4.00	3.59
50×32	19	3/1	14.30	9.10	6.27	4.90	10.45	9.25
		2/2	—	8.61	—	5.88	—	11.31
		1/1	4.47	3.23	2.10	1.78	3.62	3.30
	27	3/1	10.66	6.08	4.80	3.53	8.28	7.35
		2/2	—	10.90	—	5.83	—	12.15

* Yarn twist, in turns per inch.
† Tear energy in inch-pounds per inch.
‡ Tear force P_u in pounds.
§ Normalized tear force (tear force divided by breaking strength, P_u/B.S.).

the superiority of the continuous-filament fabrics over the staple-fiber fabrics depends very much upon the twist in the yarns.

In the warp tests, most of the continuous-filament fabrics are superior when the yarns have twists of less than 13 turns per in. and inferior when the twist is greater than about 17 turns per in.

The filling tear data show most of the continuous-filament fabrics to be superior below yarn twists of about 13 turns per in. and inferior for yarn twists above about 19 turns per in.

Figures 21*a* and *b* and 22*a* and *b* show all the tear force and normalized tear force values for the fabrics designed for the Quartermaster study of form factors.

To show the overall effect of yarn structure on the tear strength of the fabrics, irrespective of weave and texture, the curves in Figure 22*a* and *b* have been averaged and replotted in Figure 23*a* and *b*. In Figure 24*a* and *b* the strength of the yarns corresponding to the values in 23*a* and *b* have been plotted to show the effects of yarn structure on the yarn strength.

Aside from its own tensile strength, the most important property of a yarn in influencing the tear strength of a fabric is its surface or yarn-to-fabric

TABLE V. Tear Strength vs. Texture and Weave *

Nominal Texture	Weave	Tear Energy (w)	Tear Energy (f)	P_u in lb (w)	P_u in lb (f)	P_u/B.S. (w)	P_u/B.S. (f)
		Continuous Filament Fabrics					
	1/1	5.24	5.08	2.84	2.72	3.72	3.29
68×52	3/1	8.72	7.47	4.34	3.93	5.04	4.67
	2/2	12.98	8.85	6.44	4.97	7.35	6.06
	1/1	5.42	5.06	2.83	2.78	3.44	3.29
50×52	3/1	8.58	7.56	4.32	4.07	5.62	5.03
	2/2	15.06	11.22	7.28	6.64	9.15	7.94
	1/1	7.25	5.40	3.77	3.21	4.50	3.86
50×32	3/1	—	9.88	—	5.48	—	6.42
	2/2	—	—	—	—	—	—
		Staple Fiber Fabrics					
	1/1	4.09	3.37	2.05	1.81	3.84	3.04
68×52	3/1	6.58	5.14	3.04	2.72	4.58	4.64
	2/2	8.31	5.63	4.07	3.08	6.90	5.25
	1/1	4.08	3.75	2.00	1.95	3.40	3.52
50×52	3/1	6.18	6.57	3.17	3.23	5.30	5.41
	2/2	8.98	7.25	4.31	4.05	7.55	6.88
	1/1	5.17	3.38	2.49	1.94	3.88	3.37
50×32	3/1	11.39	7.30	5.30	4.12	8.88	7.95
	2/2	—	9.07	—	5.28	—	10.24

* This is a summary of the data in Table IV eliminating the twist subdivisions by averaging the amounts for the three twists. For explanation of terms see footnotes to Table IV.

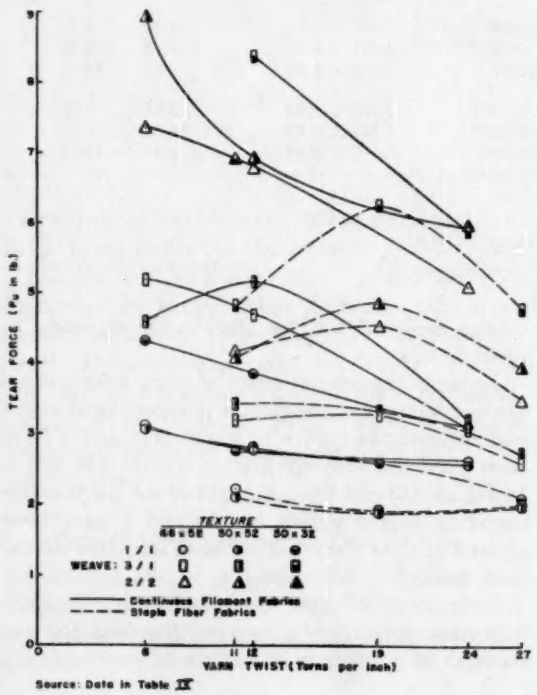

Fig. 21a. Tear force vs. yarn twist of different weaves and textures—warp.

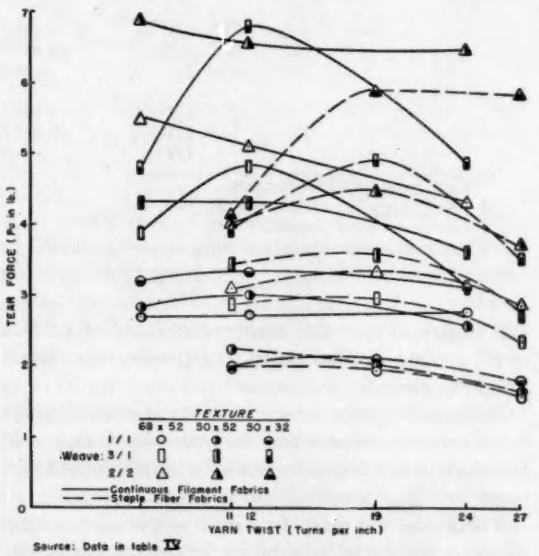

Fig. 21b. Tear force vs. yarn twist of different weaves and textures—filling.

friction. Thus, if the fiber used or the amount of twist given the fiber affects the friction, then these factors will influence the tear strength.

Until further work is done on the relationships between yarn structure and yarn friction and be-

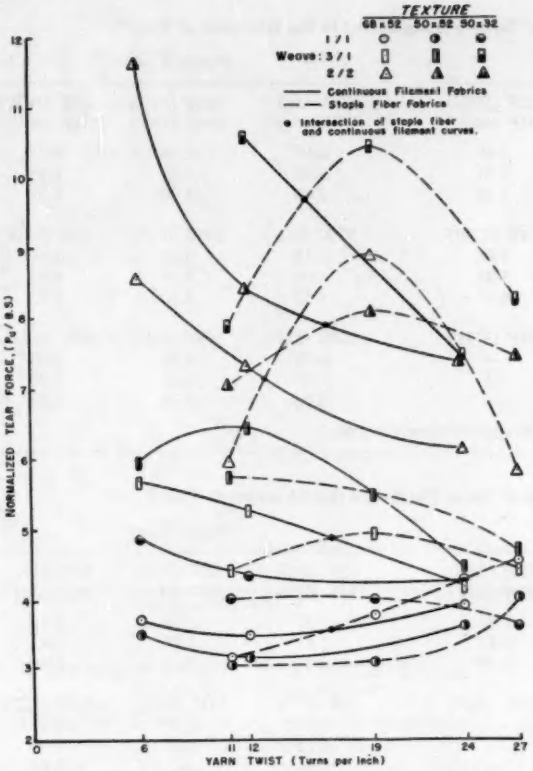
TEXTURE
68 x 52 50 x 52 50 x 32
Weave: 1/1 3/1 2/2
Continuous Filament Fabrics
Staple Fiber Fabrics
Intersection of staple fiber and continuous filament curves.
NORMALIZED TEAR FORCE, (Pw/B.S.)
YARN TWIST (Turns per inch)

Fig. 22a. Normalized tear force vs. yarn twist—QMC form fabrics—warp.

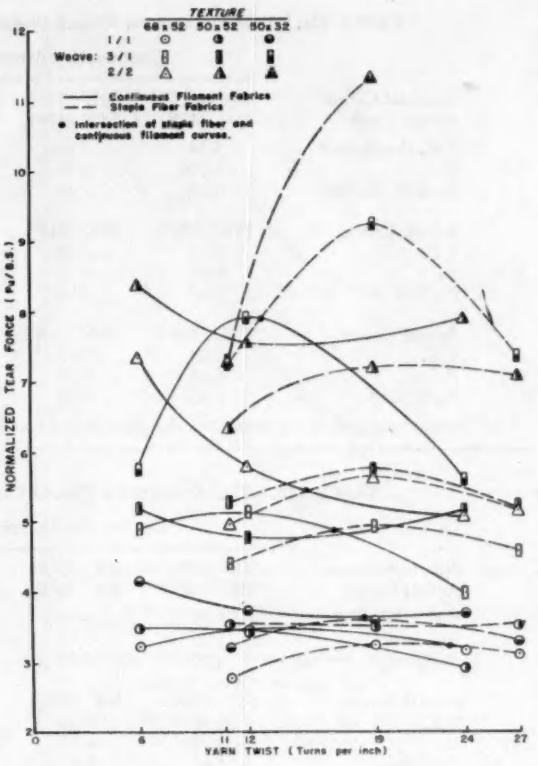
TEXTURE
68 x 52 50 x 52 50 x 32
Weave: 1/1 3/1 2/2
Continuous Filament Fabrics
Staple Fiber Fabrics
Intersection of staple fiber and continuous filament curves.
NORMALIZED TEAR FORCE (Pw/B.S.)
YARN TWIST (Turns per inch)

Fig. 22b. Normalized tear force vs. yarn twist—QMC form fabrics—filling.

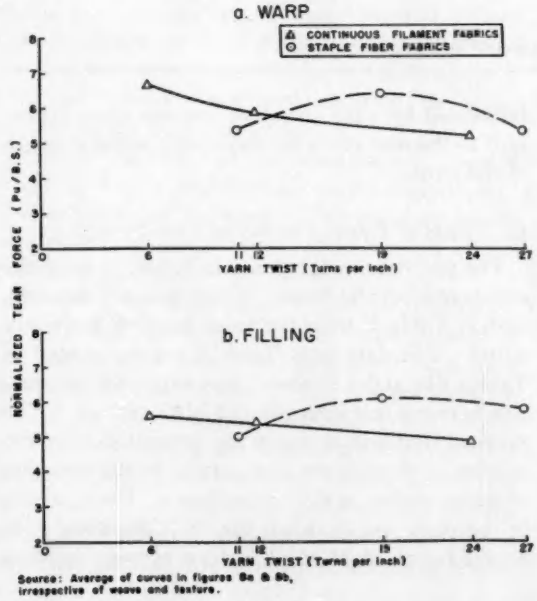
a. WARP
CONTINUOUS FILAMENT FABRICS
STAPLE FIBER FABRICS
NORMALIZED TEAR FORCE (Pw/B.S.)
YARN TWIST (Turns per inch)
b. FILLING
YARN TWIST (Turns per inch)
Source: Average of curves in figures 8a & 8b, irrespective of weave and texture.

Fig. 23. Average of normalized tear force vs. yarn twist.

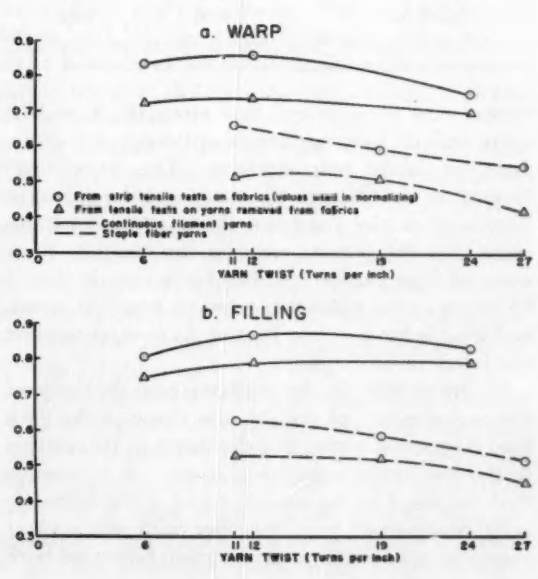
a. WARP
From strip tensile tests on fabrics (values used in normalizing)
From tensile tests on yarns removed from fabrics
Continuous filament yarns
Staple fiber yarns
YARN TWIST (Turns per inch)
b. FILLING
YARN TWIST (Turns per inch)

Fig. 24. Yarn strength vs. yarn twist.

TABLE VI*a*. Tear Strength vs. Thread Count of Yarns Perpendicular to the Direction of Tear *

		Continuous Filament			Staple Fiber		
	Nominal Count	68W (52F)	50W (52F)	32F (50W)	68W (52F)	50W (52F)	32F (50W)
	Actual Count	74W (42F)	58W (47F)	34F (56W)	75W (51F)	59W (50F)	32F (56W)
	T.E. (in.-lb/in.)	5.24	5.43	5.40	4.09	4.08	3.38
1/1	P_u	2.84	2.83	3.21	2.05	2.00	1.94
	P_u/B.S. (lb/lb)	3.72	3.44	3.86	3.84	3.40	3.37
	Actual Count	77W (55F)	58W (54F)	34F (57W)	77W (51F)	59W (51F)	32F (58W)
	T.E.	8.71	8.58	9.88	6.58	6.18	7.30
3/1	P_u	4.34	4.32	5.48	3.04	3.17	4.12
	P_u/B.S.	5.04	5.62	6.42	4.58	5.30	7.95
	Actual Count	77W (55F)	57W (55F)	35F (57W)	77W (52F)	58W (52F)	33F (56W)
	T.E.	12.98	15.07	—	8.31	8.98	9.07
2/2	P_u	6.43	7.29	—	4.07	4.31	5.28
	P_u/B.S.	7.35	9.16	—	6.90	7.55	10.24

* Thread count of yarns *parallel* to the direction of tear held approximately equal.

TABLE VI*b*. Tear Strength vs. Thread Count of Yarns Parallel to the Direction of Tear †

		Continuous Filament			Staple Fiber		
	Nominal Count	52F (68W)	52F (50W)	50W (32F)	52F (68W)	52F (50W)	50W (32F)
	Actual Count	42F (74W)	47F (58W)	56W (34F)	51F (75W)	50F (59W)	56W (32F)
	T.E.	5.09	5.06	7.25	3.37	3.75	5.17
1/1	P_u	2.72	2.78	3.77	1.81	1.95	2.49
	P_u/B.S.	3.29	3.29	4.50	3.04	3.52	3.88
	Actual Count	55F (77W)	54F (58W)	57W (34F)	51F (77W)	51F (59W)	58W (32F)
	T.E.	7.47	7.56	—	5.14	6.57	11.39
3/1	P_u	3.93	4.07	—	2.72	3.23	5.30
	P_u/B.S.	4.67	5.03	—	4.64	5.41	8.88
	Actual Count	55F (77W)	55F (57W)	57W (35F)	52F (77W)	52F (58W)	56W (33F)
	T.E.	8.85	11.22	—	5.63	7.25	—
2/2	P_u	4.97	6.64	—	3.08	4.17	—
	P_u/B.S.	6.06	7.94	—	5.25	6.88	—

† Thread count of yarns *perpendicular* to the direction of tear held approximately equal.

tween yarn friction and tear strength, it will be quite difficult to determine an optimum yarn structure for fabric tear strength. The helix angle formed by the fibers in the yarns and the degree of flattening of the yarn may be important parameters. At the present stage in the research, however, all that can be specified for a yarn is that it be strong, even when subjected to repeated stress, and that it have as low friction as possible against the fabric or other yarns.

In the section on the mathematical synthesis of the tear diagram of the del, the shape of the yarn load-elongation curve was discussed in its relation to the tear load-elongation diagram. It is possible that the shape of the loading curve of the mechanically conditioned yarn together with the pullout characteristics of the yarn in a given fabric are both influenced by yarn structure and are more important to the tear strength than the breaking strength of the yarn.

C. Effects of Fabric Texture on Tear Strength

The test data as tabulated in Table IV show the effects of fabric textures. These data are summarized in Table V with the twist subdivisions eliminated. The data from Table V are rearranged in Tables VI*a* and *b* to show more explicitly the relation between tear strength and fabric texture. The nominal and actual count are presented with the number of threads per inch parallel to the direction of tear contained within parentheses. For example, in the plain weave, when the 68 × 52 fabric with actual count of 74 × 42 is torn across the warp

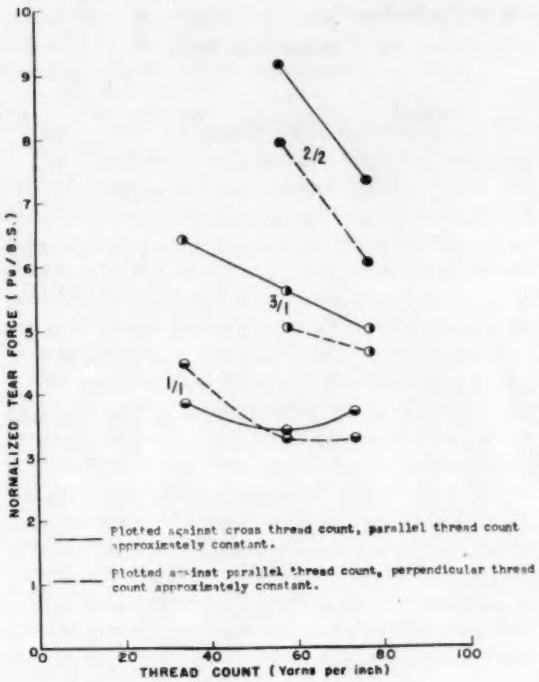
NORMALIZED TEAR FORCE (Pw / B.S.)
THREAD COUNT (Yarns per inch)
2/2
3/1
1/1
Plotted against cross thread count, parallel thread count approximately constant.
Plotted against parallel thread count, perpendicular thread count approximately constant.

Fig. 25a. Normalized tear force vs. thread count: continuous-filament fabrics.

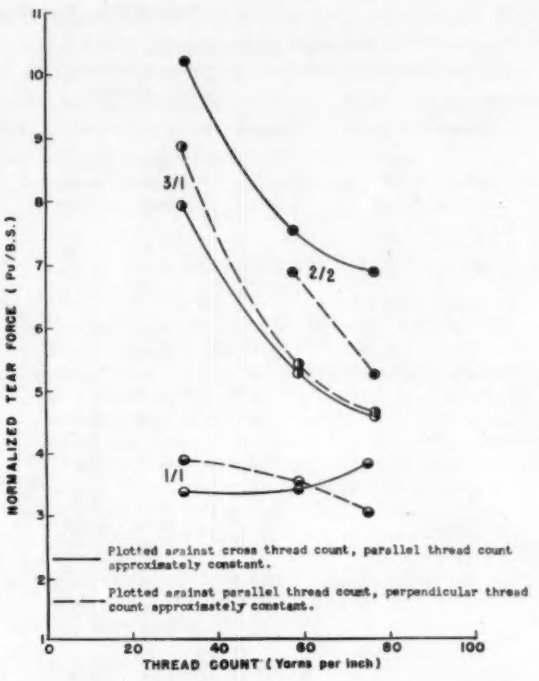
NORMALIZED TEAR FORCE (Pw / B.S.)
THREAD COUNT (Yarns per inch)
3/1
2/2
1/1
Plotted against cross thread count, parallel thread count approximately constant.
Plotted against parallel thread count, perpendicular thread count approximately constant.

Fig. 25b. Normalized tear force vs. thread count: staple fiber fabrics.

threads, there are 74 warp threads per in. (which are being torn across) and 42 filling threads parallel to the direction of tear. Figures 25*a* and *b* show the normalized tear force plotted against the thread count of the yarns perpendicular to the direction of tear and against the thread count of the yarns parallel to the direction of tear.

In both the twill and the basket weave, there is a distinct loss in tear strength as the thread count in *either* direction increases. This effect occurs for both the continuous-filament fabrics and the fabrics constructed of staple-fiber yarns.

However, the plain-weave fabrics act differently. When plotted against the thread count parallel to the direction of tear, the normalized tear force decreases as the number of threads per inch increases for both continuous-filament and staple-fiber fabrics. When the normalized tear force for the staple-fiber plain weaves is plotted against the thread count of the yarns perpendicular to the direction of tear, the same trend is observed, i.e., a reduction of tear strength with increasing thread count. In the continuous-filament plain weave this trend does not evidence itself. On the contrary, whether the plain weaves are examined neglecting twists or fabric by fabric, there seems to be no distinct trend, although the fabric with the lowest thread count in the cross-direction seems to be the strongest in tear.

This anomaly in the behavior of the continuous-filament plain weave is probably attributable to factors other than thread count, such as yarn crimp and yarn flattening (see Table VII). It is probable, therefore, that the normalized tear force should be investigated as a function of the corrected warp and filling cover factors rather than as a function of the thread counts alone [4]. It is planned to do this in future work.

The normalized tear force was used for this study in an attempt to eliminate the effect of the individual yarn strength itself. If the tear energy or tear force were used the trends would be slightly different, at least for the plain weaves, but the normalized tear force seems to be a better criterion of tear performance, especially when fabrics com-

TABLE VII. Yarn Crimps in Fabrics Studied (%)

Continuous-Filament Fabrics					Staple-Fiber Fabrics				
Nominal Texture	Twist (t.p.i.)	Weave	Crimps (w)	Crimps (f)	Nominal Texture	Twist (t.p.i.)	Weave	Crimps (w)	Crimps (f)
		1/1	8.00	6.28			1/1	6.56	9.13
	6	3/1	1.46	9.90		11	3/1	1.72	10.16
		2/2	0.49	9.26			2/2	0.53	12.22
		1/1	10.40	5.72			1/1	11.34	8.27
68×52	12	3/1	3.49	8.39	68×52	19	3/1	4.63	9.63
		2/2	1.41	9.43			2/2	2.35	11.53
		1/1	9.69	3.32			1/1	12.36	8.13
	24	3/1	6.88	8.78		27	3/1	4.65	10.40
		2/2	4.05	6.90			2/2	2.55	9.11
		1/1	2.04	11.62			1/1	0.85	16.20
	6	3/1	0.77	8.62		11	3/1	0.19	13.48
		2/2	0.50	8.99			2/2	0.00	10.02
		1/1	3.44	9.75			1/1	4.33	15.37
50×52	12	3/1	0.38	12.40	50×52	19	3/1	1.18	14.99
		2/2	0.44	10.50			2/2	0.81	12.74
		1/1	6.67	8.15			1/1	5.90	12.93
	24	3/1	3.19	12.20		27	3/1	1.99	15.76
		2/2	0.73	11.10			2/2	0.36	14.45
		1/1	1.54	8.18			1/1	0.55	11.98
	6	3/1	0.83	8.08		11	3/1	0.16	7.98
		2/2	0.61	6.55			2/2	0.01	8.80
		1/1	1.37	8.76			1/1	3.56	10.48
50×32	12	3/1	0.62	10.10	50×32	19	3/1	0.99	12.46
		2/2	0.44	7.79			2/2	0.99	9.97
		1/1	7.24	3.77			1/1	4.31	7.61
	24	3/1	2.82	7.72		27	3/1	0.72	11.92
		2/2	1.52	7.52			2/2	0.52	9.91

prised of yarns of different tensile strengths are being compared.

Since the cover factors of a fabric have been shown to be of considerable importance in tear strength, most of this analysis will deal with the relationships between tear strength and the cover factors parallel and perpendicular to the direction of tear. The data, however, have been tabulated and plotted against the number of threads per inch in the warp and filling directions. One of the objectives of the future work on this project will be the quantitative analysis of these data as a function of the cover factors of the fabric.

The cover factor in the direction of tear controls the amount of jamming which occurs ahead of the del and also the pullout force of the yarns parallel to the tear. Thus the tear strength should increase as the cover factor goes down in the direction of tear. As the cover factor parallel to the tear decreases, the amount of trellis action and jamming near the del also increases, further strengthening the del system. Just what the relationship is between the tear strength and each of these cover factors has not yet been determined quantitatively but the general trends have been shown by the data as plotted in Figure 25*a* and *b*.

As also indicated by these data, there is a definite effect attributable to the types of weave. For the basket weave, in both the continuous-filament and the staple-fiber fabrics, the tear strength increases much faster for decreasing texture than in the plain-weave fabrics. There is reason to suppose that some type of weave factor, such as described by Backer [1], may be another important parameter

influencing, or perhaps replacing, the "dimensional stability in the plane of the fabric" as used in this discussion.

IV. Conclusions

The mechanics of a woven fabric undergoing tongue tear have been analyzed from the load-elongation curve of the individual yarn through the del geometry to the synthesis of the load-elongation diagram of the del structure. The effects of the tails and the fabric structure in parallel with the del were studied and finally all three components were examined as they combine into one system.

The purpose of this theoretical work was to set up hypotheses which could be checked against experimental data. Such hypotheses make for a more scientific approach to testing and, when modified by the results of the experimental check, may illuminate some of the mechanics involved. Of more immediate practical importance, however, is the contribution of the theoretical analysis to the predictability of tear strength, both for analysis of fabrics already constructed and for the design of new fabrics. These objectives have guided both the experimental and theoretical phases of this work. From the results as described in this report, it should be possible to evaluate tongue-tear tests more scientifically and to design high tear-strength fabrics with a better appreciation of the relative importance of the parameters involved.

Last but not least, further research in tear should be able to benefit from the results included here.

Literature Cited

1. Backer, S., "Cover Factor Adjustment for Twill Weaves" (Letter to the Editor), Textile Research Journal **22**, 435–436 (1952).
2. Gardner and Barnes, *Transients in Linear Systems*, Wiley and Sons, New York, Vol. I, Chap. IV, Sec. 7; Chap. VII, Sec. 5 (1942).
3. Krook and Fox, "Study of Tongue-Tear Test," Textile Research Journal **15**, 389–402 (1945).
4. Painter, E. V., "Mechanics of Elastic Performance of Textile Materials; Graphical Analysis of Fabric Geometry," Textile Research Journal **22**, 153–168 (1952).
5. Preisman, Albert, *Graphical Constructions for Vacuum Tube Circuits*, McGraw-Hill, New York, 237 pp., illus. (1943).

Manuscript received April 15, 1955.

Rate of Dyeing[1]

John H. Skinkle

Professor of Chemistry, Lowell Technological Institute, and Executive Director, Lowell Technological Institute Research Foundation

As part of a continuing investigation of the kinetics of dyeing, the author and certain of his students have for a number of years been obtaining accurate time-exhaustion measurements under carefully controlled conditions. These data have been principally determined on wool because it was thought that the mechanism of fiber-dye combination was more precisely known for this fiber than for any other; this is still believed to be true although the degree of certainty of this knowledge is not as great as had been previously thought.

Initial attempts to verify conventional diffusion formulas by means of the data having consistently failed, it was thought advisable to return to fundamental principles and see whether alternative rate-determining mechanisms might correlate better with these data.

[1] Presented at the Fall Meeting of the Fiber Society in Montreal on September 14, 1954.

Part I: The Driving Pressure Concept

In the rate of transfer of either energy or matter a general relationship exists:

$$\text{Rate of flow} = k\left(\frac{\text{Driving pressure}}{\text{Resistance}}\right)$$

The simplest example of this relationship is Ohm's

Law as applied to direct current where rate of flow (current) equals electromotive force (voltage) divided by resistance (ohms). In this particular case, and within reasonable limits, the resistance remains constant and, if the voltage is also kept constant, then a constant current results. Under other conditions, however, resistance may not be constant and voltage also may not be constant so that a plot of current against voltage which gives a straight line in the first instance gives a curved relationship in the second. Similarly, for the flow of liquids the driving pressure is the pressure difference on the system; for the flow of vapor the driving pressure is the difference in partial pressure of the vapor exerted on the system, and for the flow of heat the driving pressure is the difference in temperature.

The Classical Diffusion Theory

Conventionally, diffusion of a dissolved substance through a solution is expressed by the Fick Equation:

$$ds/dt = -D(\Delta c/x)$$

where

s = Amount of solute diffused
t = Time
c = Concentration
x = Distance
D = "Diffusion coefficient"

and where concentration difference is constant and distance is finite; or by

$$ds/dt = -D(dc/dx)$$

when concentration varies nonlinearly with distance. In this case, the driving pressure is assumed to be difference in concentration and the resistance is distance. Since it is believed that concentration does not vary linearly with distance in the case of diffusion of dye into a fiber, the Fick Equation has been transformed into a general form in terms of measurable quantities:

$$dc_f/dt = -D(d^2c_f/dx^2)$$

where c_f = concentration of dye in fiber and D is a constant or the still more general form,

$$\frac{dc_f}{dt} = \frac{d\left(D\,\frac{dc_f}{dx}\right)}{dx}$$

when D is not a constant.

TABLE I. Test of Hill Equation on Wool Fiber (Color Index # 1054)

	Loose Fiber				Chopped Fiber		
	Data	Hill	Calc.		Data	Hill	Calc.
t	E/E_∞	kt	k	t	E/E_∞	kt	k
1	0.090	0.0013	0.0013	1	0.062	0.0008	0.0008
2	0.169	0.0055	0.0028	4	0.145	0.0037	0.0009
4	0.206	0.0090	0.0022	9	0.253	0.014	0.0016
6	0.278	0.017	0.0028	16	0.395	0.037	0.0023
8	0.336	0.026	0.0033	25	0.535	0.077	0.0031
12	0.416	0.042	0.0035	36	0.695	0.145	0.0040
20	0.546	0.079	0.0040	49	0.819	0.23	0.0047
30	0.665	0.135	0.0045	64	0.910	0.35	0.0055
40	0.745	0.175	0.0044	81	0.952	0.475	0.0059
60	0.855	0.27	0.0045	100	0.979	0.65	0.0065
80	0.911	0.35	0.0044	121	0.992	0.75	0.0062
100	0.942	0.42	0.0042	144	0.997	0.88	0.0061
120	0.965	0.55	0.0046	169	1.000	1.00	0.0059
135	0.992	0.75	0.0056				
150	0.996	0.88	0.0055				
160	1.000	1.00	0.0063				

These general equations are not capable of integration without simplifying assumptions, one of which involves the constancy of dye concentration at the surface of the fiber throughout the dyeing, and the others of which are concerned with the idealization of the geometry of the fiber and the equality of all individual fibers.

Hill's derivation [1], assuming diffusion into infinitely long cylinders of radius r, results in a series,

$$c_f/c_{f\infty} = 1 - 0.692(e^{-5.785\,kt} + 0.190e^{-30.5\,kt} + 0.0775e^{-74.9\,kt} + \cdots)$$

where $c_{f\infty}$ is concentration of dye in the fiber at equilibrium and $k = D/r^2$. The series is not readily usable and use is generally made of the equation by reference to tables or graphs of $c_f/c_{f\infty}$ against kt.

While satisfactory results have been reported for constancy of k, the author has consistently obtained poor results, as shown in Table I where the Hill Equation is tested by dyeing data of known accuracy, which will be referred to later.

The other simplification of the Fick Equation by Speakman and Smith [4] treats the dyeing of fiber, again at constant surface concentration, as diffusion of a dye into one side of a slab of infinite thickness. Under these conditions, the equation simplifies to

$$c_f/c_{f\infty} = 2(Dt/\pi)^{\frac{1}{2}}$$

According to this, a plot of $c_f/c_{f\infty}$ (or E/E_∞) against $t^{\frac{1}{2}}$ (where E = fraction of dye exhausted) should yield a straight line as long as the assumed conditions are approximated; that is, until the advancing

dye in the fiber reaches the center of the fiber or during the period of "ring dyeing"; theoretically also this straight line should start at zero time. Using actual data, a straight line usually is obtained for a portion of any dyeing when the results are plotted in this manner. Usually, however, the straight line does not begin at zero time but is preceded by an initial curved portion, so that the resulting curve is sigmoid in shape and extrapolation of the straight line usually intersects the $t^{\frac{1}{2}}$ axis.[2] Vickerstaff [5] suggests a skin effect as the cause of the initial curvature, but such a skin effect would be exerted over the whole period of dyeing and would not be confined merely to the initial stages. This initial curvature may be decreased or even eliminated by changes in the physical conditions of the dyeing experiment especially by (1) increasing the amount of agitation [3] and (2) simplifying the geometry of the fiber sample [2]. That is, yarns have less curvature than fabrics; loose fiber, less than yarns; and chopped fiber, least of all.

The use of chopped fiber plus a large amount of agitation tends to make all fibers equally and immediately accessible to the dye solution and decreases the initial curvature. This suggests that this initial curvature might be due to penetration delays, but thorough saturation with either water or blank dyebath (dyebath with all chemicals except the dye), while it decreases the curvature, does not eliminate it [2]. In other words, the sigmoid shape of the E/E_∞ vs. $t^{\frac{1}{2}}$ curve remains in nearly all cases, in spite of all attempts to eliminate it by altering presently known factors. This suggests that the curve shape differs from the theoretical for one of the following reasons:

1. One or more of the assumptions inherent in the theoretical relationship is incorrect.
2. The whole theoretical relationship is incorrect but some other relationship exists which gives a sigmoid shape when plotted in this manner.
3. The true relationship is the sum of two or more mechanisms, one of which probably is diffusion. In this case, the other mechanism would seem to be confined to the first part of the dyeing period and probably does not consist of either swelling or acid penetration, since initial treatment with a blank dyebath for a relatively long period of time does not eliminate the sigmoid shape.

[2] Some cases of intersection of the E/E_∞ axis by the straight line extrapolation are given in the literature. These are examples of the dyeing of cotton with vat dyes.

Considering the first possibility above, the theoretical model upon which the relationship

$$E/E_\infty = 2(Dt/\pi)^{\frac{1}{2}}$$

is based consists of a large number of fibers of identical composition and surface characteristics and of identical size immersed in a dyebath from which dye is migrating to the surface of the fibers at a rate such that the surface concentration of dye is constant during the dyeing process. Under such conditions, if the fiber is already swollen and has its amino groups ionized by previous treatment with a blank dyebath, dye should be immediately deposited on the surface of all the fibers equally so that the dye in the cross-sections of the fibers would appear as thin rings. Continued dyeing should produce thicker rings until the dye reaches the axis of the fiber (or the center of the cross-section). This should occur for all fibers at the same time. Continuing still further, these fully but lightly dyed fibers should continue to take up more dye—all at the same rate—until all fibers are heavily and equally dyed and finally no more dye is adsorbed. Figure 1*a* shows at the top the number of fibers which might be expected at each stage of the dyeing on examination of the cross-section. At the bottom is shown the relationship between E/E_∞ and $t^{\frac{1}{2}}$ which would result; in this plot the coordinates are reversed from their usual position to facilitate comparison with the top graph. Note that an initial straight line on the diffusion plot corresponds to the period of ring dyeing on the cross-section plot. Figure 1*b* shows the effect of either one of two variations from the model. Either some fibers differ in reactivity from the others or are less acces-

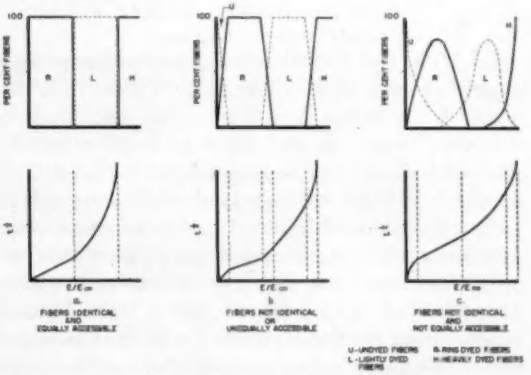

Fig. 1. Theoretical models of diffusion.

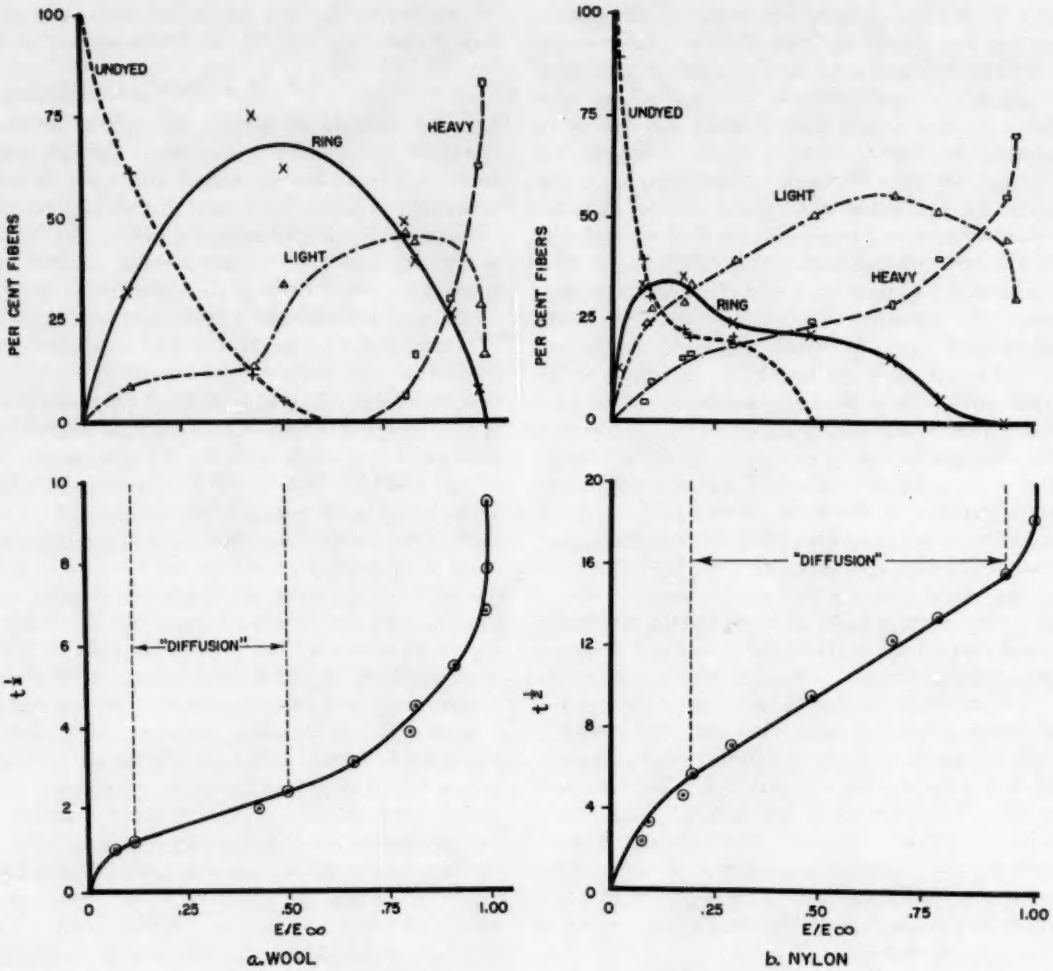

Fig. 2. Actual dyeings: *a*, Wool; *b*, Nylon.

sible. The dye initially starts ring dyeing on some fibers but some remain undyed for a short time; the result is an initial period in which two kinds of fibers are present so that the slope is different from that of Figure 1*a*. Then a second period follows in which all fibers are ring dyed, which corresponds to the first slope of Figure 1*a*; then follows further curvature after ring dyeing ends. Figure 1*c* represents deviation from the model in *both* of the manners above, and to a larger degree, so that at all times during the dyeing there are at least two, and sometimes three, types of dyed fibers in the cross-sections. In this case the period during which ring dyeing is at a maximum (although not 100%) may correspond to a straight-line portion on the diffusion plot, but is preceded by a curved portion, and is unlikely to have the same slope as in Figure 1*a* or 1*b*. However, the presence of a straight-line portion of the diffusion plot corresponding in position to the period of maximum ring dyeing would at least indicate that diffusion is the principal mechanism involved, even if the actual fibers only approximate the model fibers. It would also follow that the nearer the actual fibers approached the properties of the model fibers, the closer should be the correspondence between the straight line of the

diffusion plot and the period of maximum ring dyeing. That this is not the case may be seen in Figures 2*a* and 2*b*. Wool, which has a variable diameter, variable chemical composition, and a variable surface, has its "diffusion period" coincide fairly well with the period of ring dyeing, although the number of undyed fibers and lightly but completely dyed fibers are by no means negligible. Nylon, on the other hand, which is much more uniform in size, composition, and surface, shows much poorer coincidence of "diffusion period" with ring dyeing; in fact, ring dyeing has passed its maximum and is decreasing before the so-called "diffusion period" begins. During the "diffusion period" of nylon the fibers are approximately 50% fully but lightly dyed, 30% fully and heavily dyed, and only about 20% ring dyed.

Based on the above reasoning, it would seem that one or more of the assumptions used in the

$$E/E_\infty = 2(Dt/\pi)^{\frac{1}{2}}$$

simplification are incorrect and that the straight-line portion of the curve is related only by chance if at all to that period of dyeing which might be considered as principally diffusion.

Literature Cited

1. Hill, *Proc. Roy. Soc.* (*London*) **104B**, 39 (1928).
2. Setty, *L. T. I. Thesis* (1953).
3. Shippee, *L. T. I. Thesis* (1952).
4. Speakman and Smith, *J. Soc. Dyers Colourists* **52**, 121 (1936).
5. Vickerstaff, *Physical Chemistry of Dyeing*, Interscience Publishers, New York, p. 240 (1950).

Manuscript received March 8, 1933.

Microwave Dielectric Measurements on Single Fibers[1]

J. J. Windle and T. M. Shaw[2]

Western Utilization Research Branch, Agricultural Research Service, United States Department of Agriculture, Albany 10, California

Abstract

Microwave techniques which have proved successful at frequencies of 3,000 and 9,300 Mc for the determination of the complex dielectric constant of fiber bundles have been extended to include a frequency of 26,000 Mc, where for the first time measurements on a single wool fiber have proved to be feasible. Such measurements make it possible to compare directly the results of electrical and mechanical measurements on the same single fiber. In addition, the single-fiber technique has provided a convenient, rapid, and nondestructive method for the determination of the average mass of adjacent 1-cm sections of the fiber along its length. Variations as large as two-fold in mass per unit length are sometimes encountered within a single wool fiber. The occurrence of these variations and their effect upon mechanical measurements are discussed.

Introduction

The dielectric properties of a material are a manifestation of interactions between an applied electric field and the electrons, atoms, and molecules of the substance. These properties are not observed directly but are inferred from effects of the specimen upon some parameter of the measuring apparatus, i.e., the capacitance and resistance of a condenser or the frequency or Q-factor of a resonant cavity. The dielectric properties are utilized in elucidating facts about the molecular structure of the material. It is usually the case, however, that changes in the apparatus parameter also depend upon such macro-

[1] Portions of this paper, under the same title, were presented at the meeting of the American Physical Society, Berkeley, California, December 28–30, 1954.

[2] Present address, Southwest Research Institute, San Antonio, Texas.

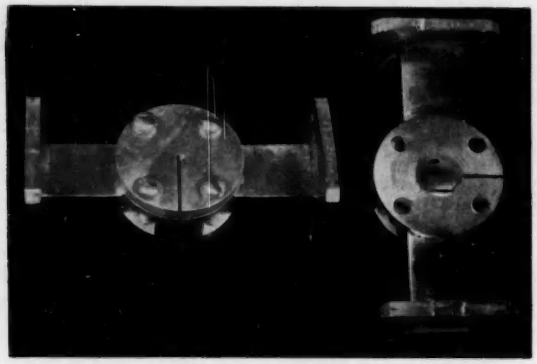

a b

Fig. 1. *a*, Photograph of slotted cylindrical cavity resonant at 26,000 Mc; *b*, top plate has been removed to show interior details.

scopic properties of the specimen as its density or its shape. Thus when the dielectric properties are known, the dielectric apparatus frequently can be used to characterize the macroscopic properties of the specimen. In this paper the techniques developed to measure the dielectric properties of single wool fibers at 26,000 Mc are discussed and are applied to the determination of the mass per unit length and its variation along the fiber. This work is part of a study of the dielectric properties of wool-water systems, for which the results obtained at 3,000 and 9,300 Mc have already been published [6]. The dielectric properties of the wool-water systems at 26,000 Mc will be published elsewhere.

Experimental

A microwave cylindrical-cavity resonator operating in its fundamental mode has almost ideal characteristics for dielectric measurements on fibers. In this mode the electric field is axial with its maximum intensity along the axis of the cylinder. For a single fiber or a specimen composed of a bundle of parallel fibers placed coaxially within the cavity and extending from top to bottom, the electric field is everywhere tangential to the fiber surface. When the radius of the specimen is small compared to the cavity radius so that the fibers are in a region of essentially constant electric field, a particularly simple formula (equation 1) relates the observed change in resonant frequency to the dielectric constant of the fiber substance.

Although the effect of a single fiber on the resonant frequency of a cavity can be detected at both

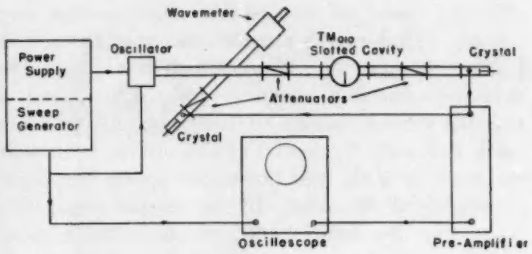

Fig. 2. Schematic diagram of test setup used at 26,000 Mc for dielectric measurements on single fibers.

3,000 and 9,300 Mc, fiber bundles composed of a few hundred to a thousand or more parallel fibers are required to get frequency changes within the sensitivity of the wavemeters employed. For the same percentage change ($\sim$0.03%) in resonant frequency, however, fewer fibers are required when using the 9,300-Mc cavity because of its smaller diameter. The diameter and, therefore, the resonant frequency of a cavity suitable for measurements on a single fiber can be estimated from the requirements at 3,000 and 9,300 Mc for measurements on fiber bundles. The factors which relate the observed change in resonant frequency to the dielectric constant of the material are given in equation 1[3]

$$\Delta f = 1.855\ (\epsilon' - 1)(c/a)^2 f_0 \qquad (1)$$

where Δf is the change in resonant frequency f_0 of a resonator of radius a when a specimen of radius c and dielectric constant ϵ' is coaxially inserted. (For specimens of irregular cross section, the radius is defined as that of a cylindrical specimen of the same length, mass, and density.)

Equation 1 is valid only when the specimen radius is small compared to the radius of the resonant cavity. For the fiber bundles used at 3,000 and 9,300 Mc a ratio of specimen to cavity radius of the order of 1:200 was found to be satisfactory. If this ratio is to be maintained for a single fiber with a radius of the order of 20 μ, then the radius of the corresponding cavity resonator would have to be of the order of 0.40 cm. A resonator of this radius would have its fundamental frequency near 30,000 Mc. Dielectric measurements on single wool fibers should be feasible, therefore, at microwave frequencies in the neighborhood of 30,000 Mc.

A cylindrical resonator with a radius of 0.44 cm, resonant at a frequency of 26,000 Mc, has been con-

[3] See Appendix for derivation of this equation.

structed. This frequency was chosen because the microwave oscillator available had its maximum output at this frequency. Figure 1 shows two photographs of this resonator. The top plate has been removed in one photograph to show interior details. The cavity has an internal height of 1 cm. This height was chosen to give the highest Q-factor commensurate with the suppression of all unwanted modes of resonance. The top surface of the cavity has about a 1° bevel from the center to the periphery so that the top plate, which is flat, will make good electrical contact at the inside surface. This was found to be necessary because the Q-factor depends strongly upon the excellence of this contact. The cavity is provided with a narrow (0.040 cm) radial slot to facilitate the introduction and removal of the fiber. Such a slot can be considered as a perturbation of the cavity boundaries and only slightly alters the Q-factor and resonant frequency of the cavity [7]. Finally, the cavity has been silver plated to improve the surface conductivity and, therefore, the Q-factor. The air-filled resonator has a Q-factor of approximately 60% of the theoretical value for a resonator of these dimensions. A single wool fiber causes a frequency shift of the order of 5 Mc, which can be measured with a precision of about 2% by means of an absorption-type wavemeter provided with an optical lever.

Figure 2 is a schematic diagram of the test setup. The microwave energy from a Raytheon QK 277 klystron is passed by means of a system of wave guides and attenuators to the resonant cavity and from there to a 1N26 crystal detector. The output frequency of the klystron is measured by means of an absorption-type wavemeter [2]. Both the cavity and wavemeter outputs are amplified by means of a preamplifier provided with a differential input balanced to ground and displayed in opposition upon an oscilloscope. The klystron and the horizontal plates of the oscilloscope cathode-ray tube are swept by means of a sawtooth voltage obtained from the sweep generator in the klystron power supply.

Results and Discussion

The single-fiber cavity resonator can be used to study variations in fiber properties which may occur along the length of a single fiber. This is possible because the internal height of the cavity is small compared to the length of a wool fiber. (This height can be made even smaller than the 1 cm of the present cavity, but at a sacrifice of sensitivity owing to a reduction in cavity Q-factor.) The effects of different sections of the same fiber upon the resonant properties of the cavity can be compared rapidly and nondestructively by observing the change in resonant frequency due to each section as it is passed through the cavity.

One property that was investigated by this method was the linear density of wool and its variations along the length of the fiber. It was observed that the change in resonant frequency, Δf, due to different sections of the same fiber sometimes varied by as much as a factor of two. Referring to equation 1, such changes in Δf could be due to variations in the dielectric constant of the fiber substance, in its density, or in its linear density (i.e., the mass per unit length since $c^2 = (m/l)/(\rho\pi)$ where m/l is mass per unit length and ρ is the density). Studies that we have made on the density and dielectric constant indicate that these properties do not vary significantly between fibers of different wools; therefore it would seem unlikely that variations in these parameters within a single fiber would be large enough to cause a two-fold change in Δf. It is well-known, however, that wool fibers are neither perfectly circular nor uniform filaments; therefore, variations in cross-sectional area or mass per unit length within a single fiber may be large enough to account for the observed changes in Δf.

If the assumption is made that the density and dielectric constant of the fiber substance are uniform, then Δf will be proportional to the average mass per unit length of the fiber section included within the cavity. By measuring the change in resonant frequency as successive sections of the fiber are passed through the cavity, the average mass per unit length of each section can be determined. The average mass of adjacent 1-cm sections of a single Lincoln-type wool fiber has been determined by this method. To confirm the result, the same fiber was cut into the same 1-cm sections, and each section was weighed by means of a microbalance. The results are shown in Figure 3. At the present time the estimated experimental error in the microwave result is about twice that for the microbalance, as shown by the vertical line through the experimental points. Within this uncertainty the correlation is good and establishes the feasibility of this method and shows that the assumption of uniform density and dielectric constant along the fiber is correct.

Figure 3 also shows that this Lincoln fiber, representing a year's growth, has superimposed upon the small irregularities in linear density or cross-sectional area a gross variation in which the mass per unit length has decreased at one point by about a factor of two. This is by no means unique for this wool. A similar type of variation (differing only in degree) has also been observed in Suffolk, Rambouillet, Navajo, and Columbia wools. On the other hand, when evidence of this gross variation was sought in extra long Merino fibers representing several years' growth it was not found. The five wools showing the gross variation were all grown in California under the same environmental conditions. The Merino was a foreign wool of unknown origin. The position of the region of smallest cross-sectional area in each of the five wools occurred at approximately the same relative distance ($\sim\frac{1}{3}$) from the root end. If uniform increase in length per unit time is assumed, then this point corresponds to the months of December or January in the yearly growth period. Unfortunately, further details concerning the environmental conditions under which these wools were grown are unknown, and therefore the possible causes for the thinning of the fibers cannot be ascertained.

Such irregularities in the mass per unit length must profoundly influence the mechanical properties of the fibers. The proper interpretation of the stress-strain curves, for example, must take these variations into account. The determination of the average mass per unit length of a fiber by means of the vibroscope will be in error if the fiber does not have a uniform mass per unit length [4]. In some instances the vibroscope can be used to detect the presence of nonuniformities in cross section, but in other cases the presence of gross irregularities can go almost unnoticed. As an example of this, a vibroscopic determination of the average mass per unit length was made on a selected 4-cm section of a Lincoln fiber for which the average mass per unit length of adjacent 1-cm sections had been determined by means of the cavity resonator. The 4-cm section was especially selected to include a region of large cross-sectional area variation. Figure 4 is a schematic profile drawing of this section. The average mass per unit length for the whole 4-cm section as determined by the vibroscope was 18.5 μg/cm. The average mass per unit length of each 1-cm section in micrograms per centimeter as determined by the resonant cavity is given by the numbers in parentheses in Figure 4. The average mass per unit length for the whole section as found by the vibroscope is practically identical to the average for sections 1–3 as determined by the resonant cavity.

In this example section 4 had very little influence upon the vibroscope result; yet section 4 is the most critical portion of the fiber with respect to a mechanical measurement. The stress-strain curve for this fiber as determined at a constant rate of loading on the stress-strain apparatus in use at this laboratory [5] is shown in Figure 5. This curve differs from the normal stress-strain curve for wool (dashed curve in Figure 5) in the appearance of the so-called secondary yield point. The occurrence of the secondary yield point can be understood from the following qualitative argument. In the usual method of procedure, the rate of loading is set by the average cross-sectional area of the fiber as determined from the vibroscopic result. For this particular fiber, this results in one quarter of the fiber (section 4) being subjected to a larger stress than the other three sections because of its smaller cross-sectional area; therefore, as the fiber is stretched,

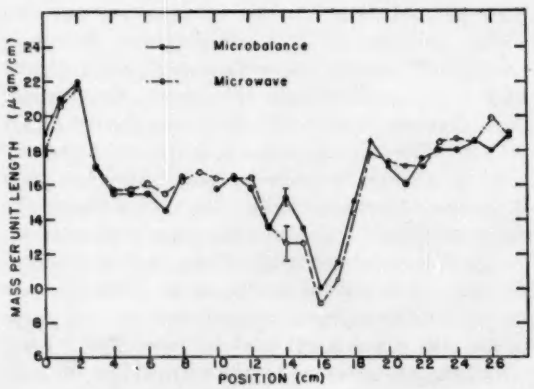

Fig. 3. Mass per unit length of single Lincoln fiber vs. position along fiber determined by resonant cavity (broken line) and by microbalance (solid line). The gap in the microbalance curve at 9 cm results from the loss of this fiber segment during the microbalance measurements.

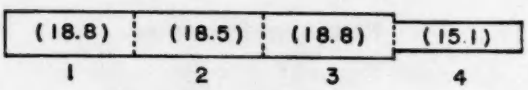

Fig. 4. Schematic profile diagram of fiber section which showed a secondary yield point in the stress-strain curve. The numbers in parentheses are the average mass per unit lengths of the numbered sections as determined by means of the resonant cavity.

section 4 will pass its yield point (primary yield point on curve) and begin to "flow" before the other sections reach their yield point. When the yield stress for the other section of the fiber has been reached, another yield point due to this portion of the fiber appears in the stress-strain curve, and this has been called the secondary yield point.

In further support of this explanation, other fibers which previously had shown secondary yield points were then checked for uniformity in the cavity resonator and each showed marked irregularities. Fibers which showed a normal stress-strain curve were found to be much more uniform. This result tends to confirm the analysis of other researchers [3] that the occurrence of a secondary yield point is a result of nonuniform stress along the fiber due to variations in the fiber cross section and is not of molecular origin.

From these examples it is evident that care must be used in selecting fibers for certain mechanical tests to insure uniformity of cross section throughout the filament. The cavity resonator provides a simple and rapid method for selecting such fibers. By merely passing the fiber through the cavity and observing the constancy of Δf, the uniform fibers can be quickly separated from the nonuniform ones. If this is the only information desired a more simplified test setup than the one shown in Figure 2 should be feasible.

Acknowledgment

The authors wish to thank R. A. O'Connell of the Wool Unit of this Laboratory for many stimulating discussions and for performing the stress-strain measurements and L. M. White of the Analytical Unit for the microbalance determinations.

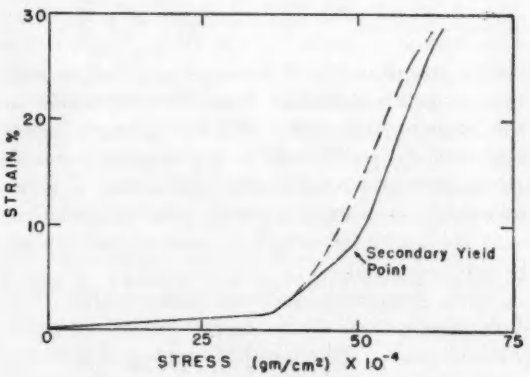

Fig. 5. Stress-strain curve at constant rate of loading for irregular Lincoln fiber. The dashed curve is the normal stress-strain curve for a uniform wool fiber.

Mathematical Appendix

Bethe and Schwinger [1] have developed a perturbation theory which gives the change in resonant frequency (f_0) of a cavity due to some small change in the cavity. If the change is due to the presence of some material of dielectric constant ϵ' with permeability equal to 1, then

$$\frac{\Delta f}{f_0} = (\epsilon' - 1)\frac{\int_v \vec{E}_1 \cdot \vec{E}_2 \, dv}{2\int_V E_1^2 \, dV} \tag{2}$$

where v and V are the volumes of the dielectric and cavity respectively, and E_2 and E_1 are the perturbed and unperturbed electric field intensities. When E_2 can be obtained from E_1 then equation 2 can be evaluated. For the case where the electric field is everywhere tangential to the surface of the dielectric, E_2 can be set equal to E_1. (Ideally the dielectric should end with the field lines on the cavity walls. In practice this condition is only approximated since the fibers actually extend beyond the walls.)

For a cylindrical resonant cavity operating in the TM_{010} mode the solution of Maxwell's equations expressed in cylindrical coordinates gives for the electric field $E_1 = AJ_0(kr)$ (the time dependence $e^{j\omega t}$ is understood). J_0 is a Bessel function of the first kind and A is a constant involving the amplitude of the field and permeability and dielectric constant of free space. Substituting for E_1 into equation 2 and integrating gives

$$\frac{\Delta f}{f_0} = (\epsilon' - 1)\left\{\frac{(c^2/2)[J_0^2(kc) + J_1^2(kc)]}{a^2[J_0^2(ka) + J_1^2(ka)]}\right\} \tag{3}$$

where c and a are the radii of the cylindrical dielectric specimen and cavity respectively. Now $k = 2.405/a$ and so

$$J_0(ka) = 0, \quad J_1(ka) = 0.519$$

Thus equation 3 becomes

$$\frac{\Delta f}{f_0} = (\epsilon' - 1)\left\{\frac{Bc^2/2}{a^2(0.519)^2}\right\} \tag{4}$$

where $B = [J_0^2(kc) + J_1^2(kc)]$. For thin specimens in the limit as $c \to 0$, $B \to 1$ so equation 4 becomes

$$\frac{\Delta f}{f_0} = (\epsilon' - 1)\frac{c^2}{a^2}\frac{1}{0.539} \qquad (5)$$

or rewriting

$$\Delta f = 1.855(\epsilon' - 1)(c/a)^2 f_0$$

which is equation 1 in the text.

Literature Cited

1. Bethe, H. A., and Schwinger, J., *NDRC Report D1–177*, U. S. Dept. Commerce, Office of Tech. Services, PB 18340 (March, 1943).
2. Bleaney, B., Loubser, J. H. N., and Penrose, R. P., *Phy. Soc. (Lond.) Proc.* **59**, 185 (1947).
3. Burte, H. M., TEXTILE RESEARCH JOURNAL **18**, 635 (1948).
4. Montgomery, D. J., *J. Appl. Phys.* **24**, 1092 (1954).
5. Preusser, H. M., O'Connell, R. A., Yeiser, A. S., and Lundgren, H. P., TEXTILE RESEARCH JOURNAL **24**, 118 (1954).
6. Windle, J. J., and Shaw, T. M., *J. Chem. Phys.* **22**, 1752 (1954).
7. Windle, J. J., and Shaw, T. M., *Phys. Rev.* **93**, 952 (1954) (A).

Manuscript received April 18, 1955.

Molecular Properties of Milkweed Cellulose

T. E. Timell and J. L. Snyder

McGill University and Pulp and Paper Research Institute of Canada

Abstract

The seed hairs of the common milkweed (*Asclepias syriaca*, L.) have been found to contain 39.6% alpha-cellulose, 35.3% pentosan (chiefly xylan), and 15.1% lignin. The alpha-cellulose fraction was entirely composed of anhydroglucose, the hemicellulose portion of anhydroxylose units. The original material, in addition, also contained minor amounts of arabinose and uronic acid residues.

Direct nitration of the untreated fibers gave a cellulose nitrate with glucose as the only constituent sugar in a yield corresponding to a content of 29% cellulose in the original material. The average degree of polymerization of the nitrate was 5800, as determined viscometrically with corrections applied for the effects of rate of shear and nitrate substitution on the intrinsic viscosity.

Fractional precipitation of the nitrate derivative was carried out with acetone water as the solvent-nonsolvent system. The chain-length distribution had only one peak and exhibited a considerable right-hand skewness. The lower D.P. limit was 2500 and the upper 8000, with the maximum located at a D.P. of 4000.

SEED hairs have, except for cotton, found little use for either textile or other purposes. The better-known sources include kapok, tree cotton, cat-tail floss, milkweed floss, and cotton grass [17]. Of these, only the first and the last genus seem to have been more thoroughly investigated. Zapf [18], studying the seed fibers from kapok (*Ceiba petandra*), found this material to contain 35% cellulose, 45% pentosan, 18% lignin, and an undetermined amount of uronic acids. Extraction with methanol and bleaching with chlorine dioxide gave in 35% yield a cellulose material which still, however, contained 11% pentosan and 3.6% uronic acids. When this product was nitrated and fractionally precipitated, a chain-length distribution was obtained which contained three maxima within a D.P. range of 70 to 2200. It is very probable, however, that the purification of the original material had resulted in a considerable degradation, and the work therefore would seem to offer little information as to the molecular weight or polymolecularity of the native material.

Gralén, Berg, and Svedberg [4] investigated the fibers from various species of Swedish cotton grass (*Eriophorum*). These seed hairs contained approximately 40% cellulose, 30% pentosan, mostly xylan, and 3–5% uronic acids. Methoxyl groups were also present but no lignin or methyl pentoses. The ni-

trated material was only partly soluble in acetone, a property that was ascribed to the high content of hemicelluloses. Extraction with 18% aqueous sodium hydroxide left 29% of the material undissolved. Sedimentation-diffusion measurements on the cuprammonium solution of this alpha-cellulose suggested a molecular weight of 710,000. In view of later experience, however, this value was probably much too high.

Milkweed floss is a material which attained some commercial importance in the United States during the Second World War as a substitute for kapok. These seed fibers consist of a single cell and are outstanding for luster and softness [17]. Like kapok, milkweed floss has a low density and is not easily wetted, and it is therefore an excellent material for lifebelts and similar equipment. Most of it is obtained from the common milkweed (*Asclepias syriaca* L.) which grows all over the continent. This species has been reported to contain approximately 36% alpha-cellulose and 20% lignin [10], whereas another (*A. cornuti*) has been found to analyze for 39.9% alpha-cellulose, 31.2% pentosans, and 18.2% lignin [5].

The present investigation was mostly concerned with the physical properties of the cellulose component of the common milkweed, i.e., its molecular weight and molecular-weight distribution. In a following study the hemicellulose portion will be more closely studied.

Results

Freshly collected milkweed fibers were extracted with ethanol benzene and cold water. The results of a series of analyses, all carried out by standard methods, are given in Table I. Alkaline extraction of chlorite holocellulose indicated a lower alpha-cellulose content than a similar treatment of a chlorinated material, and this was probably due to loss of carbohydrates in the former case. The values obtained were rather close to those reported previously for *Asclepias cornuti*. Qualitative analysis by paper chromatography of the hydrolyzates from the alpha-cellulose and hemicellulose portions showed that only glucose was present in the former and only xylose in the latter fraction, whereas the arabinose and uronic acid residues also present in the original material had been removed. These results were in marked contrst to those noted by similar treatment of wood [15] and pulps, where such a clear separation apparently is not possible.

TABLE I. Analytical Data for Milkweed Floss, Based on Extractive-Free Oven-Dry Fibers

Material	Per Cent
Chlorine holocellulose	83.7
Alpha-cellulose, chlorine method	39.6
Alpha-cellulose, chlorite method	38.0
Pentosan	35.3
Lignin	15.1

The degree of polymerization was estimated viscometrically, using the relationship recently developed by Conrad and co-workers [9] between the D.P. and the intrinsic viscosity of a series of cellulose nitrates:

$$\text{D.P.} = K \cdot [\eta]_{500}$$

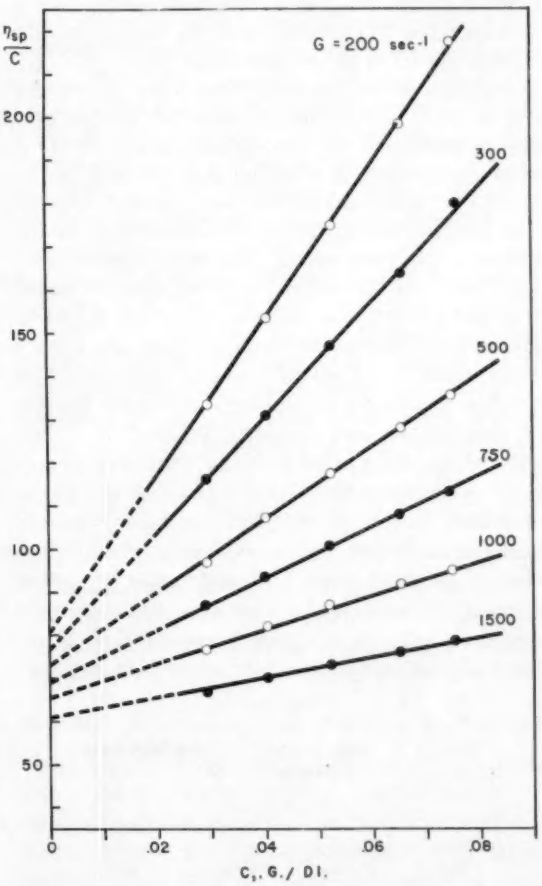

Fig. 1. Relation between reduced viscosity and concentration at various rates of shear for an ethyl acetate solution of nitrated milkweed cellulose.

In this equation, D.P. was determined from sedimentation-diffusion data and $[\eta]_{500}$ was the intrinsic viscosity of the nitrate (nitrogen content, 13.60%) in ethyl acetate as measured at a constant rate of shear of 500 sec^{-1}. The procedure used in the present study for obtaining $[\eta]_{500}$ has been described in detail previously [12]. Triplicate experiments were carried out, which all checked well. Figure 1 shows a typical plot of reduced viscosities against concentrations, indicating the great influence of the shear rate on the intrinsic viscosity. After correction for the nitrate substitution [6], the intrinsic viscosity averaged 72.5 dl/g, corresponding to a D.P. of 5800 [9]. The intrinsic viscosities of the fractions isolated in the fractionation experiments as well as those in Table I were measured in acetone with a Cannon-Fenske viscometer and converted to the corresponding D.P. values with the help of a calibration curve, described elsewhere [15].

Nitration of the extractive-free fibers was carried out at +6°C with a standard nitration mixture containing nitric acid, phosphoric acid, and phosphorus pentoxide, known to effect no degradation of cellulose [2]. After purification, the nitrated material was exhaustively extracted with acetone and the solutions poured into water. The percentage of cellulose, based on the original material, was calculated from the amount and nitrogen content of the white fibrous precipitate. The results of three preliminary experiments are given in Table II. The yield of cellulose apparently did not vary within the interval of time studied and amounted to 28–29%. Only 75% of the alpha-cellulose in the fiber was accordingly recovered as the nitrate, a fact that was rather surprising in view of the good correlation that evidently exists between nitrate yield and alpha-cellulose content for both wood [15] and pulps [1]. The intrinsic viscosities, which were measured in acetone, decreased only slightly with increasing time of reaction. Glucose was the only constituent sugar of the nitrate derivatives, and this was not entirely unexpected in view of the known insolubility of nitrated xylan.

TABLE II. Nitration of Untreated Milkweed Fibers at +6° C

Time (hr)	Yield (%) Nitrated Fibers	Cellulose	$[\eta]$ (dl/g)
20	68.8	28.9	38.6
71	71.2	27.9	37.2
92	70.3	27.9	36.7

An additional quantity of material was nitrated for 20 hr under similar conditions and with the same results, and this product, containing 13.66% nitrogen, was used for determining the chain length and chain-length distribution of the nitrate.

The cellulose nitrate was fractionally precipitated from 0.15% aqueous acetone solution by gradual removal of the solvent. Lack of material prevented application of a two-stage procedure, duplicate one-stage experiments being carried out instead. Previous results with native wood cellulose [15] had indicated that a one-stage technique was likely to give the same results as one involving refractionation, provided a minimum number of 15–20 fractions were taken. In the present case, 17 fractions were isolated in each experiment and the procedure was accordingly considered as reasonably reliable, especially as the chain-length distribution could be expected to be less complicated than that of a wood cellulose [8].

The results obtained in one of the experiments are summarized in Table III, those noted in the other being essentially the same. As in several other instances [13, 15], the nitrogen content increased from the first fraction to attain a maximum in the middle range, where it stayed constant, after which it decreased rapidly for the last few fractions. The average nitrogen content was 13.73% after fractionation, which showed that no denitration occurred.

TABLE III. Fractionation of Nitrated Milkweed Cellulose

Fraction No.	Weight (%)	$[\eta]$	Nitrogen (%)	$[\eta]_{corr.}$	D.P.
1	3.5	37.0	13.30	40.7	6800
2	3.4	39.4	13.35	42.6	7600
3	3.0	39.6	13.43	41.8	7300
4	4.7	39.8	13.75	37.8	5780
5	6.0	39.7	13.73	38.0	5830
6	5.1	40.1	13.76	37.8	5780
7	7.7	39.6	13.80	36.9	5460
8	2.5	38.0	13.75	37.1	5500
9	6.2	36.2	13.70	34.9	4760
10	12.2	35.8	13.75	34.0	4450
11	11.1	33.4	13.66	32.6	4010
12	9.0	32.7	13.73	31.3	3650
13	5.5	30.4	13.70	29.4	3200
14	6.0	27.8	13.56	28.2	2970
15	4.3	25.6	13.26	28.5	3030
16	6.7	22.0	13.00	27.3	2820
17	3.1	9.4	12.24	15.1	1510

The corrections which had to be applied to the intrinsic viscosities to adjust them to a constant nitrogen content of 13.60% were never negligible, and sometimes considerable, and most notably so for the last fractions. Except for a few irregularities, the degrees of polymerization decreased gradually from a maximum of 7600 for the second fraction to 2820 for the next to the last one. The last fraction had a D.P. of only 1510, or almost 50% lower than the next preceding one, and in view of this difference it was not included in the chain-length distribution curves. It is interesting to note in this connection that the high values exhibited by the first three fractions would not have appeared if the low degree of substitution had not been accounted for in these cases.

The weight-average D.P. of the fractionated material was 4620, while the original viscosity average was 5800. These values are theoretically equivalent in the case of cellulose nitrates, and the discrepancy was probably due to degradation occurring during the fractionation. This reduction of the average D.P., while changing the overall chain-length distribution to lower D.P. values, was not believed to have significantly altered the character of the distribution. The number-average D.P. was only slightly lower than the weight-average, viz., 4250, and the relative nonuniformity was accordingly very low.

The integral and differential weight-distribution curves are given in Figure 2. The frequency distribution had a maximum located at a D.P. of 4000 and showed considerable right-hand skewness, the lower D.P. limit being 2500 and the higher, 8500.

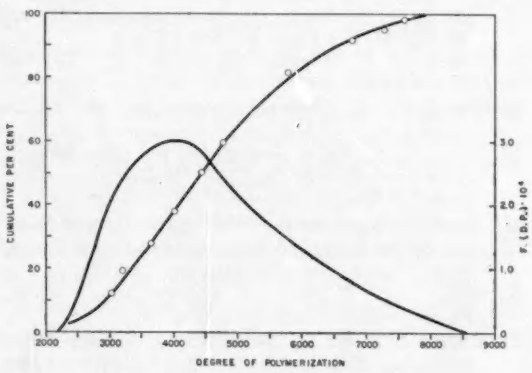

Fig. 2. Integral and differential weight distribution of milkweed cellulose.

Discussion

The milkweed fiber had a rather interesting composition, apparently comprising only two main constituents, namely, an exceedingly high-molecular-weight cellulose part and a probably low-molecular-weight hemicellulose portion, the latter consisting chiefly of xylan. This composition was very similar to that of the related kapok fiber and, as far as the content of cellulose and xylan was concerned, also to that of the cotton grass. The molecular weight compared closely with that of native ramie but was higher than that of cotton or flax [14]. Despite the presence of this high D.P. cellulose, the fiber has very poor strength properties due to the high content of xylan.

The chain-length distribution was different from that of cellulose from cotton, flax, and ramie. The first two of these materials have been shown to have a D.P. distribution with one maximum and a pronounced left-hand skewness, whereas ramie cellulose seems to have a narrow, almost Gaussian distribution [14]. Wood celluloses usually appear to have two maxima in their molecular-weight distribution and thus also differ from milkweed cellulose in this respect [15].

Although it appears probable that the hemicellulose portion of the milkweed is largely composed of a xylan polysaccharide, the chemical and physical properties of the latter are still unknown. It is hoped, however, that some of these problems can be elucidated in the near future when more material becomes available for further studies.

Experimental

Material

Milkweed floss, 20 g, was collected in September 1954 from mature but unopened bolls. The material was extracted with a 1:2 mixture of ethanol benzene and with cold water, but otherwise left untreated.

Methods

Analytical Procedures. The content of holocellulose in the extractive-free fibers was determined by the chlorination method of Van Beckum and Ritter according to TAPPI standard method T 9 m-45. Alpha-cellulose was estimated by extraction with 17.5% aqueous sodium hydroxide of the chlorine holocellulose and also by a similar extraction of a

chlorite holocellulose, prepared according to the directions of Wise, Murphy, and D'Addieco [16]. Analysis for lignin was carried out by the method described in TAPPI T 13 m-54 and pentosan analysis according to T 223 m-48, assuming in the latter case a 92.5% yield of furfuraldehyde from xylose and with no correction applied for the formation of hydroxymethyl furfuraldehyde.

Nitrogen was estimated by a semimicro Kjeldahl procedure [14] employing recrystallized potassium nitrate as a reference substance. Denitration was performed with 20% aqueous ammonium hydrosulfide as described elsewhere [15]. The denitrated product was hydrolyzed with sulfuric acid according to the procedure of Saeman and co-workers [11]. Separation on the paper chromatogram was carried out with the solvent systems ethyl acetate-acetic acid-water (9:2:2) and butanol-pyridine-water (10:3:3). Whatman No. 1 filter paper was used and development allowed to proceed for 40 and 80 hr. respectively. The spraying reagent was aniline hydrogen phthalate.

Intrinsic viscosities were determined for three ethyl acetate solutions of the unfractionated nitrate at various rates of shear, as described in detail elsewhere [12]. The value obtained at an average shear rate of 500 sec^{-1} was adjusted to a standard nitrogen content of 13.60% by the equation developed by Lindsley and Frank [6]. The corresponding D.P. was calculated from the intrinsic viscosity by the relationship of Newman, Loeb, and Conrad [9]. In all other cases, viscosities were measured in acetone with a Cannon-Fenske viscometer, extrapolated with Martin's equation [7] to zero concentration, corrected for nitrate substitution, and finally converted to degrees of polymerization with the help of a calibration curve [15].

Nitrations. Nitrations were carried out at +16°C for various lengths of time with the nitration mixture of Alexander and Mitchell [2], which contained nitric acid, phosphoric acid, and phosphorus pentoxide in the weight proportions of 64:26:10. The nitrated material, orange-colored and considerably swollen, was recovered as described previously [15] and nitrolignin was partially extracted with methanol. After weighing, the fibers were dissolved in acetone; insoluble portions were removed by centrifuging; and the clear solution poured into water to yield a white fibrous precipitate. Extraction was continued until no further material was removed, after which the cellulose nitrate was dried *in vacuo* at +50°C for 2 hr and weighed.

Fractionations. Cellulose nitrate, 1.45 g, was dissolved in 950 ml of 93% aqueous acetone and fractionally precipitated at 25°C by slowly removing the acetone with air, as described previously [15, *cf.* 8]. The total time required for isolating 17 fractions was approximately 10 hr, the last fraction being obtained by evaporation of the solution to dryness. The weight of the various fractions ranged from 36 to 175 mg, the total amounting to 1.44 g. A second experiment, carried out in the same way, gave similar results.

Acknowledgment

The authors wish to express their gratitude to Mr. D. Stoltzenburg, who carried out a part of the experimental work.

Literature Cited

1. Abadie, F. A., and Ellefsen, Ö., *Norsk Skogind.* **6**, 192 (1952).
2. Alexander, W. J., and Mitchell, R. L., *Anal. Chem.* **21**, 1487 (1949).
3. Björkquist, K. L., Jörgensen, L., and Wallmark, A., *Svensk Papperstidn.* **57**, 113 (1954).
4. Gralén, N., Berg, S., and Svedberg, T., *Ber.* **75**, 1702 (1942).
5. Juillet, A., and Delga, J., *Mém. services chim. état (Paris)* **32**, 378 (1948).
6. Lindsley, C. H., and Frank, M., *Ind. Eng. Chem.* **45**, 2491 (1953).
7. Martin, A. F., Paper presented at the American Chemical Society Meeting, Memphis (April, 1942).
8. Mitchell, R. L., *Ind. Eng. Chem.* **45**, 2526 (1953).
9. Newman, S., Loeb, L., and Conrad, C. M., *J. Polymer. Sci.* **10**, 463 (1953).
10. Rheineck, A. E., *Pharm. Arch.* **10**, 69 (1939).
11. Saeman, F. J., Moore, W. E., Mitchell, R. L., and Millett, M. A., *Tappi* **37**, 336 (1954).
12. Timell, T. E., *Svensk Papperstidn.* **57**, 777, 844, 913 (1954).
13. Timell, T. E., *Svensk Papperstidn.* **58**, 1, 234 (1955).
14. Timell, T. E., Paper presented at the 127th Meeting of the American Chemical Society, Cincinnati, Ohio (1955).
15. Timell, T. E., Paper presented at the Summer Meeting of the Technical Section, Canadian Pulp and Paper Association, Québec, Qué. (1955).
16. Wise, L. E., Murphy, M., and D'Addieco, A. A., *Paper Trade J.* **122**: (2), 35 (1946).
17. Whitford, A. C., in Mauersberger, H. R., editor, *Matthews' Textile Fibers,* Sixth Ed., John Wiley and Sons, New York, pp. 439–456 (1954).
18. Zapf, F., *Makromol. Chem.* **10**, 71 (1953).

Manuscript received May 20, 1955.

On the Bulk Compression Characteristics of Wool Fibers

P. C. deMaCarty[1] and J. H. Dusenbury[2]

Textile Research Institute, Princeton, New Jersey

Abstract

A method has been found to prepare bulk samples of wool fibers in such a way that reproducible compression tests may be performed upon them. An evaluation of the bulk compression characteristics of 29 widely different wool samples shows that compressive load, rather than resilience, serves to bring out differences among them. This finding suggests that quality differences among wools, as determined by handling, are related to differences in the wools' resistance to compression rather than to differences in compressional resilience.

For these 29 wool samples there is an inverse relationship between compressive load and mean fiber diameter. Although this finding is in agreement with similar results reported for cotton fibers, it conflicts with the predictions from a theoretical model that has been proposed to explain the compressional behavior of wool. The theoretical model, which was based on a consideration of bending forces only during compression, has been claimed to fit results found for 310 samples of Merino wool. There is, therefore, an implication either that there is a different dependency of resistance to compression on fiber diameter within a wool breed as compared to that among different breeds or that the proposed theory is inadequate.

When the compressing piston size is varied at a constant sample size for a Targhee 60's wool card sliver, it is found that the effective volume of fibers being compressed is greater than the volume of fibers beneath the piston, probably because of fiber-to-fiber entanglements. The experimental results indicate that a constant area should be added to the compressing piston areas in order to achieve a constant compressive stress. This area increment is independent of sample diameter, providing the sample diameter is sufficiently greater than that of the compressing piston, and this area increment decreases with increasing degree of compression.

Introduction

An important characteristic of a mass of fibers is its behavior during compression. With wool in particular, the "handle" of a sample of bulk fibers is often given special consideration when the quality of the wool is estimated. Such an assessment of quality often involves an operation of squeezing by hand, that is, a subjective kind of bulk compression test. It is the threefold purpose of this paper to describe a quantitative method for measuring the bulk compression of wool fibers, to discuss the effect of varying experimental conditions on the test results, and to estimate the importance of the different parameters that may be derived from such measurements.

[1] Textile Engineer.
[2] Assistant Director of Research.

The compression characteristics of fibers in bulk have been described by several authors [4, 10, 11, 15, 17], and the subject has been reviewed briefly by Kaswell [8]. In addition, other writers have discussed the compressional and resilience characteritics of yarns and fabrics [1, 5, 12, 13], but these works will not be considered here.

Resilience is a property that has been often discussed and sometimes measured in connection with studies on fibers in all forms from single fibers to finished fabrics. Many definitions have been proposed in the literature, but the one mentioned most frequently has been that described by Dillon in 1947 [3]:

$$\text{Resilience} = \frac{\text{Energy of Retraction}}{\text{Energy of Deformation}} \qquad (1)$$

In this instance, resilience is the ratio of the energy

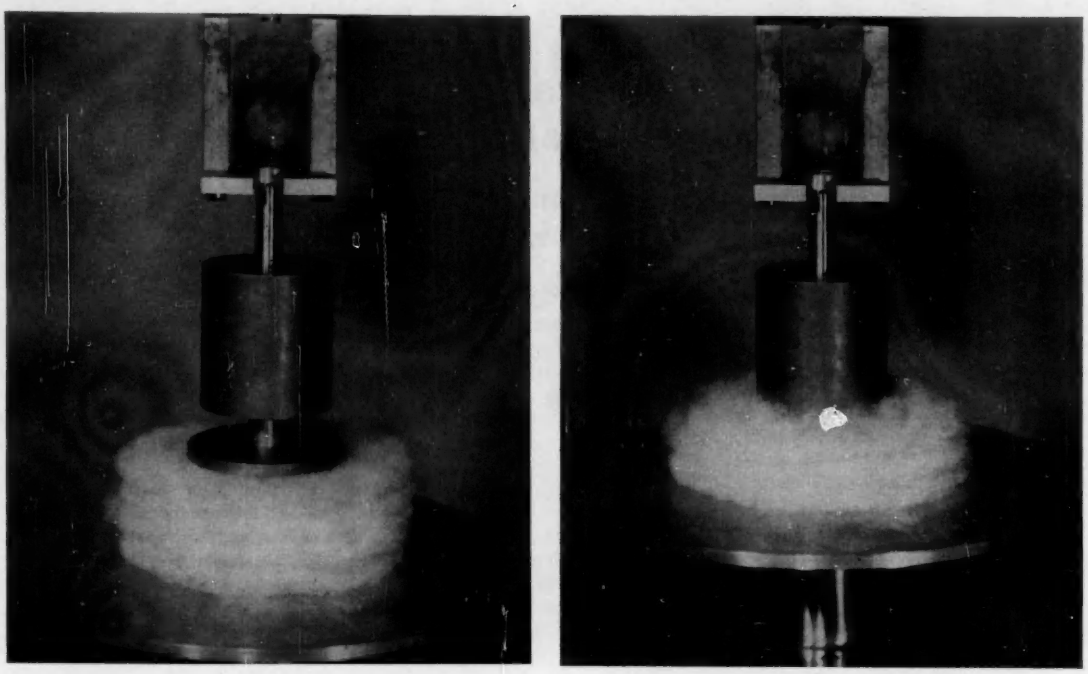

a *b*

Fig. 1. Compression test on 5.50-in. diameter sample with 3.00-in. diameter piston. *a*, Prior to compression; *b*, at 90% compression.

recoverable when a deforming force is removed from a test specimen to the energy initially absorbed by the specimen during deformation. It is to be noted that this definition does not attempt to take into account whether the deformation is tensional, compressional, shearing, bending, or a complex combination of various types of strain.

In his now classic 1944 Marburg Lecture, Smith [14] discussed resilience and attempted to relate it to the "hand" of fabrics, and later, in 1946, Mark [9] discussed the relationship of resilience to certain functional characteristics of fabrics in a generalized and qualitative fashion. In 1948, Hamburger [6] proposed the use of another parameter, the elastic performance coefficient, which relates the properties of a "conditioned" sample (previous loading to remove secondary creep) to those of the same sample prior to loading. He pointed out that it is possible for two materials to exhibit the same elastic-performance coefficient in tension and yet differ in another important property, the extensibility. He proposed that differences in this property should be evaluated by yet another parameter, the extensibility coefficient.

No attempt will be made here to define additional parameters related to resilience. Instead, it will be shown that resilience, defined according to equation 1, is not a parameter suitable for characterizing the bulk compression characteristics of wool fibers and that the load measured at certain fixed compressions of an initially "strain-free" sample provides a better measure of differences among wool samples.

Experimental Procedure

All sample preparations and testing operations were carried out at the standard conditions of 70°F and 65% R.H. The compression experiments were carried out with an Instron Tensile Tester [7] equipped with apparatus designed and constructed in this laboratory. This apparatus consists of a compressing piston with an attached weight that is suspended by appropriate linkages from an Instron Load Cell "C." During a compression test, the

Staple Length (200 fibers)
Mean length = 2.14 in.; standard deviation = 1.46 in.

Staple-Length Distribution

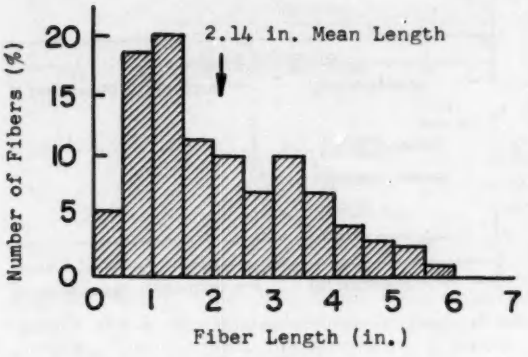

Single-Fiber Properties (50 fibers)

Property	Mean Value	Coefficient of Variation (%)
Diameter	27.5 μ	15
Uncrimping stress	0.084 $\times 10^6$ g cm^{-2}	16
Stress at 5% ext.	0.81 $\times 10^6$ g cm^{-2}	10
Stress at 20% ext.	1.00 $\times 10^6$ g cm^{-2}	7
Stress at break	1.28 $\times 10^6$ g cm^{-2}	19
Elastic modulus	26.0 $\times 10^6$ g cm^{-2} for 100% ext.	17
Extension at break	33.8%	29

Fig. 2. Physical properties of Targhee 60's wool card sliver.

cross-head is lifted to compress a test specimen, and the compressive load is measured by the amount of "unloading" that occurs during the test of the assembly suspended from the load cell. Special provision is made to prevent jamming and possible rupture of the strain gage because of uncontrolled upward motion of the cross-head. The sample being tested is placed on a plate mounted on the cross-head.

In Figure 1*a* may be seen a 5.50-in. diameter sample situated beneath a 3.00-in. diameter piston prior to compression from an initial gage length of 2.00 in.; in Figure 1*b* the same sample is shown at a compression corresponding to 90% of gage length. With the use of the Instron extension-cycling controls, the sample was compressed to a predetermined extent and immediately retracted at the same rate.

In one set of experiments, those to be considered in the greater detail here, the samples were prepared

Fig. 3. Method used in preparation of test specimens.

from card sliver made from the 1952 clip of 60/62's wool from mature Targhee ewes. This wool is one of nine lots grown at the U. S. Sheep Experiment Station in Dubois, Idaho, whose processing characteristics are now being extensively studied at Textile Research Institute. This wool was selected because of its intermediate character of fineness as an apparel wool and because its physical properties had already been determined. These properties, including a staple-length distribution histogram, are shown in Figure 2 [16]. The single-fiber properties listed in Figure 2 were measured on fibers removed from top rather than card sliver, but they provide a good representation of the properties of fibers from the card sliver.

As received, the Targhee 60's card sliver had a uniform distribution of fibers, and these were rearranged into cylindrical assemblies of known weights and dimensions. The rearrangement was done in a way to insure sample homogeneity; that is, it insured that the distribution of fibers was uniform throughout the sample and that there was no preferential orientation of single fibers with respect to any of the dimensions of the cylindrical sample. The importance of uniform and reproducible preparation of samples can hardly be overemphasized in bulk compression experiments.

The method used to prepare test specimens is shown in Figure 3. Strips of card wire of the type used on a fancy roll were glued to a board and marked with circles of diameters corresponding to

TABLE I. Sample Sizes and Weights

Sample Diameter (in.)	Sample Weight (g)	Specific Volume ($cm^3\ g^{-1}$)
3.25	2.00	136
5.50	5.72	136
9.80	18.20	136

those of the desired test specimens. Fibers were gently embedded in these wires (Figure 3) in such a way as to prevent breaking or excessive stretching. This was done by tamping down small amounts of fibers from a predetermined weight of wool into the area within a prescribed circumference until an even bulk density of material was obtained throughout. Cylindrical samples, 2 in. in height, were prepared in this way, each sample consisting of four layers about ½ in. thick. The reproducibility of results from sample to sample indicated that uniformity among different samples was good and that no special effects were produced as a result of compressing layered samples. After preparation each sample was allowed to "relax" for at least one day prior to subsequent testing. In those cases where a sample was tested with one size compressing piston and later tested with a piston of different size, the sample was reprepared lightly and allowed to "relax" between tests.

Three sample sizes were used with their corresponding weights determined so as to preserve the same 2.00-in. depth for each size (Table I); that is, the sample depth and the weight of fiber per unit volume of test sample were kept constant, regardless of the sample diameter. The circular compressing pistons used varied in ½-in. intervals of diameter from ½ through 3 in. The gage distance between the plate mounted on the cross-head and the compressing piston was 2.00 in. and, in the case of the experiments carried out on the Targhee 60's wool card sliver, the compressing distance was 1.80 in., or 90% of the sample thickness. At this setting, the first detectable load or resistance to compression by the sample could be measured by the Instron Load Cell. Compression-decompression cycles were run at a constant cross-head speed of 2.00 in./min, corresponding to a compression rate of 100% of gage length/min.

In Figure 4 are shown two typical load vs. compression curves obtained by compressing a 5.50-in. diameter sample with a 3.00-in. diameter piston. The compression of 1.80 in. corresponds to the distance AD (1st cycle) or $A'D'$ (7th cycle) of Figure 4. The direction of travel of the cross-head was reversed automatically at points D and D', where the compressive loads had reached the values of B and B', respectively. The Instron tester may be set to perform compression-recovery cycles in succession. With the use of such an arrangement, after the curve of the first cycle was recorded, five more cycles were run and only the corresponding maximum loads at 90% compression were recorded. Two minutes were allowed to elapse after cycle 6. Compression-recovery cycles 7 and 8 were then run, allowing a 2-min wait between them. It was found that values observed for loads at 90% compression and secondary creep had reached constant values at cycles 7 and 8. Probably the effects of creep, stress relaxation, and the 2-min interval between cycles all interacted to produce steady-state values for the loads at 90% compression and the extent of secondary creep. The following three types of parameters were evaluated, as indicated from the curves in Figure 4: loads at various compressions during the compression portion of the test, secondary creep, and resilience. Since the values for the compressive loads were nearly the same for cycles 7 and 8, the mean values from these two cycles were used for the analysis discussed later in this paper.

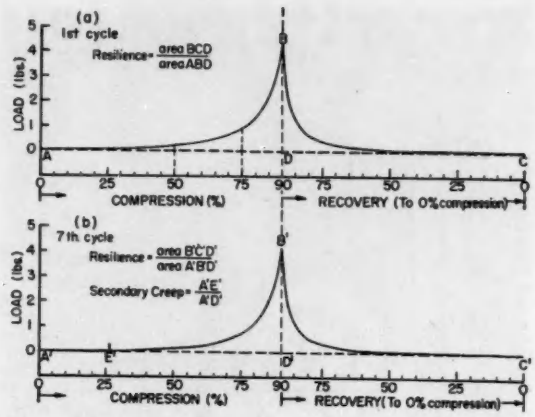

Fig. 4. Load vs. compression plots when 5.50-in. diameter sample is compressed with 3.00-in. diameter piston.

As another check on the reproducibility of the experiments, several load-relaxation experiments were carried out. Because of the response characteristics of the recorder pen at the moment of stopping the cross-head and starting to measure load relaxation, the samples were compressed at 10% of

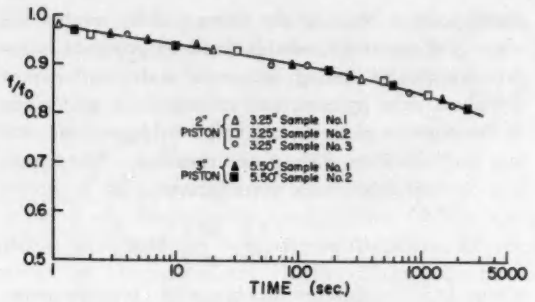

Fig. 5. Load relaxations of several samples at 90% compression.

gage length/min rather than at the 100%/min rate used in other experiments. The data were then plotted as f/f_0 vs. the logarithm of time, where f is the load measured at any time after stopping the cross-head at 90% compression and f_0 is the load when the cross-head is stopped and load relaxation starts to be measured.

It was found that smooth curves drawn through such data for different samples were superimposable, as demonstrated in Figure 5, where points taken from the data of five separate experiments are shown to fit on the same curve. It will be noted that three of the experiments involve a 2.00-in. diameter piston with 3.25-in. diameter samples and two are concerned with a 3.00-in. diameter piston compressing 5.50-in. diameter samples. The experimental conditions are different enough from those reported by Finch [4] so that no direct comparison may be made with his data for wool. He reported, however, an "essentially linear" relationship between f/f_0 and log time up to 1000 sec, whereas this situation holds only approximately in our experiments. After about 300 sec, all of the curves derived from the original data show a distinct tendency to become concave downwards.

In another set of experiments, performed in this laboratory by Demiruren in connection with his doctoral thesis at the University of Wyoming [2], the experimental technique previously described was used to determine the compressional characteristics of 29 samples of wool of widely varying staple lengths and fiber diameters. Demiruren used one set of conditions for all his experiments: a 1.50-in. diameter piston compressing 3.25-in. diameter samples weighing 2.00 g each to 75% compression at the constant rate of 100% of gage length/min. From his measurements he evaluated the three parameters: load at 75% compression, secondary creep, and resilience.

Discussion of Results

With the loads developed at 90% compression used as a criterion, comparison was made of the results when 3.25-in. diameter samples were compressed without confining walls (Figure 1) and within a cylindrical confining wall. Under the test conditions used (1.00, 2.00, and 3.00-in. diameter pistons), there was no difference between the walled and wall-less experiments. This indicates that, at least in these experiments, frictional effects caused by the proximity of the outer edge of a compressing piston to the inner surface of a confining wall are unimportant.

In making measurements on samples of a Bengals cotton, Rees found in 1948 [11] that the presence or absence of confining walls had a slight effect on values observed for compressional resilience. In his work the compressing piston was in contact with the inner walls of the confining cylinder, whereas in this work an appreciable distance existed between them. The experiments reported here show the experimental variance of compressional resilience values to be rather high and would indicate that the differences in resilience observed by Rees may not be statistically significant. As a result of his walled vs. wall-less comparisons, Rees adopted as a standard method tests carried out without confining walls, the method used in the experiments with which this paper is concerned.

The results of the previously described measurements by Demiruren [2] are most interesting. Over the wide range of wools tested, the resilience values obtained showed a very weak dependence on mean fiber diameter and mean staple length, whereas the secondary creep and maximum load values (75% compression) appeared to be considerably more sensitive to changes in fiber dimensions. The compressive load appeared to be most sensitive, with loads observed for a 70's wool (fine grade) being about 10 times greater than those observed for a 36's wool (extremely coarse grade). Correlation coefficients illustrating these observations are shown in Table II. These results indicate that subjective differences between wool fiber types, as determined by hand squeezing, may be due to differences in maximum load values rather than to differences in resilience.

TABLE II. Compression Test Correlations

(Correlation coefficients observed for mean values of 29 different wool samples)

Variable "Y"	vs.	Variable "X"	Simple Correlation Coefficient (r)
Maximum load		Fiber diameter	−0.702***
Maximum load		Fiber length	−0.755***
Resilience		Fiber diameter	+0.322
Resilience		Fiber length	+0.380*

*** Correlation significant at 0.1% level.
* Correlation significant at 5% level (r = 0.367 or more).

The inverse relationship between the compressive load and the fiber diameter indicates further that the measurements reflect a cooperative property of the entire fiber assembly rather than properties of the individual fibers such as the bending or extensional moduli of elasticity. If one considers the compressive loads to depend *only* upon bending or extensional moduli of the single fibers and considers the loads to be simple additive functions of the loads on the single fibers, it may be shown that these loads should either vary directly with the square of the fiber diameter, in the case of pure bending, or be independent of fiber diameter, in the case of pure extension. The crimp of the single constituent fibers may well be important, however, and should be considered in a more detailed analysis than that mentioned briefly above.

A more sophisticated analysis of this kind of problem has been performed by van Wyk [15], who derived a relationship between the pressure (compressive load) and the volume of the mass of fibers being compressed. He assumed that the compression consisted only of bending the fibers and he treated the mass of fibers as a randomly oriented group of cylindrical rods. Twisting, slippage, and extension of the fibers were ignored, and consideration was given to the number of times one rod would come in contact with another during compression. The equation derived from these considerations is

$$dp = -\left(\frac{kY}{12v^4}\cdot\frac{m^3}{\rho^3}\right)dv \qquad (2)$$

where dp is the differential change of pressure corresponding to the differential change of volume dv; k is a constant of proportionality; Y is Young's modulus through bending; v is the volume of the mass of fibers; and m and ρ are the mass and density, respectively, of the wool fibers. It is to be noted that this equation predicts that compressive loads should be independent of fiber diameter. Integration of equation 2 leads to a relationship in which the pressure varies with the inverse cube of the volume, a relationship which appeared to be satisfied by data obtained by van Wyk on three different Merino wool samples.

In testing 310 different Merino wool samples, van Wyk found no correlation between resistance to compression and fiber diameter, an apparent confirmation of equation 2. Unfortunately, such a selection of wool samples would not provide a very wide range of fiber diameter. The much wider range considered by Demiruren and Burns [2] provides a more severe test of van Wyk's theoretical model, and, as already noted, their results show a negative dependence of compressive load on fiber diameter. After an attempt to eliminate the effect of crimp differences among the 310 Merino wools, van Wyk

TABLE III. Typical Values of Parameters Obtained from Load vs. Compression Curves

5.50-in. Diameter Samples Taken to 90% Compression by

		1.00-in. Diameter Piston			2.00-in. Diameter Piston			3.00-in. Diameter Piston		
Sample No.	Cycle No.	Maximum Load (lb)	Secondary Creep (%)	Resilience (%)	Maximum Load (lb)	Secondary Creep (%)	Resilience (%)	Maximum Load (lb)	Secondary Creep (%)	Resilience (%)
1	1	0.640	—	61.7	2.04	—	44.7	4.36	—	50.8
	7	0.618	32.6	65.0	2.00	29.4	62.5	4.20	29.6	61.8
	8	0.614	34.5	58.8	2.00	28.3	54.5	4.20	26.7	59.8
2	1	0.636	—	56.1	2.04	—	57.2	4.49	—	54.2
	7	0.614	29.6	51.3	2.00	34.7	63.5	4.37	29.9	62.8
	8	0.612	38.6	58.4	2.00	35.8	54.6	4.35	27.0	63.4
3	1	0.648	—	45.9	2.03	—	58.5	4.34	—	48.3
	7	0.628	34.1	58.3	1.96	33.0	45.0	4.27	27.9	62.8
	8	0.620	33.7	61.6	1.96	32.4	46.0	4.26	27.8	73.0

found a positive partial correlation coefficient between compressive load and fiber diameter and mentioned "that an influence of fibre diameter may be masked by the crimping." Again, it is to be noted that the range of crimp, measured as number of crimps per unit length, among Merino wools may not provide a severe enough test of the theory.

There are two possible explanations for the apparent disagreement between the experiments reported by Demiruren and Burns [2] and those of van Wyk [15]. One is that the dependence of resistance to compression on fiber diameter may be different within a single breed of sheep from what it is among different breeds. Such a difference might be related to a similar one involving crimp levels within a breed as compared to those among breeds. Only further experimentation can tell the answer to this problem.

Another, and perhaps more obvious explanation, is that van Wyk's theoretical model needs revision. For one thing, and van Wyk has acknowledged this as a possible objection, only the *total* length, that obtained by considering all the fibers laid end-to-end, is used in deriving the pressure-volume equation. Staple length differences have been completely ignored. Variations in "element length," the distance between adjacent points of contact in van Wyk's model, have also been ignored, but, if crimp is an important factor, it should have a significant effect on the "element length."

The only other work related to this discussion is that of Rees in 1948 [11], mentioned previously. Rees tested five different cotton breeds and found at higher pressures that the finer the cotton, the greater is its specific volume. This result means that at the same volumes (the same compressions) the compressive loads varied inversely with fiber diameter, the same type of relationship found for different breeds of wool. It is also interesting that Rees found no significant correlation of compressional resilience with fiber diameter among his five different cottons. As mentioned earlier, it is surprising in view of this that he believed the presence or absence of confining walls during a compression test could have a significant effect on the determination of resilience.

The experiments carried out on bulk samples prepared from Targhee 60's card sliver will now be considered. As mentioned previously, these involved the compression of three different diameter samples with compressing pistons of varying diameter. Some typical values of parameters derived from load vs. compression curves are shown in Table III. It may be seen that the variance of the resilience measurements is far higher than that of the corresponding measurements for compressive load. As discussed earlier, the values observed for maximum load and secondary creep have reached essentially constant values at cycles 7 and 8.

When the compressing piston size was varied at a constant sample size, it was found that the effective volume of fibers being squeezed was greater than the volume of fibers directly beneath the piston. The compressive loads, F_i, developed at a compression c were greater than expected to maintain a constant compressive stress, S_c. That is, the area of the compressing piston, A_i, needed correction by a corresponding area increment, a_i, to maintain constant stress, or

$$F_i = S_c\,(A_i + a_i) \tag{3}$$

Typical plots showing how the load developed at 90% compression (average of cycles 7 and 8) varied

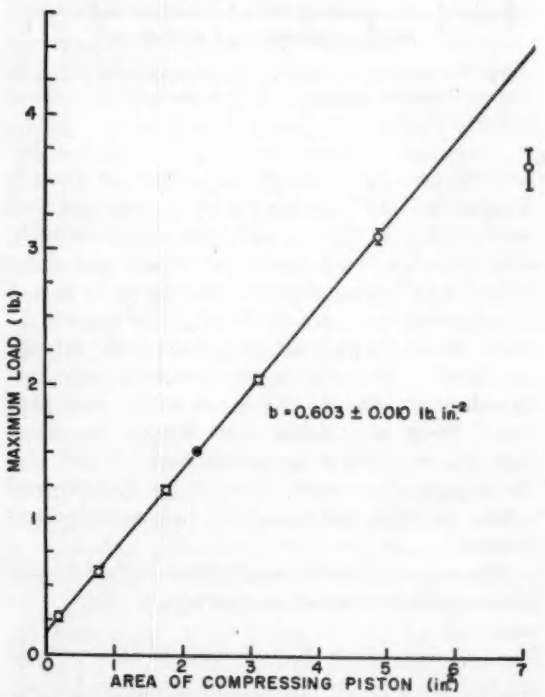

Fig. 6. Maximum load vs. area of compressing piston for 3.25-in. diameter samples at 90% compression (average of cycles 7 and 8).

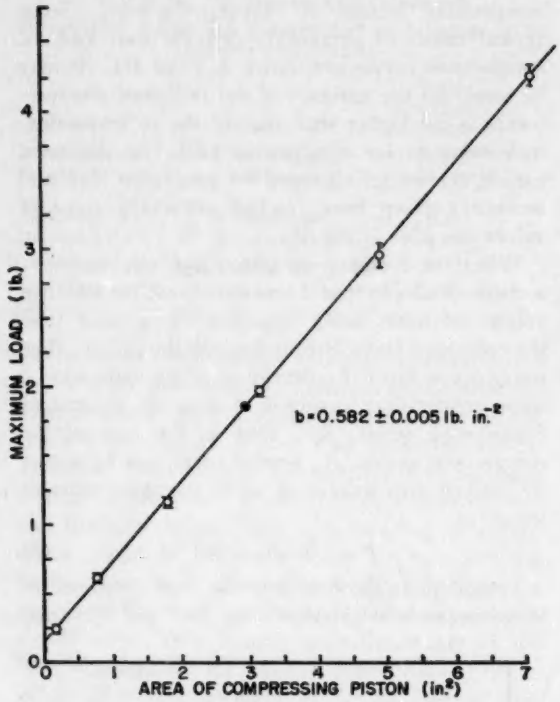

Fig. 7. Maximum load vs. area of compressing piston for 5.50-in. diameter samples at 90% compression (average of cycles 7 and 8).

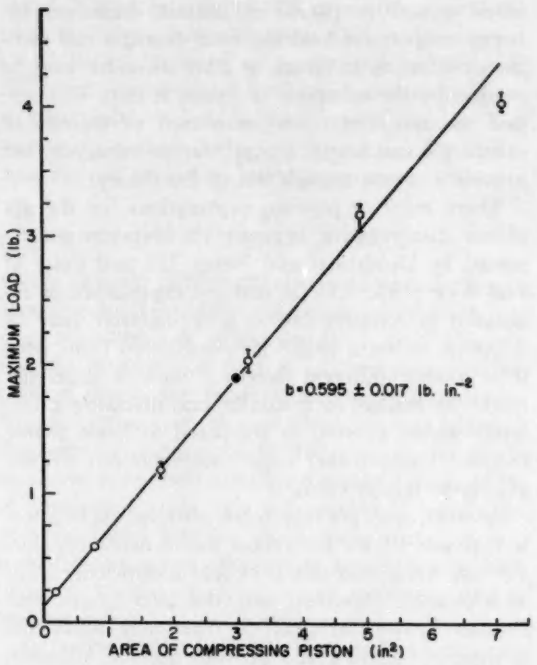

Fig. 8. Maximum load vs. area of compressing piston for 9.80-in. diameter samples at 90% compression (average of cycles 7 and 8).

with the area of the compressing piston are given in Figures 6, 7, and 8, where the sample diameter sizes were 3.25 in., 5.50 in., and 9.80 in., respectively. The indicated limits above and below each mean value (open circles) show the experimental range of the observed loads, and the solid circles indicate the mean values for each set of measurements through which the corresponding least-mean-squares lines have been drawn. It may be seen from such plots that a linear relationship exists between maximum load, F_i, and compressing piston area, A_i, and that the straight line drawn through the experimental points intercepts the "F_i axis" at a value greater than zero.

The slopes of such straight lines (dF_i/dA_i) are given by differentiation of equation 3:

$$dF_i/dA_i = S_c\,[1 + (da_i)/(dA_i)] \qquad (4)$$

The results of all the experiments indicated the value of da_i/dA_i to be zero; that is, values calculated for a_i appeared to be constant at a single compression and sample diameter over the range of piston sizes used.

An example of how this was determined is given in the data listed in Table IV. The linear relationship between F_i and A_i shows that da_i/dA_i must be a constant or zero. The values of the least-mean-squares slopes with their corresponding 95% confidence limits (the b's in Figures 6, 7, and 8) may be taken as being equal to S_c as a first approximation. Using this S_c value, the corrective area increases, a_i, may be calculated for each of the corresponding maximum load values, F_i, at all the piston sizes, A_i. These calculated a_i values are shown listed for a typical case in Table IV. A plot of the a_i values listed there vs. the radii of the corresponding compressing pistons is given in Figure 9 (open circles). It may be seen from the value given for "b" (the regression coefficient) with its corresponding 95% confidence limits that the slope of the least-mean-squares line does not differ from zero. The

TABLE IV. Typical Values Derived from Measurements of Compressive Load

5.50-in. Diameter Samples Taken to 90% Compression

Piston		Cycle 1		Average of Cycles 7 and 8	
Diameter (in.)	Area—A_i (in.²)	Max. Load—F_i (lb)	Corrective Area Increase—a_i (in.²)	Max. Load—F_i (lb)	Corrective Area Increase—a_i (in.²)
0.50	0.196	0.263	0.244	0.248	0.230
		0.270	0.256	0.254	0.241
		0.280	0.272	0.265	0.259
1.00	0.785	0.640	0.286	0.616	0.274
		0.636	0.279	0.613	0.268
		0.648	0.299	0.624	0.287
1.50	1.767	1.190	0.224	1.160	0.226
		1.200	0.240	1.170	0.244
		1.180	0.207	1.140	0.192
2.00	3.142	2.040	0.271	2.000	0.295
		2.040	0.271	2.000	0.295
		2.030	0.254	1.960	0.226
2.50	4.909	3.040	0.176	2.970	0.195
		3.170	0.394	3.065	0.358
		2.970	0.059	2.870	0.023
3.00	7.069	4.360	0.224	4.200	0.149
		4.490	0.442	4.360	0.424
		4.340	0.191	4.265	0.260
		Compressive Stresses (lb in.$^{-2}$)			
$b \pm t_{0.05}\sigma_b$		0.598 ± 0.010		0.582 ± 0.005	
		Corrective Area Increases (in.²)			
$\bar{a}_i \pm t_{0.05}\sigma_{\bar{a}_i}$		0.255 ± 0.040		0.247 ± 0.041	

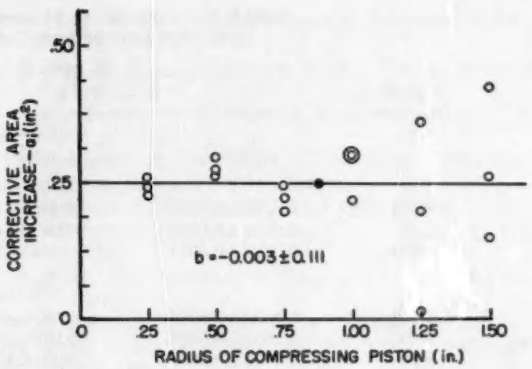

Fig. 9. Corrective area increase vs. radius of compressing piston for 5.50-in. diameter samples at 90% compression (average of cycles 7 and 8).

solid circle corresponds again to the mean values for a_i and compressing piston radius through which the calculated line has been drawn. Since there is *no* dependence of a_i upon the size of the compressing piston, it is possible to calculate a mean value of a_i and its 95% confidence level. Such calculated values for $\bar{a}_i$ are shown in Table IV.

A possible criticism of this method of analysis is that the variance of the compressive loads is greater at the larger piston sizes, and this is manifested by there being a greater variance in the calculated area increments at the larger piston sizes (Figure 9). A more rigorous analysis, in the statistical sense, would be obtained by using the logarithms of the F_i and A_i values, but such an approach is complicated by the necessity of then determining S_c as an intercept and by the presence of the summation term $(A_i + a_i)$ in equation (3).

The necessity of adding a corrective area to that of the compressing piston is undoubtedly due to fiber entanglements among fibers beneath the piston and fibers beyond the edge of the piston. Since the area increase, a_i, is constant with increasing compressing piston size, the corresponding corrective radius decreases with increasing piston size. Therefore, providing the sample size is large enough, the effect of the corrective area increase tends to vanish as the compressing piston size is increased.

Using the method of data analysis outlined previously, it was possible to calculate values of compressive stress, S_c, and corresponding area increments $\bar{a}_i$ for the three piston sizes at cycle 1 and at the average of cycles 7 and 8 for the three compressions of 50%, 75%, and 90% (Figure 4). These calculated values are listed in Table V. The area increments at low compressions were large enough to suggest that the compressive loads, in the case of the 3.00-in. diameter piston squeezing the 3.25-in. diameter samples, would be too small to fall on the straight-line plot of maximum load, F_i, vs. area of compressing piston, A_i. This was found to be the case, and, accordingly, the F_i values obtained with the 3.00-in. diameter piston were excluded from the analysis of the data for the 3.25-in. diameter samples. When, for comparison, these data were also excluded from the analysis of the data for the 5.50 and 9.80-in. diameter samples, no significant change

TABLE V. Compressive Stresses and Corresponding Corrective Area Increments Derived from Compression of Bulk Wool Samples

Sample Diameter (in.)	Compressive Stress*—S_c (lb in.$^{-2}$)		Area Increment*—$\bar{a}_i$ (in.^{2})	
	Cycle 1	Average of Cycles 7 and 8	Cycle 1	Average of Cycles 7 and 8
		50% Compression		
3.25†	0.0210±0.0025	0.0109±0.0013	1.288±0.192	1.754±0.194
5.50	0.0216±0.0020	0.0130±0.0011	1.284±0.219	0.983±0.197
9.80	0.0246±0.0017	0.0165±0.0015	1.340±0.165	0.618±0.214
		75% Compression		
3.25†	0.1035±0.0044	0.0856±0.0042	0.779±0.068	0.782±0.080
5.50	0.1064±0.0036	0.0899±0.0019	0.707±0.078	0.630±0.048
9.80	0.1106±0.0028	0.0916±0.0028	0.762±0.058	0.702±0.068
		90% Compression		
3.25†	0.621±0.011	0.603±0.010	0.247±0.030	0.237±0.025
5.50	0.598±0.010	0.582±0.005	0.255±0.040	0.247±0.041
9.80	0.613±0.021	0.595±0.017	0.270±0.079	0.258±0.065

* Limits shown are 95% confidence levels of the corresponding mean values.
† Data for 3.00-in. diameter piston excluded from the analysis.

TABLE VI. Compressive Stresses and Corresponding Corrective Area Increments Derived from Compression of Bulk Wool Samples; 3.00-in. Diameter Piston Data Excluded from the Analysis

Sample Diameter (in.)	Compressive Stress*—S_c (lb in.$^{-2}$)		Area Increment*—$\bar{a}_i$ (in.^{2})	
	Cycle 1	Average of Cycles 7 and 8	Cycle 1	Average of Cycles 7 and 8
		50% Compression		
3.25	0.0210±0.0025	0.0109±0.0013	1.288±0.192	1.754±0.194
5.50	0.0229±0.0013	0.0146±0.0013	1.123±0.078	0.703±0.145
9.80	0.0247±0.0022	0.0171±0.0018	1.327±0.148	0.542±0.169
		75% Compression		
3.25	0.1035±0.0044	0.0856±0.0042	0.779±0.068	0.782±0.080
5.50	0.1042±0.0048	0.0884±0.0030	0.754±0.046	0.667±0.025
9.80	0.1118±0.0030	0.0943±0.0043	0.735±0.044	0.628±0.074
		90% Compression		
3.25	0.621±0.011	0.603±0.010	0.247±0.030	0.237±0.025
5.50	0.592±0.014	0.576±0.018	0.202±0.047	0.240±0.048
9.80	0.631±0.021	0.619±0.021	0.218±0.054	0.182±0.056

* Limits shown are 95% confidence levels of the corresponding mean values.

was observed in the calculated values for S_c and $\bar{a}_i$ (Table VI).

The calculated corrective area increases show a marked decrease with increasing compression, and this suggests that effects caused by fiber-to-fiber entanglements extending beyond the edge of the compressing piston tend to vanish as the compression approaches 100%. The differences among the three different diameter samples are slight or negligible, save in one instance. The data for the average of cycles 7 and 8 are in general accord with those of cycle 1 except at 50% compression. Here, the effect of secondary creep was to lower appreciably the observed compressive loads. These loads were rather difficult to read from the load vs. compression plots of the Instron tester, and, accordingly, there was more inaccuracy associated with these small values than with any of the other compressive loads. This,

rather than any real differences among the three different diameter samples, is probably the cause of the apparent differences to be noted in Tables V and VI.

Acknowledgments

We thank Dr. J. H. Dillon for his encouragement and advice throughout this work and Dr. J. H. Wakelin and Professor J. C. Whitwell for helpful discussions pertaining to it. In addition, we should like to thank Mr. H. Lambert for constructing the accessory equipment used to carry out the compression measurements on the Instron tester. The work was sponsored by the Office of Naval Research, Department of the Navy.

Literature Cited

1. Cassie, A. B. D., *J. Textile Inst.* **40**, P444 (1949).
2. Demiruren, A., and Burns, R. H., Textile Research Journal **25**, 665 (1955).
3. Dillon, J. H., Textile Research Journal **17**, 207 (1947).
4. Finch, R. B., Textile Research Journal **18**, 165, 237 (1948).
5. Fox, K. R., and Schwarz, E. R., *Textile Research* **11**, 227 (1941).
6. Hamburger, W. J., Textile Research Journal **18**, 102 (1948).
7. Hindman, H., and Burr, G. S., *Trans. Am. Soc. Mech. Engrs.* **71**, 789 (1949).
8. Kaswell, E. R., *Textile Fibers, Yarns, and Fabrics*, Reinhold Publishing Corp., New York, p. 178 (1953).
9. Mark, H., Textile Research Journal **16**, 361 (1946).
10. Mutschler, H., *Textil-Praxis* **4**, 106 (1949).
11. Rees, W. H., *J. Textile Inst.* **37**, T121 (1946); **39**, T131 (1948).
12. Schiefer, H. F., *Textile Research* **3**, 505 (1933).
13. Schiefer, H. F., Stevens, H. T., Mack, P. B., and Boyland, P. M., *J. Research Natl. Bur. Standards* **32**, 261 (1944).
14. Smith, H. deW., *Am. Soc. Testing Materials Proc.* **44**, 543 (1944).
15. van Wyk, C., *J. Textile Inst.* **37**, T285 (1946).
16. Wakelin, J. H., private communication.
17. Winson, C. G., *J. Textile Inst.* **23**, T386 (1932).

Correction

Experimental Study of the Viscoelastic Properties of Textile Fibers: Dynamic Measurements from Subsonic to Supersonic Frequencies

K. Fujino, H. Kawai, and T. Horino

August 1955 **Volume XXV, No. 8** **Pages 726 and 734**

Equation 10 should read $E = (lI/Sa^2)[\{\pi^2 + (\ln \Delta)^2\}/T^2 - \pi^2/T_0^2]$.

Equation 10′ should read $\xi = (lI \ln \Delta)/(Sa^2T)$.

Equation 20 should read $E'(\ln \tau) \simeq (2/\pi)[E_2(\omega)]_{\omega=1/\tau}$.

Letters to the Editor

Short communications in the form of Letters to the Editor are intended to provide prompt publication of significant new research results and to permit an exchange of views on papers previously published in the JOURNAL. These communications are not submitted to formal review as are research papers, and the editors do not assume any share of the author's responsibility for the information given or the opinions expressed. When work previously published in the JOURNAL is the subject of critical comment, the authors of the original paper are given an opportunity to submit a reply, which will be published concurrently when possible.

The Effect of Temperature on the Adsorption of Iodine by Cellulose

AHMEDABAD TEXTILE INDUSTRY'S RESEARCH ASSOCIATION
Ahmedabad, India
June 14, 1955

To the Editor
TEXTILE RESEARCH JOURNAL

Dear Sir

Hessler and Power [1] have shown how the adsorption of iodine by cellulose can be used to estimate its crystallinity. In their method the temperature at which the adsorption is carried out is not specified and is presumably the room temperature. The room temperature in different laboratories may vary considerably and even in the same laboratory it may not be constant throughout the year. As temperature is known to have a marked effect on adsorption, this investigation was undertaken to determine its magnitude.

Preliminary experiments showed that there was considerable variation (sometimes as much as 5%) for the same material at the same temperature. This was found to be mainly due to the magnification of error in adding 2 cc of concentrated iodine solution. It was desirable to reduce this variation at a given temperature if changes in adsorption at different temperatures were to be measured with any accuracy. This was achieved by adding a larger quantity of a more dilute iodine solution. The solution was prepared by dissolving 3.125 g of iodine in 25 g of potassium iodide and 30 g of water and making up to 1 l with saturated sodium sulfate solution. Fifty cc of this solution contain approximately the same quantity of iodine as is in 2 cc of the solution used by Hessler and Power [1]. Another 50 cc of sodium sulfate solution were added as usual. Although this modification of procedure may have a small effect on the absolute value of adsorption, it should not affect the relative changes in adsorption at different temperatures. However, the total quantity of solution is reduced from 102 cc to 100 cc and so the formula for conversion must be modified to:

$$\frac{(a - b) \times 2.00 \times 2.54}{0.3} = \frac{\text{mg of } I_2}{\text{g of cellulose}}$$

The adsorption was determined at four temperatures, viz. 17.8°, 24.9°, 31.9°, and 39.0°C. (The last temperature corresponds to about 102°F, which, though unlikely, is not an impossibility in Indian laboratories!) The sodium sulfate solution was saturated at 17°C to prevent crystallization of the salt inside the fibers at the lower temperatures. Instead of conducting the experiments in open beakers, iodine-value flasks were used to prevent the escape of iodine, especially at the higher temperatures. Viscose staple fiber of 1.5 den was used throughout. Four observations were made at each temperature and the results are tabulated as shown in Table I.

These results clearly show the need of controlling and specifying the temperature at which adsorption

TABLE I. Milligrams of Iodine Adsorbed per Gram of Cellulose at Different Temperatures

Experiment No.	Temperature			
	17.8°C	24.9°C	31.9°C	39.0°C
1	143.1	135.5	126.1	118.5
2	141.4	136.3	124.5	119.4
3	143.1	137.2	127.0	118.5
4	142.2	134.6	127.0	116.8
Mean	142.5	135.9	126.1	118.3

is carried out. Control need not be better than ± 1°C, but specifying the actual temperature is important. The degree of crystallinity is measured by comparing the adsorption by the sample with the adsorption by a standard amorphous material (methocel) which is assumed to be 100% amorphous. If the two temperatures are widely different, the determination may be seriously in error. If it is not possible to carry out both the measurements at the same temperature, the adsorption value at one temperature can be converted to that at another temperature with the following equation:

$$\log_{10}\left(\frac{K_2}{K_1}\right) = 350\left(\frac{1}{T_2} - \frac{1}{T_1}\right)$$

(K_1 and K_2 expressed in the same units; T_1 and T_2 as absolute temperatures.) Here 350 stands for $-\Delta H/2.303R$ and so the heat of adsorption, ΔH, turns out to be about -1600 ca/mol.

Literature Cited

1. Hessler, L. E., and Power, R. E., Textile Research Journal **24**, 822 (1954).

A. G. Chitale

Fabric Embedding for Microtome Sectioning

Southern Regional Research Laboratory
Southern Utilization Research Branch
New Orleans, Louisiana
April 1, 1955

To the Editor
Textile Research Journal

Dear Sir:

A modified embedding technique for the preparation of fabric samples for microtome sectioning has been developed. Where other methods require the use of monomeric materials which must be polymerized in an oven [2, 4], this technique employs a viscous solution of polyvinyl alcohol [3] which hardens overnight at room temperature.

A stock solution is prepared by stirring 25 g of polyvinyl alcohol (low viscosity) in 75 g of water in a Waring Blendor;[1] 0.5% phenol is added to inhibit growth of microorganisms.

A piece of the fabric approximately ½ in. wide and 3 in. long is placed in a Petri dish 2 in. in diameter with ½ in. of the fabric strip resting against opposite sides. The dish is filled with distilled water to which 5 drops of a wetting agent are added and is placed in a vacuum desiccator; vacuum is applied for 20 min to ensure removal of air and thorough wetting of the yarns. The water is then poured off, and the stock solution diluted 1:1 with distilled water is poured over the fabric. The dish is again put in the desiccator and the vacuum applied and released alternately at intervals of 10 min for 1 hr. Finally, the dilute solution is poured off and and the sample covered (about ¼ in. deep) with the stock polyvinyl alcohol solution. With two clothespins the ends of the fabric are clipped to the sides of the dish to keep the fabric rigid and to assist later in removing the embedding when it is dry. After another hour in the desiccator with alternate application and release of the vacuum every 10 min, the dish is removed and the sample allowed to dry overnight at room temperature. The embedded fabric is then pulled out of the dish and the excess polyvinyl alcohol trimmed away.

Final preparation for the microtome requires subsequent embedding in paraffin [1]. A mold is made by wrapping a piece of paper 1½ in. by 8 in. around a wooden specimen block 1 in. by ⅔ in. and sealing the ends with Scotch Tape.[1] If the paper is properly wrapped, the box will hold melted paraffin without leaking.

The previously embedded fabric sample is centered vertically in the paper box and held in position at the upper end by a clothespin attached to a ringstand; the other end rests on the wooden specimen block. The box is then filled with melted paraffin which is allowed to cool at room temperature. After the paraffin has hardened, the paper is stripped off and the excess paraffin trimmed away. The embedded sample is now ready for sectioning with a rotary microtome.

This technique is particularly applicable to coated

[1] It is not the policy of the Department of Agriculture to endorse the products of one company over those of another company engaged in the same business. Their names are furnished merely for convenience and information.

or impregnated fabrics, the coating material of which would be affected by nonaqueous embedding media or their solvents. It permits study of the coating material as well as fabric construction.

Literature Cited

1. Allen, R. M., *The Microscope*, D. Van Nostrand Co., Inc., New York, N. Y. (1940).
2. Du Pont de Nemours, E. I., and Co., Plastics Dept., Arlington, N. J., "Embedding Specimens in 'Lucite' Methyl Methacrylate Resin," *Tech. Serv. Rept.* **4**, 4 pp. (1945).
3. Lubkin, V., and Carsten, M., *Science* **95**, 633 (1942).
4. Moore, A. T., Scott, L. W., deGruy, I. V., and Rollins, M. L., TEXTILE RESEARCH JOURNAL **20**, 620–630 (1950).

INES V. DEGRUY

Density Gradient Resolution of Cortical Cell Fractions

U. S. DEPARTMENT OF AGRICULTURE
Western Utilization Research Branch
Agricultural Research Service
Albany 10, California
June 13, 1955

To the Editor
TEXTILE RESEARCH JOURNAL

Dear Sir:

We wish to report preliminary observations of wool cortical-cell fractionation that may be of general interest to textile chemists. We have found that wool spindle-cell preparations made under a variety of conditions can very generally be separated into 2 discrete main fractions that differ in density and sulfur content. The components differing in density have been demonstrated as separate layers in density gradient columns [5]. Aqueous chloral hydrate gradient columns covering the density range 1.4 to 1.6 have been found suitable for this purpose and are preferable to columns made with electrolytes or with nonaqueous systems. Fractionation has been achieved by adding mercury to the bottom of a column showing separated layers and collecting the layers individually as they overflow. Separations of 100-mg samples are conveniently made at room temperature in gradients in 50-ml centrifuge tubes by centrifuging about 1 hr at 3000 rpm (relative centrifugal field about 2000). For precise density measurements, columns were set up in a thermostatted water bath at 30°C and the positions of cell layers compared with those of glass floats of measured density.

Spindle-cell preparations were usually made by mechanical disintegration after soaking clean wool in 6 *N* hydrochloric acid at room temperature (23 to 26°C) for 48 to 288 hr in accordance with studies of C. H. Binkley of this laboratory. The papain-bisulfite treatment described by Blackburn [1] was used for comparison. Discrete fractions have been

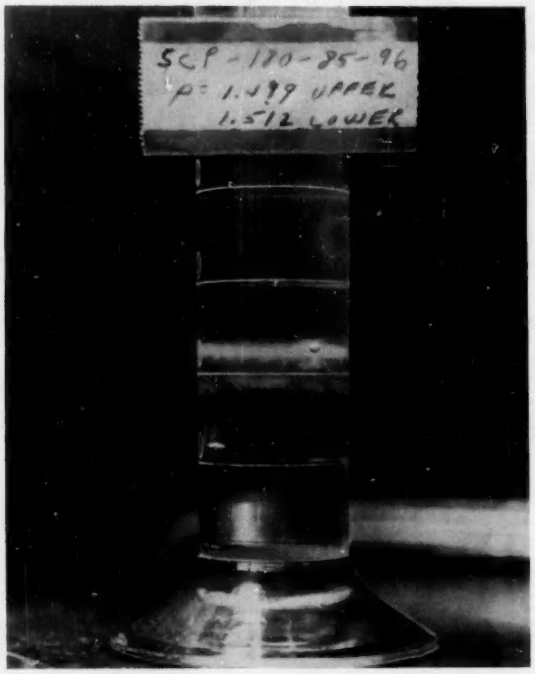

Fig. 1. Separation of two spindle cell layers of densities approximately 1.499 and 1.512 g. per cm^3 at 30°C from solvent-scoured Idaho medium wool acid-treated for 96 hours.

given by acid-treated Idaho medium (Targhee plus Columbia), Idaho Rambouillet, Australian Merino, New Mexican mohair (mature Angora doe), and papain-treated Merino wools. The total yield of spindle cells decreased with extended acid treatment, but the proportion of the heavier layer increased. The identities of both layers as spindle cells have been confirmed microscopically. In a few instances incompletely disintegrated fibers were found between the main layers or with the heavier fraction. Additional layers were sometimes observed, especially with extensively treated samples.

Spindle cells of the different fractions do not appear to differ systematically in appearance, dimensions, or staining properties as isolated, although individual cells do vary in these respects. Figure 1 illustrates the separation of two spindle-cell layers of densities approximately 1.499 and 1.512 g/cm^3 at 30°C from solvent-scoured Idaho medium wool acid-treated for 96 hr. Preston and Nimkar [5] found that wool fibers had a density of 1.5 in aqueous chloral hydrate columns and suggested that this high density (for a protein) is a result of reaction with the chloral hydrate.

The sulfur contents of the isolated fractions are of particular interest because such differences in the two cortical segments have been inferred [2, 4] from staining and partial solubilization experiments. The heavier fraction was appreciably higher in sulfur than the original fiber, while the lighter fraction was about the same as the original fiber, or only slightly enriched. For example, the Idaho Rambouillet wool, originally 3.7% sulfur, after 161 hr in acid gave a spindle-cell preparation of which the light fraction, about 26%, had 4.0% S and 15.6% N and the heavy fraction, about 74%, had 5.3% S and 15.4% N. Corresponding fractions from adult mohair (3.2% S) had 3.8% S, 15.2% N, and 4.3% S, 15.0% N, with the light fraction predominant. Cells made by papain treatment of Australian Merino wool (3.7% S) showed less enrichment. In this case the predominating heavy fraction had 4.3% S. Other results confirmed observations of Lindley [2, 3] that spindle-cell preparations may reach sulfur contents as high as 6.7%. The acid-soluble fractions are correspondingly poor in sulfur [3, 6].

Literature Cited

1. Blackburn, S., *Biochem. J.* **47**, 443 (1950).
2. Fraser, R. D. B., Lindley, H., and Rogers, G. E., *Biochim. et Biophys. Acta* **13**, 295 (1954).
3. Lindley, H., *Nature* **160**, 190 (1947).
4. Mercer, E. H., Golden, R. L., and Jeffries, E. B., Textile Research Journal **24**, 615 (1954).
5. Preston, J. M., and Nimkar, M. V., *J. Textile Inst.* **41**, T446 (1950).
6. Ward, W. H., Binkley, C. H., and Snell, N. S., Textile Research Journal **25**, 314 (1955).

Wilfred H. Ward
John J. Bartulovich

TEN YEARS OF T. R. J.

Decennial Index, 1945 - 1954

Ready for distribution in November

The year 1954 ended the first 10-year period since Textile Research Journal was established as successor to *Textile Research*, previously published by Textile Research Institute. An index to all the research papers that have appeared during this period has been prepared and is expected to be ready for distribution in November, 1955. This index of 60 pages contains both Author and Subject sections. Price, $5.00 per copy. Send orders to

Textile Research Institute
Publications Department
P. O. Box 625, Princeton, N. J.

Book Review

Introduction to Theoretical Organic Chemistry. P. H. Hermans. Edited and revised by Richard E. Reeves. Amsterdam, Houston, London, New York, Elsevier Publishing Co., 1954. xii + 507 pages. Price, $9.75.

Reviewed by Eugene Pacsu, Princeton, University, Princeton, N. J.

This book is a translation of the revised and extended text of the original book published in Dutch in 1952. Reason for writing this "elementary text" is given in the Preface, where the author states that most textbooks of organic chemistry have taken little or no cognizance of the development during the last 25 years of the theoretical aspects of organic chemistry while those dealing exclusively with such aspects are either too profound or too specialized to serve as a general introduction to the subject. Many teachers of organic chemistry at college and university level will agree with the author's diagnosis although not all of them, at least in this country, will follow him on the road outlined in this textbook toward a presumably more successful method of instruction in organic chemistry. Apparently it is the author's belief that modern organic chemistry should be taught via physics and physical chemistry, but "no more than an elementary knowledge of physics and chemistry" is required by the reader. It would be difficult, this reader believes, unanimously to agree on the minimum level where understanding of dipole moments, optical and magnetic properties of molecules, mass spectrometry, modern theory of acids and bases, reaction velocities and equilibria, redox potentials, etc., would constitute an adequate preparation for studying organic chemistry. These and similar subjects occupy more than one-half of Dr. Herman's book, which also requires thorough familiarity with what one would designate as purely descriptive or factual organic chemistry. The atom model, bonding of atoms to form molecules, resonance, stereochemistry, and attraction between molecules are other subjects dealt with in this book, which the modern organic chemist will have to master before he ventures to occupy a bench in a research laboratory. Of the more orthodox phases of organic chemistry, phenomena like tautomerism, intramolecular transformations, reactions through carbonium ions, substitution and addition reactions, and reactions which proceed via free radicals are discussed, mostly in a birds' eye fashion, referring those who seek deeper penetration to more specialized sources. Although this reviewer is one of those who firmly believes that the sharp demarcation lines still in existence between the various branches of chemistry should be gradually obliterated, he is not convinced that the author's book represents the best solution to the grave problem of how this should be accomplished. As it is, the book appears to be most useful to young organic chemists who wish to find out what they are supposed to know in physical chemistry. In any case, the author's goal of presenting an introduction to a broad field of theoretical chemistry has been achieved, and by discussing in a lucid style the essentials of up-to-date theories he deserves the gratitude of a large audience in need of an experienced guide.

Today's fabrics must be different, too!

LOOKING at the past is often amusing. Living in it can be sheer folly. For the world has changed—more people travel, more wives are working, and families are larger. That means people are busy! And busy people haven't time for tedious clothes care. That's why today's customers are looking to you for textiles that combine beauty and practicality.

Du Pont's modern-living fibers give *your* fabrics many care-free extras like wrinkle resistance, pleat and shape retention, easy washing, speedy drying and a minimum of ironing—advantages keyed to the needs of modern living.

Look to Du Pont's know-how in fiber research and fabric development to help you profit from the demands of today's market. Depend on it to help you keep pace with the changing needs of tomorrow.

DU PONT
REG. U.S. PAT. OFF.

BETTER THINGS FOR BETTER LIVING
. . . THROUGH CHEMISTRY

DU PONT'S MODERN-LIVING FIBERS

NYLON) RAYON) ACETATE) ORLON® ACRYLIC FIBER) DACRON® POLYESTER FIBER)

Neutral WOOL SCOURING WITH

LAVEPON WS-1*

FOR

1. IMPROVED COLOR AND LOFT
2. GREATER STAPLE LENGTH
3. NO ALKALI DAMAGE
4. FASTER DRYING
5. HIGHER GREASE RECOVERY

The LAVEPON WS-1 neutral scouring process has already proven highly successful on millions of pounds of apparel wools, carpet wools, pulled wools, mohair and cashmere—*at costs no more or even less than conventional alkali scours.* Why not investigate its advantages now?

LAVEPON WS-1 *is another dependable chemical product for the textile industry made by the makers of* LYKOPON.

LYKOPON and LAVEPON *are trade-marks, Reg. U.S. Pat. Off. and in principal foreign countries.*

CHEMICALS FOR INDUSTRY

ROHM & HAAS COMPANY

WASHINGTON SQUARE, PHILADELPHIA 5, PA.

Representatives in principal foreign countries